Functional characterization of Lupli, a new component of the *oskar* RNP complex in the *Drosophila* oocyte

Lukas Neidhart

September 2007

Dissertation

submitted to the

Combined Faculties for the Natural Sciences and for Mathematics

of the Ruperto-Carola University of Heidelberg, Germany

for the degree of Doctor of Natural Sciences

presented by

Lukas Neidhart (Diploma in Biology)

Born in Boston (MA), USA

Oral Examination: October 26, 2007

Functional characterization of Lupli, a new component of the *oskar* RNP complex in the *Drosophila* oocyte

Referees:

Dr. Darren Gilmour

Prof. Dr. G. Elisabeth Pollerberg

Contents

1 Introduction **11**

1.1 RNA localization . . . 11

1.1.1 Different functions in different systems . . . 11

1.1.2 Mechanisms . . . 13

1.2 *Drosophila* oogenesis . . . 15

1.3 Axis determination in *Drosophila* . . . 16

1.3.1 Establishment of the antero-posterior axis by *gurken* . . . 19

1.3.2 Determination of the dorsal-ventral axis by *gurken* . . . 20

1.3.3 Determination of the anterior-posterior axis by *bicoid* . . . 21

1.3.4 Biological role of Oskar . . . 22

1.4 *oskar* mRNA localization . . . 24

1.4.1 *oskar* mRNA distribution during oogenesis . . . 24

1.4.2 The MT cytoskeleton, motor proteins and *oskar* RNP transport . . . 24

1.4.3 The actin cytoskeleton and *oskar* mRNA anchoring . . . 28

1.4.4 *cis*-acting elements, *trans*-acting proteins . . . 29

1.5 Aim of thesis . . . 33

2 Material and Methods **35**

2.1 GFP-based protein trap screen . . . 35

2.1.1 Screening procedure . . . 35

2.1.2 Inverse PCR . . . 35

2.2 *Drosophila* genetics . . . 36

2.2.1 Fly husbandry . . . 36

2.2.2 Stocks . . . 37

2.2.3 Ectopic expression using the UAS/GAL4 system . . . 37

2.2.4 Generation of germ line clones using the FLP-FRT and FLP-DFS systems . 37

2.3 Molecular Biology . . . 40

2.3.1 Single-fly PCR . . . 40

2.3.2 RNA isolation . . . 41

2.3.3 cDNA synthesis and RT-PCR . . . 41

2.3.4 Cloning UASp-*lupli*-HA . . . 42

2.3.5 Primer list . . . 42

2.4 *lupli*$^{\Delta C}$ generation . . . 42

2.5 Antibody generation . . . 46

2.5.1 Cloning and purification of Lupli protein . . . 46

2.5.2 Injection and antibody purification . . . 47

2.6 Western blotting . . . 47

2.6.1 Phosphatase assay . . . 48
2.7 RNA affinity pull-down . . . 48
2.8 Immunostaining . . . 49
2.8.1 Immunofluorescence staining of *Drosophila* egg chambers . . . 49
2.8.2 Lupli immunostaining of egg chambers . . . 50
2.9 Software/Websites . . . 51

3 Results **52**
3.1 GFP-based protein trap screen . . . 52
3.1.1 Principle . . . 52
3.1.2 Techniques . . . 53
3.1.3 The Protein-trap consortium . . . 56
3.1.4 Observed patterns . . . 56
3.1.5 Several lines with posterior enrichment . . . 57
3.1.6 Refining posteriorly enriched lines . . . 57
3.1.7 Conclusion . . . 59
3.2 Lupli, a novel RRM domain protein . . . 60
3.2.1 GFP-trap line *P64C9* shows a posterior enrichment in the oocyte . . . 60
3.2.2 *P64C9* is a Lupli::GFP fusion . . . 61
3.2.3 *lupli* is conserved during evolution . . . 62
3.2.4 RRM protein and function prediction . . . 64
3.3 Lupli distribution during oogenesis . . . 66
3.3.1 Generation of anti-Lupli antibody . . . 66
3.3.2 Long Lupli is a phosphoprotein . . . 67
3.3.3 Lupli expression pattern during oogenesis . . . 67
3.4 Lupli is a novel component of the *oskar* RNP . . . 71
3.5 Lupli associates with the *oskar* 3' UTR . . . 72
3.6 Lupli function in *oskar* mRNA localization . . . 74
3.6.1 *lupli*$^{\Delta C}$ - an RRM-deletion mutant . . . 74
3.6.2 P element alleles of *lupli* . . . 77
3.6.3 *oskar* localization in *lupli* alleles . . . 78
3.6.4 Microtubule polarity is affected *lupli* mutants . . . 81
3.6.5 *lupli* affects Oskar protein levels . . . 81

4 Discussion **84**
4.1 Limits of the protein trap approach . . . 84
4.2 Lupli - a component of the *oskar* RNP . . . 86
4.3 Phenotype . . . 88
4.3.1 Absence of phenotype in *lupli*$^{\Delta C}$ . . . 88
4.3.2 Ectopic dot phenotype and MT polarity . . . 90
4.3.3 *lupli* and Oskar levels . . . 92
4.4 Conclusion . . . 92

Bibliography **96**

List of Figures

1.1 Examples of localized mRNAs in different organisms and cell types 12
1.2 Model for active mRNA transport 14
1.3 *Drosophila* oogenesis 17
1.4 Oocyte specification in the germarium of *Drosophila* 18
1.5 Localization of *gurken*, *bicoid* and *oskar* mRNAs in the wild type oocyte 18
1.6 Establishment of the A/P axis by Gurken signalling 20
1.7 Antero-posterior patterning systems in the *Drosophila* egg 22
1.8 *oskar* mRNA localization during oogenesis 23
1.9 Different models proposed for *oskar* mRNA localization to the posterior pole of the oocyte 26
1.10 *oskar* mRNA localization phenotypes 28
1.11 The EJC component Y14 colocalizes with Staufen at the posterior pole of the oocyte 30
1.12 Dynamics of *oskar* mRNA regulating factors from the nucleus to the posterior pole of the oocyte 32

2.1 Fly stocks used 38
2.2 UAS/GAL4 system 39
2.3 The FLP-DFS system 40
2.4 Primers used in this study 43
2.5 Homologous recombination using the ends-out system 44
2.6 General crossing scheme for homologous recombination 45

3.1 Principle of GFP-based protein trap screen 54
3.2 Layout of the Protein-trap database 55
3.3 GFP trap expression patterns in the ovary 58
3.4 Lines displaying a posterior enrichment of GFP 59
3.5 GFP expression pattern in *P64C9* egg chambers 60
3.6 Insertion of GFP into *CG32423* in line *P64C9* 61
3.7 *lupli* transcripts in the ovary 62
3.8 Lupli protein 62
3.9 Lupli is the *Drosophila* ortholog of three mamalian RBMS proteins 63
3.10 Sequence conservation of Lupli across evolution 64
3.11 Conservation of RRM domains in Lupli and its human orthologs 65
3.12 Generation and specificity of anti-Lupli antibody 66
3.13 Long Lupli a phospho-protein 68
3.14 Lupli expression in the germarium and during early oogenesis 68
3.15 Endogenous Lupli localizes to the posterior of the oocyte together with *oskar* mRNA 69

3.16 Distribution of Lupli isoforms in the oocyte 70
3.17 The posterior enrichment of Lupli depends on *oskar* mRNA 70
3.18 Colocalization of long Lupli-HA with Staufen in a *gurken* mutant oocytes 71
3.19 Posterior enrichment of Lupli does not depend on Oskar protein 72
3.20 Lupli binds biotinylated *oskar* 3'UTR 73
3.21 *lupli* locus and mutants 75
3.22 *lupli*$^{\Delta C}$ egg chambers show no defects in localization of osk-RNP 76
3.23 A truncated long Lupli transcript is present in *lupli*$^{\Delta C}$ 77
3.24 *lupli* is required for proper localization of Staufen and Oskar at the posterior pole . 79
3.25 *P64C9* is a *lupli* allele and displays the same phenotype as other *lupli* alleles . . . 80
3.26 lupli is required for oocyte polarity 81
3.27 Oskar protein levels are reduced in *lupli* mutant ovaries 82
3.28 Hatching rates of eggs laid by *lupli* mutant mothers are not affected 83

4.1 Mapping details of genes trapped by GFP 85
4.2 A Potential GKS-3 phosphorylation site in the N-terminal of long Lupli is conserved 88

Abstract

mRNA localization is a common mechanism for targeting proteins to specific locations within a cell, and is crucial for establishment of cellular asymmetries. In *Drosophila*, the two main body axis are determined by the localization of three maternal transcripts in the oocyte, *bicoid*, *gurken*, and *oskar* mRNA. *oskar* mRNA localizes to the posterior pole of the oocyte where it is translated locally, which is crucial for abdomen formation and germline development. Many of the factors regulating this process have been identified by means of genetics, and the majority of them colocalize with the *oskar* transcript at the posterior pole. However, the precise mechanism of *oskar* mRNA localization is still not understood.

To gain further insight into the process of *oskar* regulation, I aimed at identifying novel components involved in this process. I participated in a protein-trap screen where GFP fusions were randomly generated, and colocalization with *oskar* mRNA at the posterior pole of the oocyte was scored. Several lines displaying an enriched GFP signal at the posterior pole were identified. I characterized an independently generated line, in which the gene identified encodes a novel RNA recognition motif (RRM)-containing protein that I named Lupli. By immunostaining, I showed that endogenous Lupli protein displays the same distribution pattern in the oocyte as GFP::Lupli. Lupli associates with the 3' UTR of *oskar* mRNA and is a component of the *oskar* ribonucleoprotein (RNP) complex in vivo. I showed that the late short-range transport of *oskar* mRNA to the cortex is defective in *lupli* mutant oocytes at stage 9, and that the microtubule cytoskeleton is not properly polarized. Furthermore, Oskar protein levels are reduced in *lupli* mutant ovaries. My work thus led to the identification of Lupli as a new component of the *oskar* RNP complex, and suggests that its function is required for proper localization and expression of *oskar* in *Drosophila* oocytes.

Zusammenfassung

Die Lokalisierung von mRNA ist ein Mechanismus um Proteine gezielt in einer spezifischen Region der Zelle zu exprimieren und somit zur Schaffung von zellulären Asymmetrien beiträgt. In *Drosophila* werden die zwei Körperachsen durch die Lokalisierung von drei verschiedenen Transkripten bestimmt: *oskar*, *bicoid* und *gurken*. *oskar* mRNA lokalisiert am posterioren Pol der Oocyte, was essentiell ist für die Bildung der Geschlechtszellen und des Abdomens. Die meisten Faktoren, die für die Lokalisierung des *oskar* Transkripts benötigt werden, wurden durch genetische Analysen identifiziert und kolokalisieren häufig mit der *oskar* mRNA am posterioren Pol der Oocyte. Der genau Mechanismus der *oskar* mRNA Lokalisierung ist aber nach wie vor unbekannnt.

Um diesen Mechanismus besser zu verstehen war die Zielsetzung, neue Faktoren zu identifizieren, welche in diesem Prozess involviert sind. Dazu führte ich einen visuellen Screen durch, wobei durch Moblisierung eines GFP-basierten Transposons im Genom von *Drosophila* chimäre GFP-Proteine (GFP: Grün Fluoreszierendes Protein) generiert wurden. Dabei suchte ich speziell nach *Drosophila* Linien, bei welchen eine Kolokalisierung von *oskar* mRNA mit GFP am posterioren Pol der Oocyte stattfand, und mehrere solcher Linien wurden identifiziert. Zusätzlich charakterisierte ich eine vom Screen unabhängig generierte Linie, bei der GFP in ein bis dato nicht charakterisiertes Gen eingefügt war. Dieses Gen wurde *lupli* benannt und kodiert für ein RNA-Bindungsprotein. Antikörperfärbung bestätigte, dass das endogene Lupli-Protein dasselbe Expressionsmuster besitzt, wie das chimäre GFP::Lupli. Lupli assoziert mit dem 3' untranslatierten Bereich (3' UTR) der *oskar* mRNA und ist eine neue Komponente des *oskar* RNP-Komplexes (RNP: Ribonucleoprotein). Ich konnte zeigen, dass in *lupli* mutierten Oocyten währed des 9. Stadiums der Transport des *oskar* Transkripts über eine kurze Strecke zum posterioren Cortex, sowie die Polarisierung der Mikrobuli im Zytoskelett gestört sind. Im weiteren sinkt in mutierten *lupli* Oocyten der Oskar-Proteinspiegel. Meine Arbeit führte zur Identi-

fizierung von Lupli, einer neuen Komponente des *oskar* RNPs, und suggeriert, dass die Funktion von Lupli für die Lokalisierung, sowie für die Expression von *oskar* erforderlich ist.

Abbreviations and Terminology

A/P antero-posterior

BSA bovine serum albumin

CaMKIIα calcium/calmodulin-dependent protein kinase II α

Df Deficiency

D/V dorso-ventral

EJC exon junction complex

EST expressed sequence tag

GFP green fluorescent protein

GLC germline clone

grk *gurken*

hnRNP heterogenous ribonucleoprotein

IBE IMP-binding elements

iPCR inverse PCR

italics gene names

Khc Kinesin heavy chain

mRNP messenger ribonucleoprotein

MARK MAP/MT affinity regulating kinase

MT microtubule

MTOC microtubule organizing center

NGS normal goat serum

osk *oskar*

PCR polymerase chain reaction

PKA Protein kinase A

RBMS RNA binding motif, single-stranded interacting protein

RNP ribonucleoprotein

RRM RNA recognition motif

ssDNA single-stranded DNA

UAS upstream activating sequence

UTR untranslated region

Chapter 1

Introduction

1.1 RNA localization

1.1.1 Different functions in different systems

mRNA localization is an effective and widely used mechanism to spatially restrict protein activity to a specific site within a cell. It is involved in a variety of biological processes serving different functions. One function is the regulation of cell motility. In moving chick embryonic fibroblasts, for example, *β-actin* mRNA is localized to the leading edge of the cell to ensure a high concentration of polymerized actin required for motility (Figure 1.1 A) [Kislauskis et al., 1993, 1997]. *β-actin* mRNA is also localized in axonal growth cones where increased actin levels are required for motility and turning of the growing axons in response to extracellular guidance cues (Figure 1.1 B) [Zhang et al., 2001, Leung et al., 2006]. In neurons, several other mRNAs have been shown to be localized to dendrites [Steward and Schuman, 2001], in particular *CaMKIIα* mRNA, whose local translation is required for synaptic plasticity and memory consolidation [Martin, 2004, Miller et al., 2002].

Localized transcripts can also function as cell fate determinants. The best studied example is *ASH1* mRNA in the budding yeast *Saccharomyces cerevisiae*, which encodes a transcriptional regulator that represses mating-type switching [Bobola et al., 1996]. During cell division, asymmetric segregation of the *ASH1* transcript

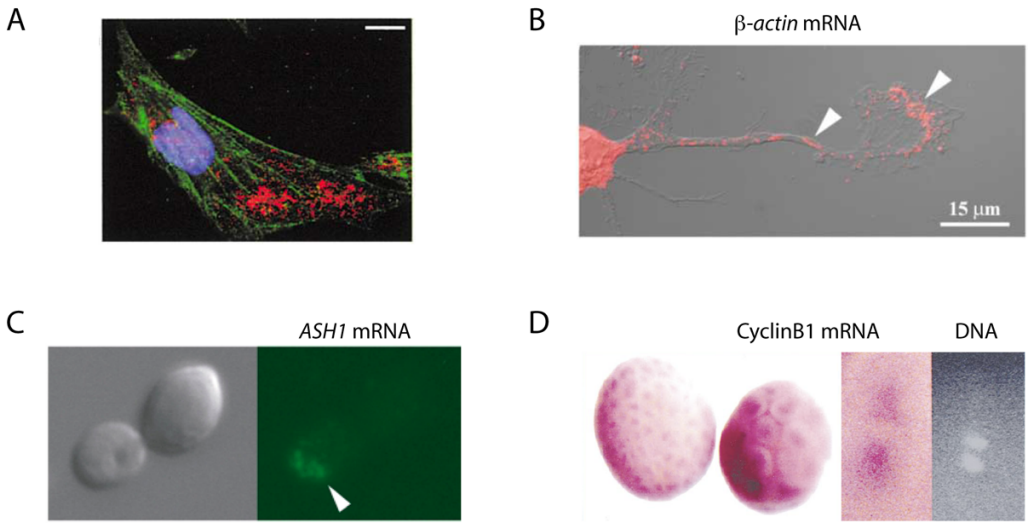

Figure 1.1: Examples of localized mRNAs in different organisms and cell types (A) Colocalization of *β-actin* mRNA (red) at the leading edge of chicken fibroblasts with phosphorylated myosin (green) and DAPI (blue). (B) *β-actin* mRNA localization in distal neurites and growth cones. (C) *ASH1* mRNA localized to the tip of the daughter cell of a mitotic budding yeast. (D) *cyclin B* mRNA is concentrated on the mitotic complexes in *Xenopus* embryos. [Groisman et al., 2000, Jansen, 2001, Kloc et al., 2002, Zhang et al., 2001]

into the budding daughter cell ensures that this cell expresses Ash1 protein (Figure 1.1 C). As a consequence, only the mother retains the capacity to switch mating-type, whereas this switch is inhibited by Ash1 protein in the daughter cell. Therefore, the two cells acquire different fates [Takizawa et al., 1997, Long et al., 1997]. Another example where an mRNA acts as a cell fate determinant is *Vg1* in *Xenopus laevis*. This transcript localizes to the vegetal pole of the oocyte and induces mesodermic tissue [Thomsen and Melton, 1993].

A localized RNA can also be used to set up a morphogen gradient in the embryo. *bicoid* mRNA is localized during *Drosophila* oogenesis to the anterior tip of the oocyte where it is anchored. After fertilization, it is translated and a gradient of Bicoid protein forms with the highest concentration at the anterior. Establishment of this gradient is necessary to switch on different sets of genes required for embryonic development [Driever and Nusslein-Volhard, 1988a,b].

At last, mRNAs localization is also a mechanism to target proteins to certain organelles or subcellular structures. *cyclin B* mRNA, for example, is specifically

localized to and translated at the mitotic spindle in *Xenopus* embryos (Figure 1.1 D). This is necessary for the integrity of the mitotic apparatus and thus, for cell division [Groisman et al., 2000]. Other transcripts, such as *metallothionein-1* (*MT-1*), *c-myc* and *c-fos*, accumulate at the nuclear periphery of mammalian cells and associate with the perinuclear cytoskeleton [Dalgleish et al., 2001, Veyrune et al., 1996, Mahon et al., 1997]. The physiological role of this is not yet clear, but it might simply be to enhance the efficiency of nuclear import of these proteins. Interestingly, cells with non-localizing *MT-1* mRNA are more susceptible to stress, as well as DNA damage, and show an increase in apoptosis after exposure to mutagens [Levadoux-Martin et al., 2001].

1.1.2 Mechanisms

Several mechanisms have evolved to localize transcripts to their subcellular location [reviewed in Johnston, 2005, Palacios, 2007]. For example, transcripts can simply diffuse passively in the cytoplasm and then get trapped locally, as is thought to be the case for *nanos* mRNA in the *Drosophila* oocyte (see Section 1.3.4 on page 22) [Forrest and Gavis, 2003]. Another mechanism is localized protection from degradation. *hsp83* mRNA, a component of the pole plasm in *Drosophila* embryos, is distributed uniformly in the early fertilized egg, but then gets degraded in the entire embryo, except in the pole plasm where the RNA is protected [Ding et al., 1993]. However, the most commonly used and best studied mechanism is active transport by molecular motors along the cytoskeleton.

Studies of different transcripts in a variety of model organisms have led to the proposal of a general model for active mRNA transport, which can be viewed as a four-step process [Jansen, 2001]. First, nuclear proteins, such as heterologous nuclear ribonucleoproteins (hnRNPs) bind to *cis*-acting elements localized in the 3' untranslated region (UTR) of the transcript (Figure 1.2) [Norvell et al., 1999, Hoek et al., 1998]. Components of the exon junction complex (EJC) may also associate with the RNA upon splicing in the nucleus [Hachet and Ephrussi, 2001].

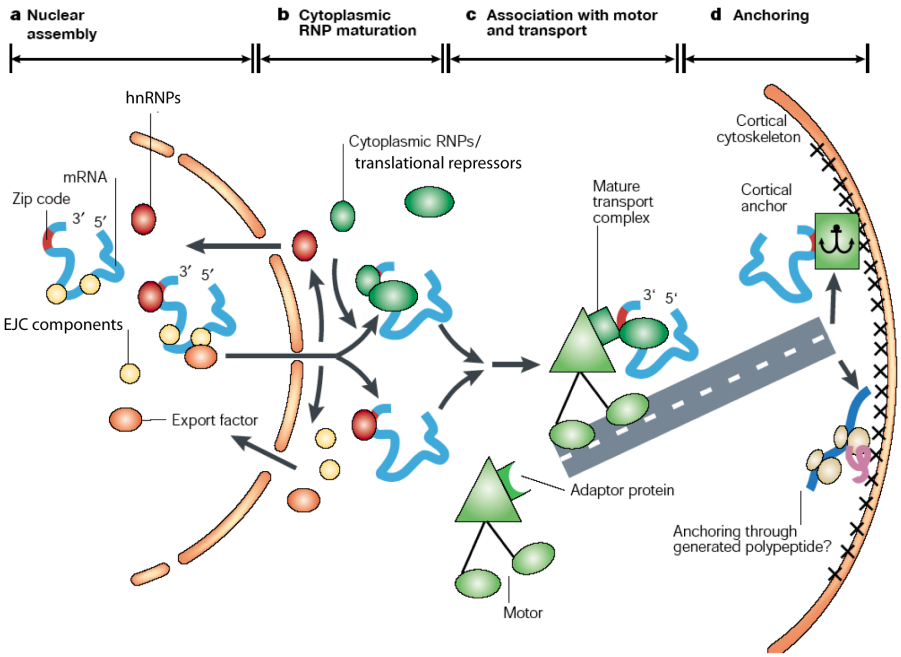

Figure 1.2: Model for active mRNA transport

(A) The transcript's (blue) localization signal, or "zip code" (red), is recognized by heterogenous nuclear ribonucleoproteins (hnRNPs, red circles) in the nucleus. Components of the exon junction complex (yellow circles) bind to the mature mRNA upon splicing. Export factors (orange oval) also assemble with the transcript. (B) The exported transcript undergoes maturation by associating with cytoplasmic hnRNPs and translational repressors, while nuclear factors may remain bound or dissociate and recycle. (C) Molecular motors (green triangle) bind to the transport complex , using adaptor proteins. The complex then gets transported to the target site along cytoskeletal structures, such as actin fibres or microtubules. (D) Once the RNP reaches its destination, it is anchored to the target site and translational repression on the transcript is relieved. [Modified from Jansen, 2001].

Second, the assembled RNA-RNP complex is then exported to the cytoplasm, where other RNA-binding proteins, including translational repressors, recognize and bind to the targeting signals of the transcript, therefore modifying the composition of the complex. Third, adaptor proteins associate with the transport complex and link it to molecular motors like myosin, dynein or kinesin [Brendza et al., 2000, Duncan and Warrior, 2002, Gonsalvez et al., 2005, Januschke et al., 2002]. These motors then actively transport the complex along the cytoskeleton (microtubules or actin filaments) to its final destination. Finally, the RNP-complex is anchored by specific factors present at the site and translational repression is relieved. Anchoring can also occur through the newly translated protein, as it is the case for *oskar* mRNA [Rongo et al., 1995].

This general model for active mRNA transport is thought to apply to all targeted transcripts. However, it is still not clear whether all employ the same strategy. For example, a direct link between a transported mRNA and a motor protein has only be shown for *ASH1* mRNA. The adaptor protein She3p binds to She2p, an *ASH1* mRNA binding protein, linking the *ASH1*-RNP to the myosin motor Myo4p, which transports the complex along actin filaments to the daughter cell [Bohl et al., 2000, Long et al., 2000, Takizawa and Vale, 2000]. Also, EJC components are required for *oskar* mRNA localization in the *Drosophila* oocyte, but seem to be dispensable for *bicoid* and *gurken* mRNAs [van Eeden et al., 2001, Hachet and Ephrussi, 2001]. Therefore, a deeper understanding of the mechanism mediating the localization of different mRNAs to different cellular compartments is required to be able to propose a general model applicable to all localized mRNAs.

1.2 *Drosophila* oogenesis

In *Drosophila*, three mRNAs, *gurken*, *bicoid* and *oskar*, are localized to different regions in the oocyte (see Chapter 1.3 on the next page). Much insight has been gained in the general understanding of how transcripts localize within cells through

analysis of the mechansim employed by these three transcripts to localize in the oocyte. The size of the oocyte, as well as the genetic tools available, make it an excellent model system to study mRNA localization in vivo.

The ovary of an adult *Drosophila melanogaster* female consists of 16 to 20 ovarioles, that constitute a succession of ovarian follicles at different stages of maturation (Figure 1.3). The ovariole can be subdivided into the anterior germarium and the posterior vitellarium. The germline stem cells reside in the germarium and divide asymetrically to give rise to a cystoblast and a new stem cell (Figure 1.4). The cystoblast will go through four rounds of mitosis with incomplete cytokinesis, forming a syncytium of 16 cells called germline cyst [reviewed in Huynh et al., 2004]. The 16 cells are interconnected via 15 actin-rich cytoplasmic bridges called ring canals. One of the two cells (pro-oocytes) that arose from the first division, and contain four ring canals, will be determined and differentiate into the oocyte. The 15 other cells will develop into nurse cells. The follicular cells that derive from the somatic stem cells in the germarium, will surround the germline cyst by forming the follicular epithelium, giving therefore rise to a stage 1 egg chamber.

1.3 Axis determination in *Drosophila*

The body axes of the fly are determined before fertilization of the egg by the correct localization of the three maternal transcripts, *gurken*, *oskar* and *bicoid*, in the oocyte (Figure 1.5) [Riechmann and Ephrussi, 2001]. The localization of these transcripts depends on the polarity of the microtubule (MT) skeleton within the oocyte. Prior to its role as the determinant of the dorso-ventral axis, Gurken (Grk), an EGF-receptor ligand, sets up MT organization that governs axis formation [Steinhauer and Kalderon, 2006].

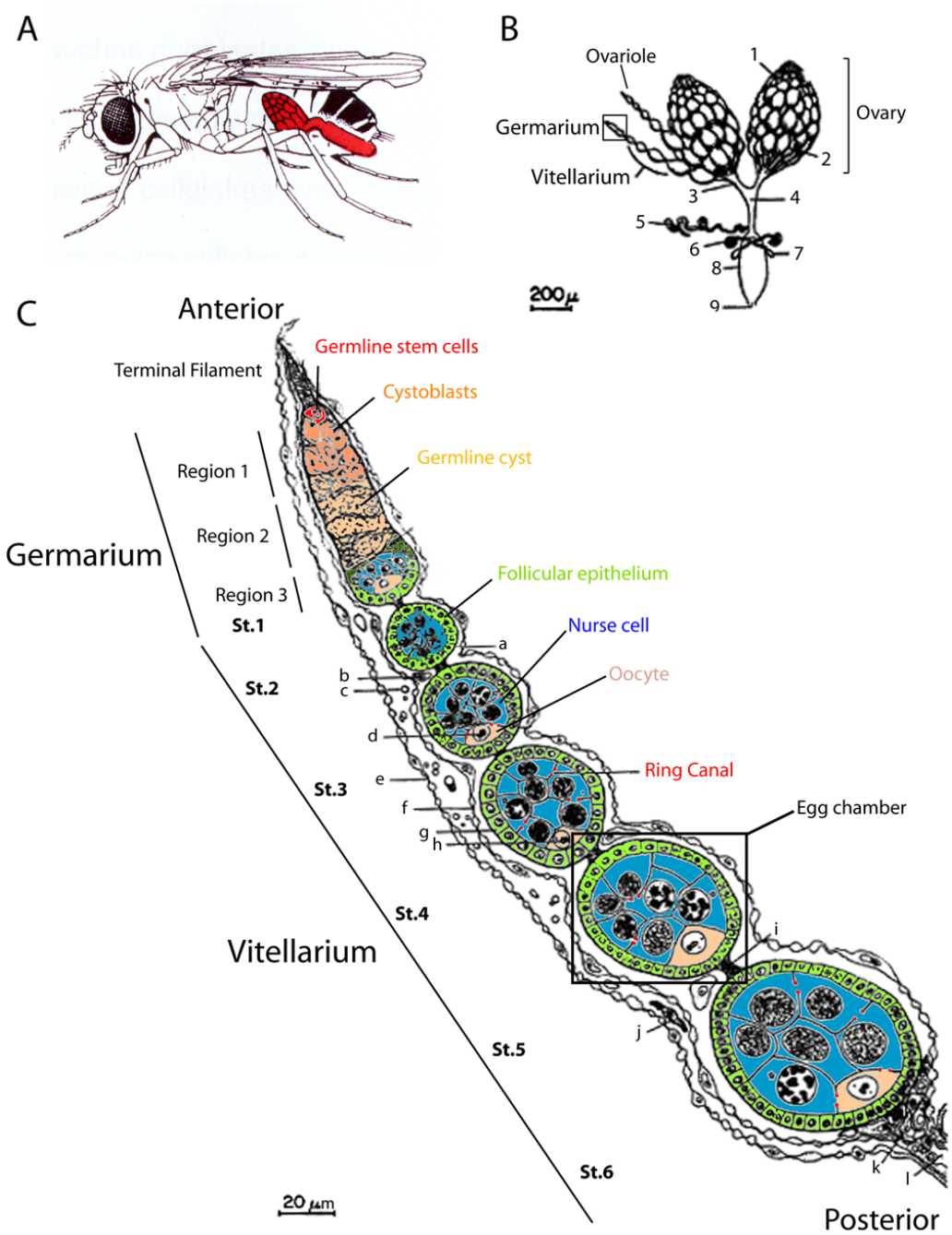

Figure 1.3: *Drosophila* oogenesis

(A) Representation of a *Drosophila* female with the position of the genital tract (red) within the abdomen. (B) Diagram of the female reproductive apparatus. Two ovarioles are shown pulled out of the ovary. 1: peritoneal sheath; 2: mature eggs; 3: lateral oviduct; 4: common oviduct; 5: seminal receptacle; 6: spermatheca; 7: accessory glands; 8: uterus; 9: vulva. (C) Diagram of an ovariole, which is differentiated into an anterior germarium and a posterior vitellarium. The germarium can be divided in three regions (for details see Figure 1.4). The vitellarium contains the maturating egg-chambers. Representative egg-chambers of each one of the first six stages of oogenesis (St.1-St. 6) are drawn. a: tunica propria; b: lumen cell; c: trachea; d: oocyte nucleus; e: peritoneal sheath; f: epithelial sheath; g: follicle cell; h: karyosome; i: follicular stalk; j: tracheal cell; k: debris; l: oviduct. Egg chamber maturation is a continuous process, not all of the depicted stages are simultaneously present in one ovarriole in vivo. [Courtesy of J.B. Coutelis, modified from King, 1970].

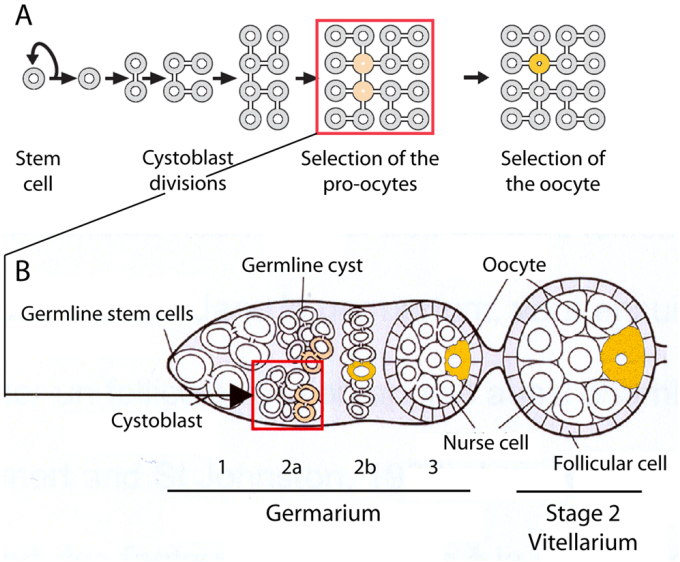

Figure 1.4: Oocyte specification in the germarium of *Drosophila*
(A) Scheme of the first division of a germline stem cell resulting in 15 nurse cells and one oocyte. The first asymetric division gives rise to a cystoblast and a stem celll. The cystoblast then divides four times with incomplete cytokinesis, to produce 16 cells, interconnected by 15 cytoplasmic bridges (ring canals). One of the two cells having four ring canals (pro-oocytes, light orange) will be selected as the oocyte (orange). (B) Diagram of the germarium and a stage 2 egg chamber. Region 1 contains the mitotically active germline cells, region 2 the differentiating germline cysts where the oocyte is selected, and region 3 a single newly formed egg chamber that represents stage 1 of oogenesis. [Modified from Huynh et al., 2004].

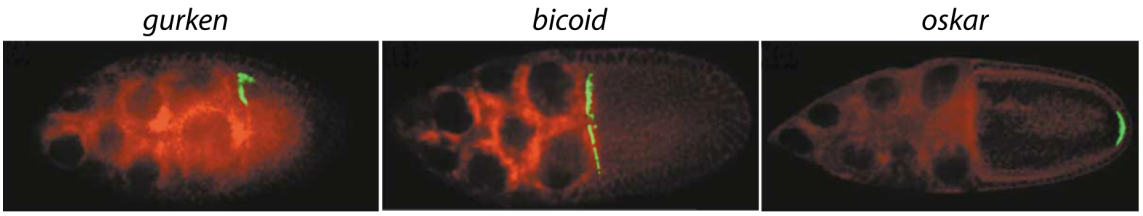

Figure 1.5: Localization of *gurken*, *bicoid* and *oskar* mRNAs in the wild type oocyte *gurken* (left) mRNA localizes in the dorsal-anterior corner of stage 9 wild type oocytes. At stage 10B, *bicoid* accumulates at the anterior cortex (middle) and *oskar* at the posterior pole (right) [Adapted from Hachet and Ephrussi, 2001].

1.3.1 Establishment of the antero-posterior axis by *gurken*

In the germarium and during the early stages (stages 2 to 6) of oogenesis, the minus-ends of the MTs are organized in the oocyte and extend their plus-ends through the ring canals into the nurse cells (Figure 1.6 A) [Theurkauf et al., 1992]. As the egg chamber buds off from the germarium and enters the vitellarium, a diffuse microtubule organising center (MTOC) localizes at the posterior cortex of the oocyte [Grieder et al., 2000], directing the localization of cytoplasmic factors including *grk* RNA and Grk protein [Neuman-Silberberg and Schupbach, 1996, 1993, Saunders and Cohen, 1999]. During these early stages of oogenesis, Grk induces the follicle cells overlying the oocyte to take on posterior fate [Gonzalez-Reyes et al., 1995, Roth et al., 1995]. By stage 7, an unkown signal is sent back from the posterior follicle cells to the oocyte, resulting in the repolarization of the MT cytoskeleton (Figure 1.6 B). In response to this reverse signal, the MTOC at the posterior of the oocyte disassembles, and the MTs nucleate from the anterior and lateral cortices of the oocyte (Figure 1.6 C). This reorganisation of the MT network is necessary for localization of the three mRNAs, *gurken*, *oskar* and *bicoid,* to the anterior dorsal corner, posterior, and anterior, respectively, of the oocyte (Figures 1.5 and 1.6 D).

Consequently, mutations in *gurken*, or in genes required for Gurken signaling, disrupt polarization of the oocyte, leading to a symmetric MT network and no defined antero-posterior (A/P) axis at mid-oogenesis [Gonzalez-Reyes et al., 1995, Roth et al., 1995]. Specifically, *grk* mutant oocytes display MT minus-ends at both the anterior and the posterior cortex, and MT plus-ends are focused towards the center of the oocyte. Furthermore, *gurken* mutations also disrupt migration of the oocyte nucleus to the anterior, and both groups of terminal follicle cells adopt the default anterior fate [Gonzalez-Reyes et al., 1995, Roth et al., 1995].

There are also other factors involved in the MT reorganization at mid-oogenesis. Protein Kinase A (PKA), for example, is thought to be required for proper polarization of MTs specifically after stage 6, as *pka* mutant oocytes display a phenotype similar to that of *grk* mutants, with the MT plus ends pointing towards the center of

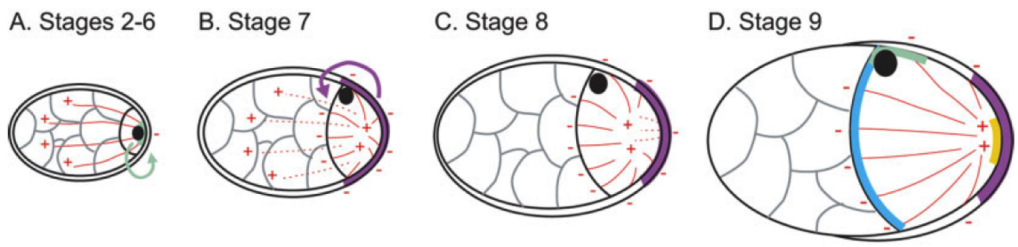

Figure 1.6: Establishment of the A/P axis by Gurken signalling
(A) During stages 2 to 6, the germline MTs (red) point from the nurse cells (plus-ends) into the oocyte (minus-ends), where an MTOC is established. Gurken (Grk) protein signals from the oocyte to the overlying follicular epithelial cells at the posterior pole. (B) At stage 7, the MT cytoskeleton completely reorganizes, presumably upon response of an unknown signal (purple arrow) that is coming from the posterior follicle cells (purple). The posterior MTOC disassembles (red dashed lines) and the MTs (red solid lines) are nucleated along the entire oocyte cortex . Migration of the oocyte nucleus (black circle) directs the localization of *grk* RNA and Grk protein (green, stage 9). (C) At stage 8, the cortical MTs disappear at the posterior pole (red dashed lines) and the MT plus-ends focus there. (D) After establishment of the A/P axis in the oocyte, *bicoid* (blue) and *oskar* (yellow) mRNAs, can properly localize to the anterior and to the posterior of the cell, respectively. MT polarity (red) is indicated by "+" or "-" to specify the general position of plus- or minus-ends. Posterior is to the right and dorsal is up. [Adapted from Steinhauer and Kalderon, 2006]

the cell [Lane and Kalderon, 1994]. Also in *par-1* mutants, MT polarity is disrupted and no A/P-axis is defined [Shulman et al., 2000, Tomancak et al., 2000]. Studies with its mammalian ortholog, the MAP/MT affinity regulating kinase (MARK), suggest that Par-1 may be directly affecting MT dynamics in the oocyte by phosphorylating MT-associated proteins [Drewes et al., 1997]. In contrast to *grk* mutants, however, migration of the oocyte nucleus in *pka*, as well as in *par-1* mutant oocytes is not affected [Shulman et al., 2000, Steinhauer and Kalderon, 2005].

1.3.2 Determination of the dorsal-ventral axis by *gurken*

The first manifestation of dorsal-ventral (D/V) asymmetry in the developing oocyte is the migration of the nucleus to the future dorsal-anterior side of the egg chamber during stage 8 (Figure 1.6 C) [King, 1970]. This migration requires the prior reorganization of the MT network that was set up by the first Grk signalling event, at the posterior pole [Gonzalez-Reyes et al., 1995, Roth et al., 1995, Theurkauf et al., 1992]. *gurken* mRNA accumulates in the dorsal-anterior corner of the oocyte, in

tight association with the oocyte nucleus during stage 8 [Neuman-Silberberg and Schupbach, 1993]. At stage 9, translation of *grk* mRNA and local release of Gurken protein specifies the adjacent follicle cells as dorsal follicle cells and that side of the oocyte as the future dorsal side. The cells that do not receive the Grk signal, instead, adopt a ventral fate and will subsequently signal back to the oocyte, defining the ventral side of the embryo [Schupbach, 1987].

1.3.3 Determination of the anterior-posterior axis by *bicoid*

In addition to *gurken* mRNA, whose asymmetric localization at the antero-dorsal corner of the oocyte defines the dorsal side of the embryo, establishment of the A/P axis depends on the asymmetric localization of *bicoid* and *oskar* mRNAs to the anterior and posterior cortex of the oocyte, respectively (Figures 1.5 B, C, and 1.6 D). *bicoid* encodes the anterior determinant required for the patterning of the head and thorax of the embryo [Frohnhofer and Nusslein-Volhard, 1986], whereas *oskar* encodes the posterior determinant necessary for formation of the abdomen and the germline [Lehmann and Nusslein-Volhard, 1986].

During stages 7 to 9 of oogenesis, *bicoid* mRNA is transported from the nurse cells into the oocyte, where it colocalizes with the minus ends of the MTs [Johnston et al., 1989] (Figure 1.6). This localization is MT-dependent, and is presumably directed by the minus-end directed motor dynein [Duncan and Warrior, 2002]. *bicoid* mRNA remains anchored at the anterior throughout the rest of oogenesis by Staufen, a conserved double-stranded RNA-binding (dsRBD) protein [Ferrandon et al., 1994]. After fertilization of the egg, the *bicoid* transcript is translated and Bicoid protein acts as a morphogen and diffuses towards the posterior of the embryo, forming a gradient that is required to regulate zygotic gap gene expression and pattern the anterior structures of the embryo [Driever and Nusslein-Volhard, 1988a,b]. Consequentlly, *bicoid* mutant embryos lack head and/or thorax, depending on the strength of the allele (Figure 1.7) [Driever and Nusslein-Volhard, 1988a].

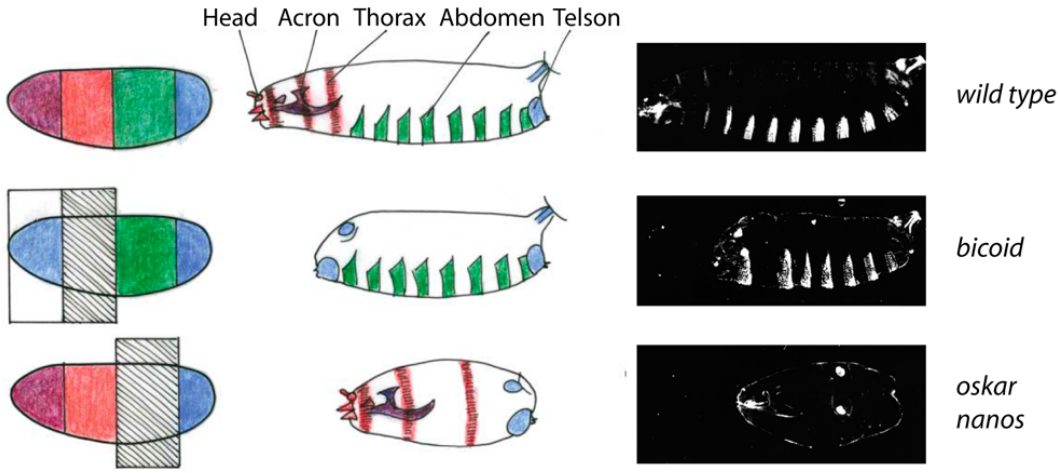

Figure 1.7: Antero-posterior patterning systems in the *Drosophila* egg
Scheme indicating which genes are responsible for patterning of the anterior (*bicoid*, middle) and posterior (*oskar/nanos*, bottom) of the embryo. The phenotypes of embryos that are either wild type, *bicoid* and *oskar* mutant (scheme in the middle, cuticule preps on the right) are shown. The colors indicate the region *bicoid* (pink) and *oskar/nanos* (green) genes are responsible for. [Modified from Nusslein-Volhard, 2004]

1.3.4 Biological role of Oskar

oskar mRNA is expressed in the nurse cells in the germarium and throughout oogenesis, but is only translated once it reaches the posterior pole of the oocyte at stage 9 [Ephrussi et al., 1991, Kim-Ha et al., 1991, Lehmann and Nusslein-Volhard, 1986, Rongo et al., 1995]. *oskar* codes for two isoforms, Long Osk and Short Osk, which are generated by the usage of two alternative start codons (M1 and M2) [Markussen et al., 1995]. Long Osk is necessary for anchoring of *oskar* mRNA and Short Osk at the posterior pole [Vanzo and Ephrussi, 2002]. Short Osk is required for the formation of the pole plasm, a specialized region of the cytoplasm that contains germline and abdominal determinants. Oskar and associated proteins recruit *nanos* mRNA, which encodes the abdominal determinant of the embryo and which is translationally repressed in the oocyte. [Ephrussi et al., 1991, Wang and Lehmann, 1991]. Upon fertilization, *nanos* mRNA is selectively translated in the posterior germ plasm. A gradient of Nanos protein emanates from the posterior of the embryo and negatively regulates translation of *hunchback* mRNA, allowing posterior zygotic gap gene activation and abdominal patterning [Johnstone and Lasko, 2001]. Additionally, pole plasm persists in the embryonic pole cells, which will give rise to the primordial

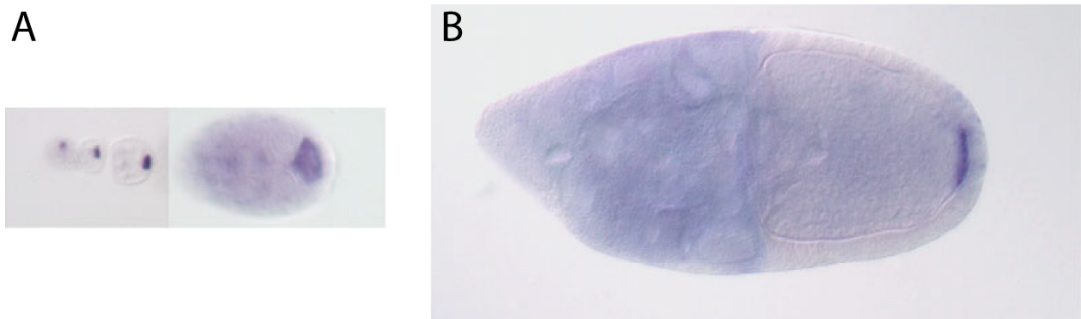

Figure 1.8: *oskar* mRNA localization during oogenesis
(A) *oskar* mRNA is expressed early during oogenesis and accumulates in the oocyte. (B) At stage 10, the transcript localizes to the posterior pole of the oocyte (B).

germline cells in the embryo.

In embryos coming from *oskar* protein null mutant mothers, the absence of Oskar activity results in an absence of formation of the abdomen, giving rise to a "posterior group phenotype" (Figure 1.7). The same phenotype is also observed in *nanos* mutant oocytes. In contrast, in weaker *oskar* alleles where Oskar activity is reduced, the embryos develop into adults, but they lack the germline. As these adults are sterile, this phenotype is called "grandchild less". Thus, the "posterior group phenotype" and the "grandchildless phenotype" reflect a differential sensitivity to Oskar activity in abdominal and germline formation. Furthermore, overexpression of *oskar* results in a duplication of the posterior structures ("bicaudal phenotype") [Ephrussi and Lehmann, 1992, Kim-Ha et al., 1995]. This phenotype is particularly penetrant when *oskar* is ectopically expressed at the anterior, using a transgene in which the *oskar* 3' UTR has been replaced by that of *bicoid*, directing Oskar activity to the anterior pole of the embryo [Ephrussi and Lehmann, 1992]. This demonstrates the capacity of Oskar to recruit all the factors of the pole plasm necessary for abdominal patterning, as well as the importance of restricting localization and translation of *oskar* mRNA to the posterior of the oocyte.

1.4 *oskar* mRNA localization

1.4.1 *oskar* mRNA distribution during oogenesis

oskar mRNA shows a dynamic pattern of localization during oogenesis. Upon synthesis in the nurse cells, the transcript accumulates in the early oocyte and seems to be enriched at the posterior cortex until stage 6 of oogenesis (Figure 1.8) [Ephrussi et al., 1991, Kim-Ha et al., 1991]. During stages 7 and 8, most of *oskar* mRNA is concentrated in the centre [Cha et al., 2002], as well as at the anterior pole of the oocyte [Ephrussi et al., 1991, Kim-Ha et al., 1991]. Interestingly, this coincides with the reversal of the MT network polarity in the oocyte upon Grk signalling (see page 19). From late stage 8, *oskar* mRNA again localizes to the posterior pole of the oocyte, forming a tight crescent. From stage 9 until early embryogenesis, the transcript is translated and Oskar protein and its transcript colocalize at the posterior pole, in tight association with the cortex.

What is the mechanism underlying *oskar* mRNA localization during oogenesis? In the following part of the introduction I will review the requirements for *oskar* mRNA localization, such as the polarity of the MT cytoskeleton, molecular motors, as well as *cis*- and *trans*-acting factors. Furthermore, I will discuss the current models and the open questions on *oskar* mRNA control.

1.4.2 The MT cytoskeleton, motor proteins and *oskar* RNP transport

How does *oskar* mRNA get transported to the posterior pole of the oocyte? And does the *oskar* RNP localize there by active transport along MT tracks (see Figure 1.2 on page 14)? It has been shown that the transport of *oskar* mRNA to the posterior pole is MT-dependent [Clark et al., 1994]. Furthermore, a marker for the plus-ends of MTs, the motor domain of Kinesin heavy chain fused to β-Galactosidase (Kin::β-GAL), localizes at the posterior pole during stages 8 and 9. The assumption is that the *oskar* mRNA localization complex gets transported by molecular

motors along MT tracks towards the MT plus ends (Figure 1.9 A) [Clark et al., 1994, Theurkauf et al., 1992]. Indeed, *kinesin heavy chain* (*khc*), encoding a component of Kinesin I (conventional Kinesin), is required for the posterior localization of *oskar* mRNA, indicating that a molecular motor may be transporting *oskar* mRNA along MT tracks (Figure 1.12) [Brendza et al., 2000]. Interestingly, *kinesin light chain* (*klc*), the gene that encodes the component of Kinesin I that usually is required for cargo binding, is not required for *oskar* mRNA transport, which suggests a novel mechanism of cargo recruitment in the case of the *oskar*-RNP complex [Palacios and Johnston, 2002].

The simplistic view of *oskar* mRNA being transported to the posterior by Kinesin I along a linear array of MTs oriented along the A/P axis has been challenged by several findings. It is becoming more evident that the MT skeleton is organized in a much more complex manner during mid-oogenesis than previously assumed. Despite the fact that Khc localizes to the posterior pole of the oocyte, staining of the oocyte with anti-tubulin antibody suggests that the posterior pole is relatively free of MTs [Cha et al., 2002]. Cha *et al.* also observed that in wild type oocytes MT minus-end markers are distributed all over the oocyte cortex, suggesting that the MTs are nucleated at the cortex and point towards the center of the cell (Figure 1.9 B). Interestingly, in *khc* mutant oocytes, the internal accumulation of *oskar* mRNA is not observed and the transcript is mislocalized around the cortex at stages 8 to 10A (Figure 1.10 A, B). This led the authors to propose a "cortical exclusion model", in which Khc transports *oskar* mRNA away from all regions of the oocyte cortex, except from the posterior pole (Figure 1.9 B).

In a different model, MTs in the oocyte have been proposed to be organized in two perpendicular subsets, one along the D/V axis, the other one along the A/P axis [Januschke et al., 2006, MacDougall et al., 2003]. Januschke and co-workers also observed an active MTOC near the nucleus, giving rise to these two MT subsets [Januschke et al., 2006]. Furthermore, by detailed analysis of the dynamic rearrangements of these MT subsets they could correlate *oskar* mRNA localization

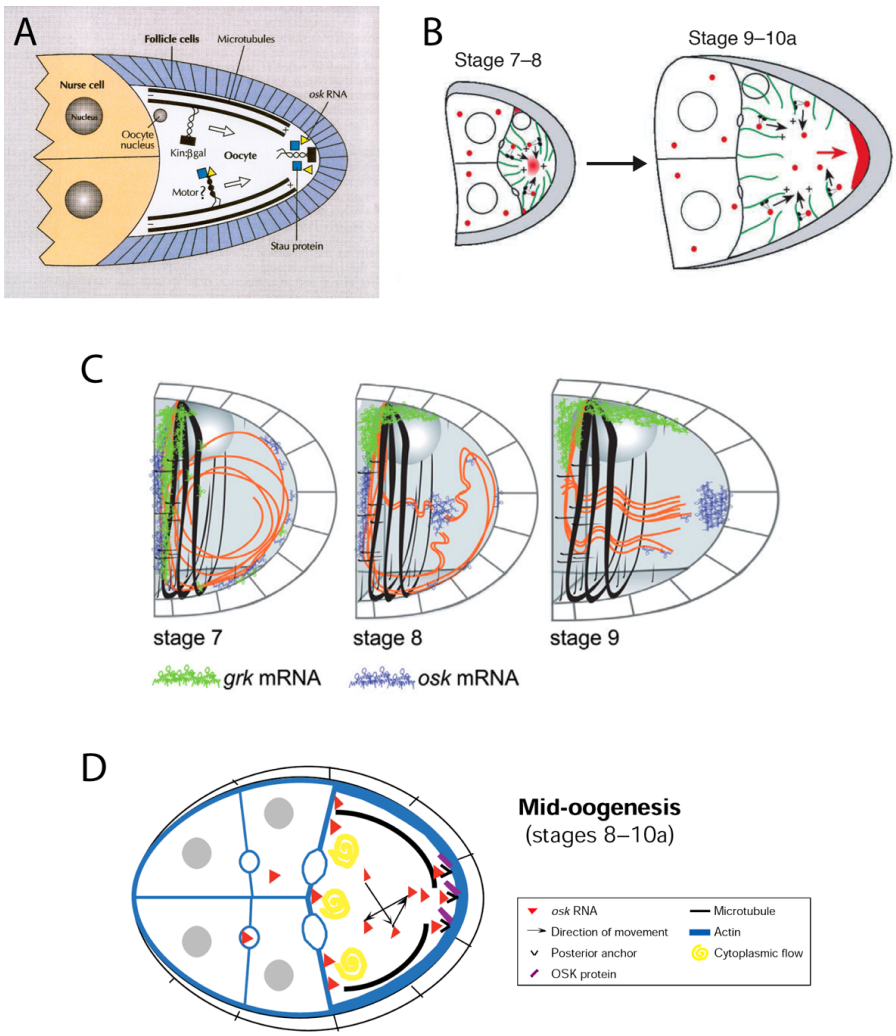

Figure 1.9: Different models proposed for *oskar* mRNA localization to the posterior pole of the oocyte

(A) Model of simple directed transport along MTs. MTs in a stage 9 oocyte are oriented with the minus ends at the anterior and plus ends at the posterior. *oskar* mRNA is transported to the posterior pole by simple plus-end movement along these MT tracks. Kin::β-GAL may mimic such a process. [Adapted from Clark et al., 1994] (B) Cortical exclusion model. MTs are nucleated from the oocyte cortex, and Kinesin associates with *oskar* mRNA and moves it to the interior of the cell during stages 7/8. During stages 9/10A, Kinesin continues to move *oskar* mRNA along MTs, but MT density decreases at the posterior due to MT destabilisation. This allows *oskar* mRNA to access to the cortical actin network only at the posterior pole, which may be enhanced by cytoplasmic movement (red arrow). [Adapted from Cha et al., 2002] (C) A model proposing that MTs are organised as two subsets along the D/V (black) and the A/P (red) axis. *oskar* mRNA localization correlates with the sequential organisation of the A/P MT subset (red) formation. The open diaphragm-like structure formed by the most central MTs transports *oskar* mRNA from the anterior towards the center. By stage 9, upon complete A/P orientation of the A/P MT subset, *oskar* is transported towards the posterior [Januschke et al., 2006]. (D) Cytoplasmic flows localize *oskar* mRNA to the anterior pole (transiently) and to the posterior pole of the oocyte where it binds to the localized anchor that is dependent on the actin cytoskeleton. The anchoring of *oskar* mRNA is stablized by Oskar protein at the posterior pole. [Adapted from Glotzer et al., 1997]

with progression of the formation of the A/P MT subset (Figure 1.9 C).

A different model has been put forward by Glotzer *et al.*, who observed that when fluorescently labelled *oskar* mRNA was injected in the vicinity of the posterior pole, some of it could still properly localize after MT depolymerization [Glotzer et al., 1997]. This led the authors to suggest that *oskar* mRNA might be passively trapped at the posterior by a pre-localized anchor, and that Kinesin might be required to generate the cytoplasmic flows that move the mRNA in the oocyte and delivering it to the posterior pole (Figure 1.9 D). However, even though the oocyte shows cytoplasmic flows at stage 9 that are kinesin-dependent [Palacios and Johnston, 2002], this slow cytoplasmic streaming is not required for the localization of the *oskar* RNP to the posterior pole [Serbus et al., 2005]. Furthermore, the localization of the injected mRNA requires Oskar protein, whereas the endogenous mRNA initially localizes to the posterior in *oskar* nonsense mutations even if not anchored there [Ephrussi et al., 1991, Glotzer et al., 1997, Kim-Ha et al., 1991]. This indicates that the localized anchor is Oskar protein itself during the later stages of the oocyte. However, as *oskar* mRNA is not translated until it reaches the posterior pole, the first pool of mRNA must be anchored by a different mechanism [Gunkel et al., 1998, Kim-Ha et al., 1995].

In addition to the MT skeleton, actin fibres might also be involved in *oskar* mRNA transport. Tropomyosin II (TmII), a protein involved in actin-based motility, is required for *oskar* mRNA localization to the posterior pole [Erdelyi et al., 1995]. However, the overall integrity of the actin network seemed not to be affected in *TmII* mutant egg chambers, and the explanation for the observed *oskar* mRNA localization phenotype still remains to be solved.

Taken together, it seems likely that several of the proposed mechanisms contribute to *oskar* mRNA localization. Both, the cortical exclusion model, as well as the dynamic rearrangement of MTs observed by Januschke *et al.* can at least partially explain how *oskar* mRNA could get transported by Kinesin into the vicinity of the posterior pole of the oocyte [Cha et al., 2002, Januschke et al., 2006]. How-

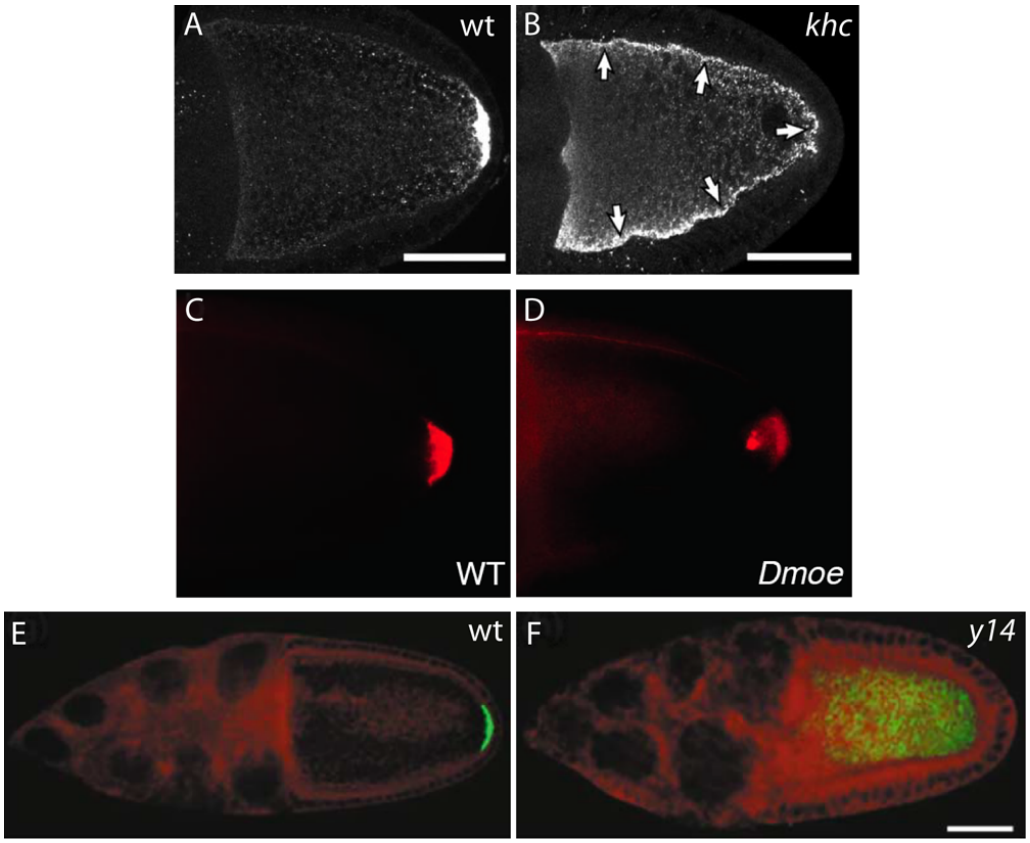

Figure 1.10: *oskar* mRNA localization phenotypes
(A, B) *oskar* mRNA localizes all around the cortex in stage 8 *khc* oocytes (B, arrowheads), whereas it localizes to the posterior pole in wild type (A) [Adapted from Cha et al., 2002]. (C, D) Staufen is used as a marker for the *oskar* RNP complex, which forms an ectopic dot close to the posterior *dmoesin* oocytes [Adapted from Polesello et al., 2002]. (E, F) *oskar* mRNA is randomly distributed in *y14* stage 10B egg chambers (F), whereas it accumulates at the posterior pole in wild type (E) [Adapted from Hachet and Ephrussi, 2001]. Scale bars represent 50 μm in A, B and F.

ever, besides the yet unanswered question of how the *oskar* RNP is directly linked to Kinesin, the two models can also not explain how *oskar* mRNA finally reaches the posterior cortex. Such a second step, or "short-range transport", could indeed be mediated by a different, MT-independent "trapping mechanism", as suggested by Glotzer *et al.* Nevertheless, the precise and complete mechanism of *oskar* mRNA transport to the posterior pole still needs to be elucidated.

1.4.3 The actin cytoskeleton and *oskar* mRNA anchoring

Once the *oskar* RNP has reached the posterior pole, it must be anchored at the cortex. Unlike *bicoid* mRNA, the anchoring of *oskar* mRNA at the posterior does

not require MTs, and instead depends on the cortical actin cytoskeleton. In *dmoesin* (*dmoe*) mutant stage 10 oocytes, the *oskar* RNP forms an ectopic dot close to the posterior pole of the oocyte, but does not form a crescent (Figure 1.10 C, D) [Jankovics et al., 2002, Polesello et al., 2002]. Furthermore, the studies indicate that Dmoesin is required for anchoring of F-actin filaments to the plasma membrane. As MT polarity is not affected in *dmoe* mutant egg chambers, this suggests that *oskar* mRNA gets transported normally to the posterior pole, but that Dmoesin is needed for the anchoring at the posterior pole.

Two actin-associated proteins, Homer and Bifocal, have also been implicated in *oskar* mRNA anchoring [Babu et al., 2004]. It was proposed that two processes that act redundantly at stage 10, one requiring Bifocal and an intact F-actin cytoskeleton and a second requiring Homer but independent of intact F-actin, mediate posterior anchoring of the *oskar* transcript.

Oskar protein itself is also involved in anchoring, as Long Osk anchors both *oskar* mRNA and Short Osk at the posterior pole [Vanzo and Ephrussi, 2002]. But as already mentioned, the initial accumulation of *oskar* mRNA at the posterior of stage 8/9 oocytes does not require Oskar protein [Ephrussi et al., 1991, Kim-Ha et al., 1991]. Therefore, the question if, and how *oskar* mRNA is anchored to the posterior cortex of the oocyte before stage 10 has not yet been answered.

1.4.4 *cis*-acting elements, *trans*-acting proteins

Whichever mechanism is used to localize *oskar* mRNA, it requires *cis*-acting localization elements in the transcript. Typically, these elements consist of stem loop structures that are recognized by RNA-binding proteins, the *trans*-acting factors, which are then thought to couple the transcript to the localization machinery and translational control. The *oskar* mRNA localization signal was orginally mapped to its 3' UTR [Kim-Ha et al., 1993], as is also the case for many other localized transcripts [Jansen, 2001]. By using chimeric constructs in a wild type background, it was concluded that the *oskar* 3' UTR was sufficient to localize the coding regions

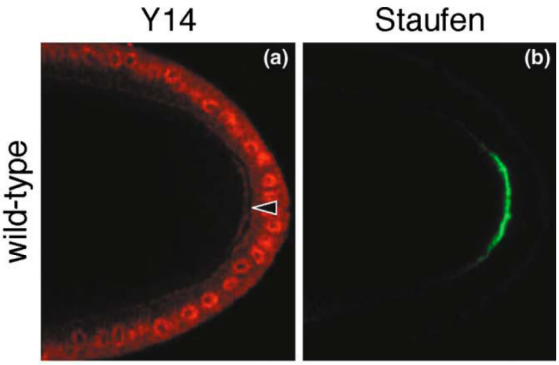

Figure 1.11: The EJC component Y14 colocalizes with Staufen at the posterior pole of the oocyte
Y14, which is required for posterior localization of *oskar* mRNA, colocalizes with Staufen at the posterior pole. Y14 (a) colocalizes with the *oskar* RNP, marked by Staufen (b), at the posterior pole of wild type stage 9 oocytes [Adapted from Hachet and Ephrussi, 2001].

of *LacZ*, *nanos* and *bicoid* to the posterior pole of the oocyte [Gunkel et al., 1998, Kim-Ha et al., 1993, Rongo et al., 1995]. The analysis of several deletions in the *oskar* 3' UTR further revealed several *cis*-acting elements that were implicated in different steps of localization: transport from the nurse cells to the oocyte, transitory accumulation at the anterior and localization to the posterior pole [Kim-Ha et al., 1993]. The authors concluded that the use of multiple *cis*-acting elements that are present in different regions of the *oskar* 3' UTR that localization may be orchestrated in a combinatorial fashion by binding of different *trans*-acting factors.

However, more recent data show that the 3' UTR alone is not sufficient for localization of *oskar* mRNA. Indeed, in the absence of endogenous *oskar*, a construct containing lacZ fused to *oskar* 3' UTR does not localize to the posterior pole of the oocyte [Hachet and Ephrussi, 2004]. The authors suggested that *lacZ-osk* 3' UTR mRNA hitchhikes on endogenous *oskar* mRNA localization complexes, and that the association of the RNA into higher-order *oskar* RNP complexes is promoted by the *oskar* 3' UTR. Thus, the previously identified *cis*-acting elements by Kim-Ha *et al.* might not represent binding sites for *trans*-acting factors implicated in transport, but rather the elements required for oligomerization during hitchhiking [Kim-Ha et al., 1993].

The study by Hachet *et al.* has also demonstrated that the splicing of the first

intron is required for posterior localization [Hachet and Ephrussi, 2004]. The function of splicing seems to be to recruit the exon junction complex (EJC), which is deposited on the mRNA, as the intron is being removed. Indeed, mutants in two core EJC components, Mago nashi and Y14, disrupt the posterior localization of *oskar* mRNA and both localize to the posterior pole (Figures 1.11 and 1.12) [Hachet and Ephrussi, 2001, Micklem et al., 1997, Mohr et al., 2001, Newmark and Boswell, 1994, Newmark et al., 1997]. A third EJC component, the RNA helicase eIF4AIII, has also been implicated in posterior transport [Palacios et al., 2004]. eIF4AIII binds to the cytoplasmic protein Barentsz, which is also necessary for *oskar* mRNA localization, indicating the the EJC recruits Barentsz to the mRNA when it is exported into the cytoplasm (Figure 1.12) [van Eeden et al., 2001, Palacios et al., 2004]. Taken together, these results indicate that formation and fate of the *oskar* mRNA localization complex therefore depends on it nuclear history.

Another important component required for *oskar* localization is the conserved RNA-binding protein Staufen [Ephrussi et al., 1991, Johnston et al., 1991, Kim-Ha et al., 1991], which presumably binds to the 3' UTR of *oskar* [Micklem et al., 2000]. It is also implicated in the localization of other *Drosophila* mRNAs, such as *bicoid* in the oocyte or *prospero* mRNA in embryonic neuroblasts [Johnston et al., 1989, Li et al., 1997]. Furthermore, its orthologs are also required for *Vg1* mRNA localization in *Xenopus laevis* [Yoon and Mowry, 2004], and are part of mRNA transport granules in mammalian dendrites [Kanai et al., 2004, Mallardo et al., 2003]. In the *Drosophila* oocyte, while the EJC components colocalize with *oskar* mRNA at the posterior pole only until stage 9, Staufen remains tightly associated with *oskar* mRNA throughout oogenesis, and is also necessary for the translation and anchoring of *oskar* at the posterior (Figure 1.12) [Johnston et al., 1991, Kim-Ha et al., 1995, Micklem et al., 2000, Rongo et al., 1995].

In addition to Staufen and the EJC, heterogenous nuclear ribonucleoproteins (hnRNPs) are also required for *oskar* localization. Hrp48, originally identified as p50, binds to the *oskar* 5' and 3' UTRs and is involved in *oskar* translational control

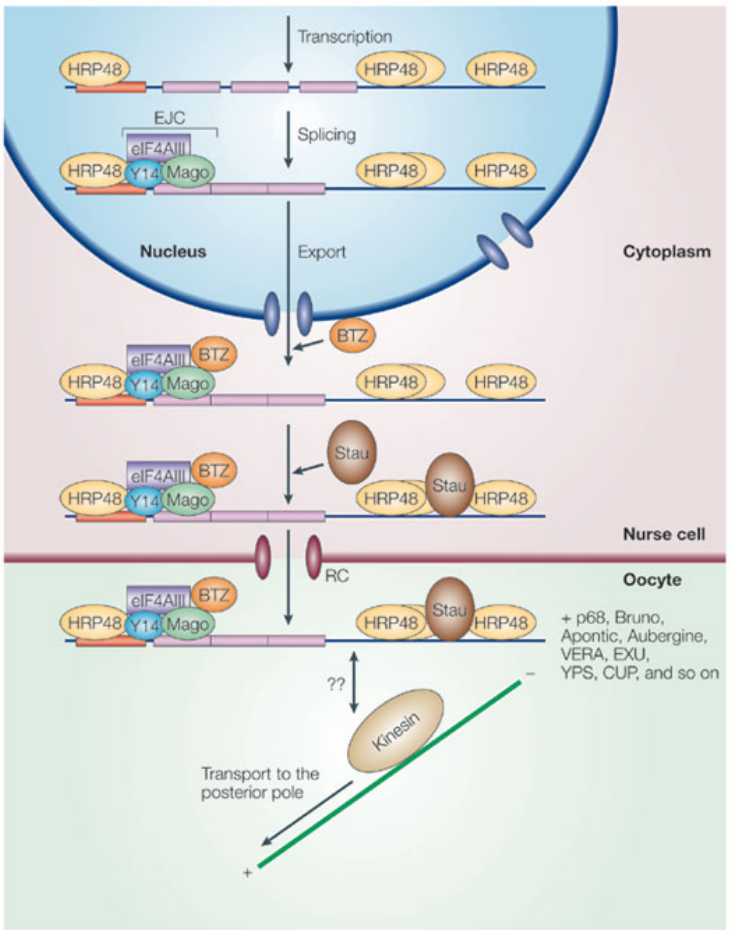

Figure 1.12: Dynamics of *oskar* mRNA regulating factors from the nucleus to the posterior pole of the oocyte
Hrp48 probably binds to *oskar* co-transcriptionally. Its association, as well as the splicing of *oskar* mRNA and the binding of EJC components is essential for *oskar* localization. Barentsz recognizes the complex by its interaction with eIF4AIII, as it is exported into the cytoplasm of the nurse cells. Staufen would then be recruited. The *oskar* particle then moves from the nurse cells to the oocyte, where it presumably associates with Kinesin to be transported along MTs to the posterior pole of the oocyte. Additional proteins associate with *oskar* mRNA in the oocyte, for example Bruno, required for translational repression during *oskar* transport to the posterior pole. EXU: Exuperantia, Stau: Staufen, YPS: Ypsilon schachtel, Mago: Mago nashi. [Adapted from Johnston, 2005]

[Gunkel et al., 1998, Yano et al., 2004], as well as in transport (Figure 1.12) [Huynh et al., 2004]. Squid, a well described hnRNP essential for *gurken* mRNA localization [Kelley, 1993, Norvell et al., 1999], also binds the *oskar* 3' UTR and is necessary for localization of *oskar* mRNA [Norvell et al., 2005]. hnRNPs therefore seem to have an important role in *oskar* mRNA localization.

More factors have been described to bind to *oskar* mRNA and/or to be essential for its localization. One of the most challenging questions that still remains, however, is how the specificity for the *oskar* transcript is achieved, when most of the factors involved are general RNA binding proteins. A likely explanation for this is the power of combining both specific and general *trans*-acting factors, which orchestrate the different steps in localization. For example, the EJC component Y14, which is required for *oskar* mRNA targeting, is dispensable for *bicoid* and *gurken* mRNA localization [Hachet and Ephrussi, 2001]. It is also probable that the composition of the *oskar* RNP is very dynamic during targeting to, anchoring and finally translation at the posterior pole. Barentsz, for example, only associates with *oskar* mRNA during transport to the posterior pole, but disappears again at stage 10, while *oskar* mRNA remains anchored at the cortex [van Eeden et al., 2001].

1.5 Aim of thesis

Players involved in targeting of *oskar* mRNA have been identified by genetic or biochemical analysis. Several colocalize with the transcript at the posterior pole. The aim of my thesis was to gain further insight into *oskar* mRNA regulation by identifying and characterizing novel components involved in this process through their co-localization with *oskar* mRNA. To this end, in collaboration with members of the lab, I performed a pilot screen where localization of GFP fusions at the posterior pole of the oocyte was scored, using a protein trap approach. Several lines displaying an enriched GFP signal at the posterior pole of the oocyte were identified (Chapter 3.1). In parallel, I have been working on an independent line identified in

a similar screen performed previously. The protein trapped by this line is encoded by a novel gene, *CG32423*, that has not been described so far. I therefore focused my project on the characterization of this gene, which I named *lupli* (Chapters 3.2 to 3.6).

Chapter 2

Material and Methods

2.1 GFP-based protein trap screen

2.1.1 Screening procedure

Plasmids were engineered in Stefan Sigrist's laboratory, Tübingen. GFP trap lines were generated in Christian Klämbt's laboratory, Münster. Ovaries were dissected in cold PBS, fixed in 4% formaldehyde in PBS for 10 min, washed three times for 10 minutes PBS with 0.1% Triton-X and mounted in mounting medium (2% n-propylgallate, 80% glycerol). Analysis was performed by confocal microscopy using a Leica SP2 microscope. Images were edited using Adobe Photoshop and uploaded in the Protein-trap database, together with a description of observed patterns and mapping data.

2.1.2 Inverse PCR

Inverse PCR (iPCR) is a method which allows the rapid amplification of DNA sequences flanking a region of known sequence [Ochman et al., 1988]. The method uses PCR, but with primers oriented in the opposite direction to usual. The template for the reverse primers is a restriction fragment that has been self-ligated to form a circle. iPCR is routinely used to amplify and identify the sequences flanking transposable element.

Fly genomic DNA was prepared using the DNAeasy kit (Quiagen). Then 15 µl of genomic DNA was used for the enzyme digestion in total volume of 25 µl for overnight at 37°C. The enzymes used for inverse PCR are 4-cutters restriction enzymes with recognition sites present once in the 5' and 3' end of the P element, such as Sau3AI or MspI. The ligation mixture was set up in a total volume of 200 µl (to promote self-ligation) and included T4 DNA ligase, ligase buffer, and the original 25 µl digest mixture. The reaction was then incubated at 16°C overnight. The next day, DNA was precipitated by adding 20 µl of 3M sodium acetate and two volumes of 100% ethanol. The mixture was left at -80°C for 30 minutes and centrifuged at 4°C for 30 minutes. The DNA pellet was washed twice with 70% ethanol and resuspended in 50 µl of water. The flanking region of the P element insertion was amplified with P element specific primers, designed to amplify out from the transposon vector sequence. The primers Pwht1 (P7, see Primer list, Section 2.3.5) and Plac1 (P5) were used to amplify the genomic fragment from the 5' end of PiggyBac and the primers Pry1 (P1) and Pry4 (P3) were used for the 3' end . The annealing temperature of the PCR reaction was set at 60°C for Pwht1/Plac1, and 55°C for Pry1/Pry4. The amplified products were sequenced using primers Sp1 (P6) for the 5' end fragments and Spep1 (P8) for the 3' end fragments. The sequence was then compared by BLAST search against the *Drosophila* genome to identify the insertion site.

2.2 *Drosophila* genetics

2.2.1 Fly husbandry

Flies were grown on standard corn meal molasses agar. All crosses were carried out at 25°C. Fly stocks were stored at 18°C and flipped once a month.

Fly food recipe: 12 g agar, 18 g dry yeast, 10 g soy flour, 22 g turnip syrup, 80 g malt extract, 80 g corn powder, 6.25 ml propionic acid, and 2.4 g methyl 4-hydroxybenzoate (Nipagin) are mixed with one liter water.

2.2.2 Stocks

(see Figure 2.1)

2.2.3 Ectopic expression using the UAS/GAL4 system

In *Drosophila*, a gene of interest can be expressed in a temporally and spatially regulated manner by using the GAL4/UAS system [Brand and Perrimon, 1993]. This system uses the yeast transcription activator GAL4, and its target, the upstream activation sequence (UAS). When GAL4 binds to UAS, it activates the transcription of the gene downstream of UAS (Figure 2.2). GAL4 can be expressed in many different patterns under the control of various *Drosophila* promoter sequences. In order to express a target gene with the pattern of a specific promoter, transgenic flies carrying the GAL4 driver under the control of a specific promoter are crossed to transgenic flies carrying UAS followed by the target gene. To drive expression in the *Drosophila* germline, a specific UAS-containing vector (UASp) is used [Rorth, 1998].

2.2.4 Generation of germ line clones using the FLP-FRT and FLP-DFS systems

In order to obtain a group of clonal cells that are homozygous mutant for a given allele, the FLP-FRT (flippase recombinase/ flippase recognition target) system was introduced into fly genetics [Golic, 1991]. The mutant allele is recombined onto a suitable FRT chromosome [Xu and Rubin, 1993] and crossed to flies carrying a heat-shock induced flippase (hs-FLP) and marker (usually GFP) on the matching FRT chromosome. To induce mitotic clones in the germ line or ovarian follicular cells, young larvae at 48-72 hours after eggs lying are heat-shocked at 37°C for 1 hour. Following heat shock, the FLP induces recombination of homologous chromosomes at the FRT sites. The recombination event results in two daughter cells: one homozygous for the GFP transgene carrying chromosome; the other homozygous for

Genotype	Source	Description
w^{1118}		reference stock used as wild type
y w; P{70FLP}11 P{70I-SceI}2B *noc*^{Sco}/CyO, *S2*	Bloomington Stock 6934	FLP and I-SceI for hom. recomb.
Df(3L)ED210	DrosDel	deficiency covering *lupli* locus
P{RS3}CB-5722-3	DrosDel	*lupli* P element allele
P{RS5}5-HA-1578	DrosDel	*lupli* P element allele
P64C9	Hanne Varmark/Shoko Yoshida	Lupli:GFP protein trap line
pCOG-GAL4VP16	Rørth, 1998	germline driver
w; grk^{2E12} *b*/CyO	Neuman-Silberberg and Schüpbach, 1993	
grk^{2B6} *b cn slbo*/CyO	Neuman-Silberberg and Schüpbach, 1993	
w;st osk^{54} *ry ss*/TM3 Sb	Lehmann and Nüsslein-Volhard, 1986	
w;osk^{84} *st e*/TM3 Sb Ser	Lehmann and Nüsslein-Volhard, 1986	
w; UASp::*Lupli-RA-HA*/Cyo		
w; UASp::*Lupli-RC-HA*/Cyo		
yw;KZ32;;*Ly*/TM3 Sb	Clark, 1994	kinesin-LacZ fusion
lupli$^{\Delta C}$*/TM3 Ser*		
w;;lupli$^{\Delta C}$FRT80B/TM3 Sb Ser		
y w hsFLP *lacZ;;ovoD* FRT80B/TM3 Sb Ser	Hsin-Ho Sung	
w hsFLP;;ubi-GFP FRT80B	Bloomington Stock 1620	

Figure 2.1: Fly stocks used

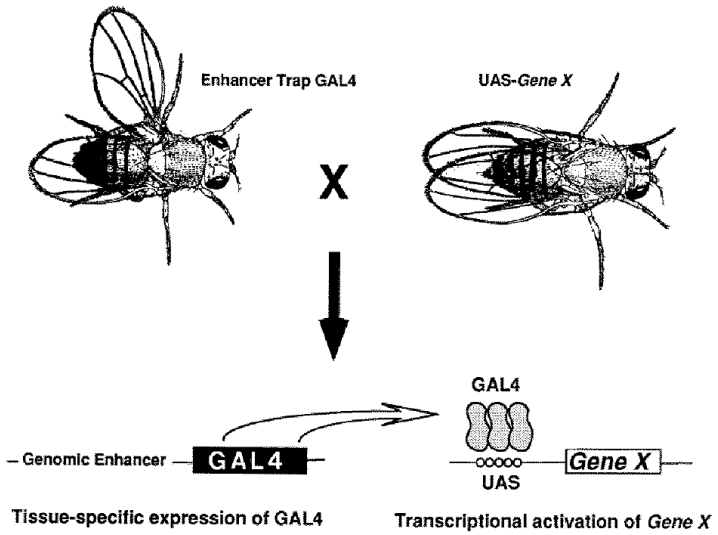

Figure 2.2: UAS/GAL4 system
A fly line expressing GAL4 (a transcriptional activator protein) is crossed to a line carrying the UAS element upstream of gene X. In the progeny, GAL4 is expressed in the tissue of interest, binds to the UAS element and activates transcription of gene X specifically in that tissue. [Adapted from Brand and Perrimon, 1993]

the mutant allele. Subsequently, the two daughter cells will give rise to two clonal groups of cells: a wild type clone with a higher level of GFP and a mutant clone lacking GFP expression. So, homozygous mutant cells are marked by the absence of GFP in a background of either homozygous wild type, GFP-expressing cells (the twin clone) or heterozygous, GFP-expressing (no recombination event) cells.

The FLP-DFS system is similar to the FLP-FRT system. However, instead of using GFP as a marker, the dominant female sterile (DFS) transgene, ovoD1 is used (Figure) [Chou et al., 1993]. In ovoD1 ovaries, oogenesis stops at early stages, but does not affect adult viability. Therefore, germline cells homozygous for the mutant allele can easily be selected, as they can proceed through oogenesis, provided that this process is not affected by the mutant allele.

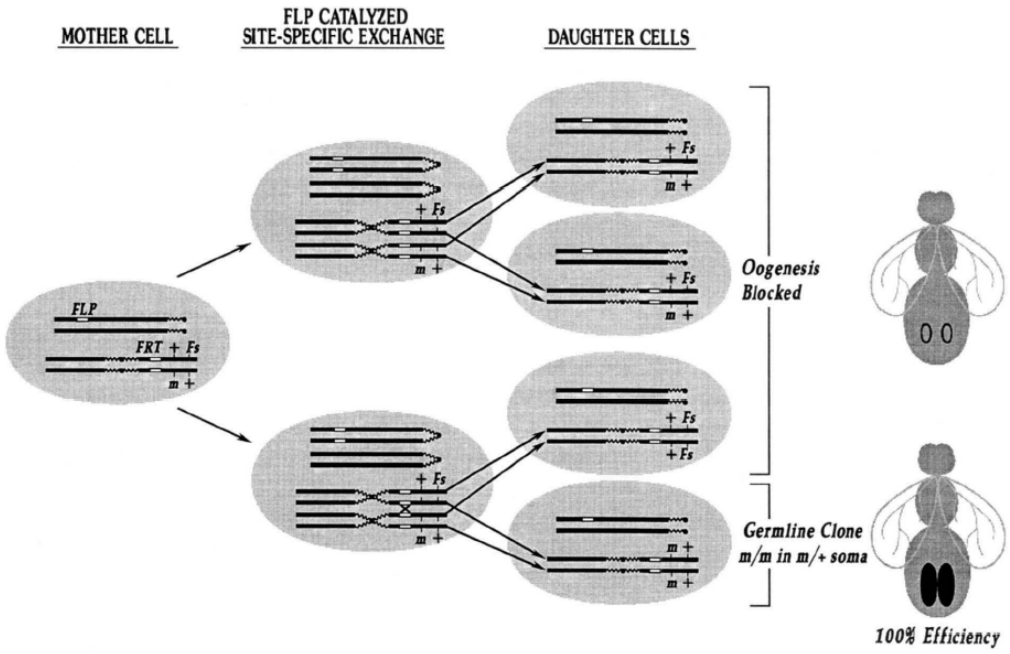

FIGURE 1.—The autosomal FLP-DFS technique. FLP-recombinase induced site-specific exchange. A chromosomal exchange that occurs in the euchromatin of a fly of genotype *Flp/Flp/+*; *FS + FRT/+ m FRT* is shown. The *X*-linked *hsp70-FLP* can provide sufficient recombinase activity following heat induction to catalyze site-specific chromosomal exchange at the positions of the *FRT* sequences. *FLP*-catalyzed recombination can result in the recovery of 100% of females with *m/m* GLCs. Atrophic ovaries are shown as empty ovals and developed ovaries as black ovals. FLP-recombinase target sequences (FRT); FS, dominant female sterile; m, recessive zygotic lethal mutation; FLP, hsp70-Flp.

Figure 2.3: The FLP-DFS system
[Original figure from Chou and Perrimon, 1996]

2.3 Molecular Biology

2.3.1 Single-fly PCR

One fly was squashed in 50 µl SB buffer (10 µM Tris-Cl, 1 µM EDTA, 25 µM NaCl) with 1 µl ProteinaseK (10 mg/ml). The solution was incubated for 1 hour at 37°C. The solution was then incubated at 95°C for 2 minutes to inactive the proteinase K. 1 µl solution was used per PCR reaction.

The PCR reaction was performed in a final volume of 20 µl and contained 2 µl of extracted genomic DNA as amplification template, forward and reverse primers (200 pM) and REDTaq PCR reaction mix (Sigma, cat. no. R2523). The PCR reaction was running on Thermal Cycler (PTC-200, MJ research) according to the following program: (1) 94°C for 10 minutes, (2) 94°C for 1 minute, (3) 59°C for 1 minute (depends on the Tm values of primers), (4) 72°C 1 minute (depends on the length of the product), (5) repeat step (2)-(4) for 34 times, (6) 72°C 10 min, (7) end

at 4°C. The amplified products were separated by electrophoresis on 1% agarose gel and visualized by ethidium bromide.

2.3.2 RNA isolation

5-10 adult ovaries were dissected and put into 1.5 ml eppendorf tube on ice. They where then dissociated by pipetting up and down with 200 µl of TRIzol (Invitrogen) until no large pieces could be seen. 800 µl of TRIzol was added and the lysate was kept at room temperature for 5 minutes. 200 µl of chloroform was added and samples were vortexed for 15 seconds. The samples were incubated at room temperature for 15 minutes before centrifugation at 14000 rpm at 4°C for 15 minutes. The aqueous phase (top or non-pink layer) was transferred into a new tube and 500 µl of isopropanol was added to precipitate the RNA. Samples were incubated at room temperature for 10 minutes, and then centrifuged for 15 minutes at 4°C. The pellet was washed with 75% ethanol (in RNase-free water) and dried at room temperature for 15 minutes. The pellet was then resuspended in 50 µl of RNase-free water. Samples were heated to 60°C in order to dissolve the RNA if necessary. Samples were stored at -80°C.

For pupal RNA isolation, entire pupae were directly dissociated by pipetting in TRIzol, and then proceeded like for ovarian RNA isolation.

2.3.3 cDNA synthesis and RT-PCR

cDNA synthesis was performed using the ThermoScript RT-PCR System (Invitrogen, cat. no. 11146-024), following the manufacturer's instructions. 5 µg of ovarian/pupal RNA were used. cDNA was synthesized using oligo(dT) primers for 1 hour at 50°C.

RT-PCR was performed using an adapted single-fly PCR protocol (see Section 2.3.1).

Transcripts were amplified using these primers (for sequences see Primers list,

Section 2.3.5): *lupli*-RA: P62/P68, *lupli*-RB: P64/P68, *lupli*-RC: P66/P67, *lupli*-RD: P65/P68

2.3.4 Cloning UASp-*lupli*-HA

Coding regions of long *lupli* (RA) and short *lupli* (RC) were amplified by PCR, using the follwing primers and ESTs as templates: RA, EST LD400280 (primers P69/P70), RC, EST RH63980. The amplified 1.7 kb (RA), 1.1 kb (RC) fragments were cloned into pENTR/D-TOPO, using the Gateway System (Invitrogen). Constructs were checked by sequencing. The *lupli* coding regions were cloned by recombination (Gateway Technology, Invitrogen) from the pENTRY constructs into the UASp-based destination vector pPWH (The Drosophila Gateway Vector Collection[1]) [Rorth, 1998]. pPWH adds 3 HA-tags at the C-terminus of the insert. These constructs were used to generate transgenic stocks by germline-mediated transformation in the w^{1118} background.

2.3.5 Primer list

(see Figure 2.4)

2.4 *lupli*$^{\Delta C}$ generation

lupli$^{\Delta C}$ was generated using the ends-out homologous recombination system [Gong and Golic, 2003]. To replace both RRMs of *lupli*, I designed primers to amplify the flanking sequences, R and L, corresponding to genomic regions +10,648 to +14,520 (primers P55 and P52, see Primer list) and +21,226 to +25,205 (primers P53 and P54) relative to the transcription start site of the short *lupli* (RC) transcript (Figure 2.5). The two flanking sequence, or homologous arms, were cloned into the pW25 vector [Gong and Golic, 2004] and used to generate transgenic (donor) flies, carrying w^+ as a marker.

[1]http://www.ciwemb.edu/labs/murphy/Gateway

No.	Name	Restriction sites	Sequence
P1	Pry1		CCTTAGCATGTCCGTGGGGTTTGAAT
P3	Pry4		CAATCATATCGCTGTCTCACTCA
P5	Plac1		CACCCAAGGCTCTGCTCCCACAAT
P6	Sp1		ACACAACCTTTCCTCTCAACAA
P7	Pwht1		GTAACGCTAATCACTCCGAACAGGTCACA
P8	Spep1		GACACTCAGAATACTATTC
P52	k.o.N-ter_R	KpnI(GGTACC)	ggtaccGCCCTGTTGGTTCTGATTCT
P53	k.o.C-ter_F	AscI (GGCGCGCC)	ggcgcgccCTTCAAGACGCCCGATCC
P54	k.o.C-ter_R	BsiWI(CGTACG)	cgtacgCTGTGCCAGTTGTTGTTGCT
P55	k.o.N-ter_aF	NotI(GCGGCCGC)	gcggccgcAATCCGCTCAGGCAATACAC
P62	RA_F		TCGGCTGCGCAAACTTATATT
P63	RA_R		GGCGCCGTATAGCGGTAG
P64	RB_F		CACACACAAAACCCAGACAC
P65	RD_F		CAAACCTGCTCACCATTAGC
P66	RC_F		CTCCCGTCGTTTTGAGATCA
P67	RC_R		CAGACCGCGAATGTAGAGAT
P68	RA_R2		GGGTAGAGCGCCCTTGAGT
P69	RA_rescF		CACCATGCACCCACGATACAGC
P70	RA_rescR		TTTGGGAGCGGCTTGATG
P72	RC_rescF		CACCATGGGTCCCAACGGCACG
P78	pW25_F_wto3'flank		GCAAACACAATCACACAAATGTGC
P79	pW25_R_wto5'flank		AGTGAGAGAGCAATAGTACAGAGAGG
P81	check_5'flankB		TTTCCGTCTGCTAAAACAAAAGAAC
P82	check_3'flankA		TGCTCAGGAATGTTGTTTGTGGTGA
P84	k.o.5'_F		ACAAGAAGGAAGCTGCAACCCATT
P85	k.o.5'_R		ATTTTGGGGATGGCAGAACAATTT
P86	k.o.3'_F		CACCATCGAATCCAACAAACCAAT
P87	k.o.3'_R		AAGCCAACGCCTAAGCGAAAAATA
P117	RA_qRT_F		CGAAATTTCAATAATCACAAGTCAA
P163	Yelena's oligo 2		GGGAGCGGCTTGATGTGGATAC
P168	Yelena's short sense		CGAACACCAACACGAACATGG

Figure 2.4: Primers used in this study

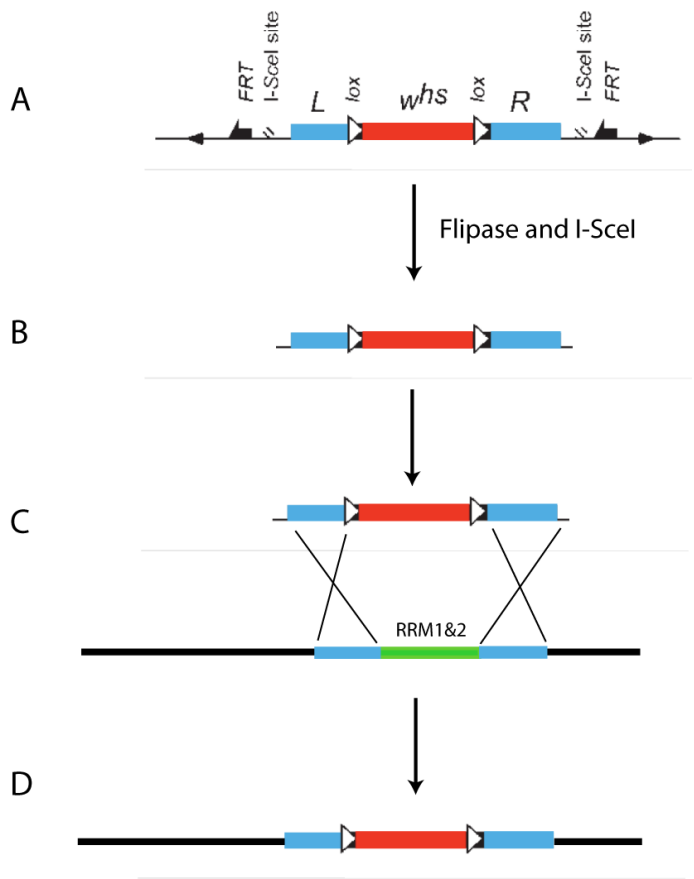

Figure 2.5: Homologous recombination using the ends-out system
The targeting scheme. (A) Homologous arms (L and R, approx. 4 kb each) flanking the *lupli* RRMs to be deleted, indicated as blue boxes, were cloned into the P-element vector, pW25, with the indicated features. (B) FLP and I-SceI generate the extra chromosomal linear donor. (C) Recombination between the homologous arms of the donor and the corresponding region in the genome (thick black bar) should generate the indicated deletions shown in (D). [Adapted from Gong and Golic, 2004]

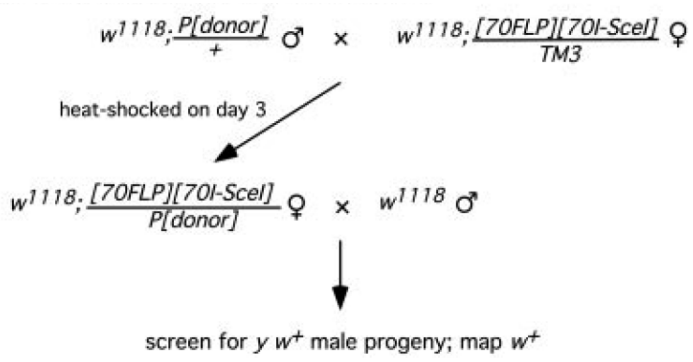

Figure 2.6: General crossing scheme for homologous recombination [Adapted from Gong and Golic, 2003]

A similar crossing scheme as developed by Gong and Golic was applied [Gong and Golic, 2003]. Donor males were crossed with virgins carrying the recombination transgenes (*P{70FLP}11 P{70I-SceI}2B noc*^{Sco}*/CyO*) which expresses the FLP site-specific recombinase and I-*SceI* endonuclease (Figures 2.5 and 2.6). I used three subsequent heat-shocks of 1 hour each at 37°C to induce expression of these enzymes. The FLP and I-*SceI* then linearize the donor molecule, allowing it to undergo homologous recombination with the target locus (Figures 2.5 B, C). These targeting events occur in the germ line. In the progeny, aprroximately 2000 virgin flies were selected for mosaic or white eyes, suggesting that the excision event was successful in these flies, and crossed to w^{1118} male flies carrying double balancer chromosomes. Red-eyed male flies were individually balanced to establish lines. Of 226 mutant alleles obtained, 51 had insertions on the third chromosome, as anticipated. A single line was obtained where excision of the RRMs was successful, as assessed by single-fly PCR on homozygous adult flies or pupae (primers P84/P85 for 5' region of RRMs, primers P86/P87 for 3' region). Genomic PCR on adult flies confirmed the insertion of the mini-white cassette in the correct locus by amplifying a genomic fragment spanning from inside the cassette beyond the flanking sequences (primers P78/P82 and P79/P81) using Phusion High-Fidelity DNA Polymerase (Finnzymes, cat. no. F530S, 100U)

2.5 Antibody generation

2.5.1 Cloning and purification of Lupli protein

The full-length coding sequence of the short Lupli isoform was amplified from a cDNA library generated from w^{1118} flies by RT-PCR , using primers P168 and P163, and cloned into and pGEX-5X-2 (GE Healthcare Life Sciences, cat. no. 27-4585-01). This construct was transformed into *E. coli* strain BL21(DE3) cells. The colony was cultured in 50 ml LB at 37°C overnight. 15 ml bacterial culture was used to inoculate 3 l of LB. The culture was incubated for about 2 hours at 37°C until the OD_{600} reached 0.4-0.5. IPTG was then added to a final concentration 250 μM to induce protein expression. The culture was grown at 30°C for another 2 hours. The bacteria were pelleted by centrifugating at 4000 g for 20 min at 4°C and then resuspended in 40 ml Lysis buffer (PBS, 1% Triton X-100). The lysate was frozen in liquid nitrogen and kept at -80°C. When required, the lysate was then thawed in water at RT to lyse bacteria. $MgCl_2$ (5 mM final concentration) and DNAase powder were added and incubated at RT until DNA was destroyed. The lysate was passed through a French press to lyse the cells. The lysate was centrifuged at 3000 g for 30 min (55000 rpm for TI-75 rotor). The supernatant was mixed with glutathione sepharose 4B beads (Amersham Biosciences) for 2 hours at 4°C on wheel. Before mixing, three lysis buffer washes were used to remove methanol from 2 ml of beads (bed volume). The beads were spun at 600 rpm for 5 min and the supernatant was removed. Beads were washed 3 times in 30 ml of wash buffer (PBS, 1% Triton X, 1 mM DTT) to remove non-specific binding proteins. The protein was then eluted in 2 ml of elution buffer (50 mM Tris-HCl, 150 mM NaCl, 20 mM glutathione, 1 mM DTT, pH 8.0) on wheel at 4°C for 30 min, and the protein concentration was mesured by Bradford assay.

2.5.2 Injection and antibody purification

GST-Lupli was injected into rats and rabbits with RIBI adjuvant (R-700 for rats, R-730 for rabbits, serum production by LAR EMBL service).

GST-Lupli was coupled to NHS-activated HiTrap column (GE Healthcare, cat. no. 17-0716-01) according to the manufacturer's instructions. For affinity purification, the Lupli serum was recirculated over the column overnight at 4°C . The column was washed with washing buffer (0.5 M NaCl, 0.1% Triton X100, Phosphate-buffered saline, PBS) followed by elution with 0.1M glycine pH 2.6 in Eppendorf tubes containing 10% (v/v) of 2M Tris pH 8. The antibody was dialysed overnight in PBS/50% glycerol and stored at -20°C.

2.6 Western blotting

Ovarian extracts were obtained by crushing 10 pairs of ovaries in 200 µl 2x Laemmli Buffer with a plastic pestle. Samples were boiled at 95°C for 5 minutes and 10 µl from each was loaded on SDS-polyacrylamide gel. Proteins were separated by elecrophoresis with a constant current of 15 mA per mini-gel. Proteins were transferred to PVDF membrane Imobilon-P (Millipore, cat. no. IPVH00010) using a constant current at 120 mA per mini-gel for 1 hour. The membrane was rinsed with water and incubated in Ponceau S solution for several minutes. The membrane was then washed with water several times and total protein levels were checked. The membrane was blocked with 5% milk/PBS or, if anti-Oskar was used, 5% milk/TTBS (25 mM Tris-Cl, pH7.5, 150 mM NaCl, 0.1% Tween 20) for 1 hour. Next, the membrane was incubated with primary antibody diluted in 5% milk/ PBT (PBS, Triton X 0. 1%) or or milk/TTBS (for anti-Oskar) for 2 hours at room temperature. Primary antibodies used in this study are rat anti-Lupli crude serum (1:1000 for 1st bleed, 1:3000 for 3rd bleed), rabbit anti-Kinesin heavy chain (1:10000, Cytoskeleton), rabbit anti-Oskar (1:2000), rabbit anti-Bruno (1:1000). The membrane was rinsed once, then washed for 15 minutes 3 times with PBT or TTBS

(anti-Oskar). Two alternative secondary antibody types were used, either conjugated to a fluorescent dye, or to HRP. For fluorescent secondary antibodies, the membrane was incubated with anti-rat AlexaFluor 680 (1:8000, Molecular Probes) or with anti-rabbit IRDye800 (1:2000, Rocklan) for 1 hour at room temperature, rinsed, washed 3 times for 15 minutes with PBT, and reveiled with Fluorescence Scanner (Licor). For HRP-conjugated secondary antibodies (GE Healthcare), the membrane was incubated with secondary antibodies, diluted in 5% milk/PBT or 5% milk/TTBS (anti-Oskar) for 1 hour at room temperature. The membrane was rinsed once and washed for 3 times 15 minutes with PBT. The membrane was rinsed with enhanced chemiluminescence reagent by mixing equal volumes of the Enhanced Luminol Reagent and the Oxidizing Reagent (NEL105, PerkinElmer). The membrane was exposed to Kodak X-OMAT MR Film for 10 seconds to 5 minutes.

2.6.1 Phosphatase assay

Wild type fly ovaries (10 ovaries per sample) were dissected in cold PBS and crushed with plastic pestles. Extracts were incubated with phosphatase mix (1 unit alkaline phosphatase from calf intestine, Roche Molecular Biochemicals, 200 units lambda protein phosphatase, New England Biolabs) and inhibitor mix (100 µM vanadate, 2 µM microcystine L-R) in 50 µl alkaline phosphatase buffer for 1 hour at 37°C. Samples were then boiled in 2x Lämmli buffer at 95°C and subjected to western blot.

2.7 RNA affinity pull-down

Wild type fly ovaries (40 ovaries per sample) were dissected in cold PBS. Ovaries were washed 2 times with 60 µl PBS, 1 time in hypotonic buffer (10 mM HEPES, pH 7.4 KCl, 10 mM potassium acetate, 1.5 mM magnesium acetate, 2.5 mM DTT), then one time in hypotonic buffer plus protease inhibitors (Complete, Roche). Supernatant was taken off and 1 volume of hypotonic buffer (including protease inhibitor) was

added to 1 volume of ovaries. Ovaries were smashed with a plastic pestle (30 strokes) and centrifuged for 10 min at 10'000 rpm (Eppendorf centrifuge) at 4°C. Supernatant was recovered and gycerol was added to ovarian extract to final concentration of 5% (3 µl was kept to load as "Input" on SDS-page polyacrylamide gel later). 40 µl of streptavidin beads per biotinylated RNA probe (kindly provided by Sonia Lopez de Quinto) were washed 3 times in 1 ml of MB-TEN^{100} buffer (10 mM Tris-HCl pH 8.0, 1 mM EDTA pH 8.0, 100 mM NaCl), resuspended in 50 µl MB-TEN^{100} buffer. Beads were homogenized by pipetting, then 200 µl MB-TEN^{100} and 2 µl RNA probes (conc. 0.5 µg/µl) were added. Samples were incubated on wheel for 20 min at room temperature. Beads were washed 2 times with MB-TEN^{1000} (10 mM Tris-HCl pH 8.0, 1 mM EDTA pH 8.0, 1 M NaCl), then washed 2 times in binding buffer (10 mM HEPES pH 7.9, 3 mM MgCl, 5 mM EDTA pH 8.0, 5% glycerol, 2 mM DTT, 0.5% IGEPAL, 40 mM/150 mM KCl, 3 µg/µl Heparin, 0.5 µg/µl yeast tRNA). 30 µl of ovarian extract were incubated with a mix containing 100 µl 2x concentrated binding buffer, 600 µg Heparin, 10 µg yeast tRNA, 55 µl H_2O, 60 units RNase inhibitor, and RNA-coated streptavidin beads, for 1 hour on wheel at 4°C. Supernatant was kept and beads were washed 5 times in binding buffer (without Heparin and without tRNA). Bound proteins were eluted by adding 2 times concentrated loading buffer (=Lämmli buffer) and incubated for 5 min at 90°C. The bound fraction was then loaded on SDS-page polyacrylamide gel, together with "input" fraction and "supernatant" fraction, and western blot was performed.

2.8 Immunostaining

2.8.1 Immunofluorescence staining of *Drosophila* egg chambers

Ovaries were dissected from females in cold PBS and fixed in 4% formaldehyde for 20 minutes. They were then washed 2 times for 10 minutes in PBST (PBS with 0.1% Triton-X). Ovaries were permeablized in PBS with 1% Triton-X for 1

to 4 hours, then blocked in blocking buffer (0.3% Triton-X, 0.5% BSA in PBS) for 1 hour. Ovaries were incubated overnight with primary antibody in blocking buffer. Primary antibodies were used in this study: rat anti-Staufen (1:2000), rabbit anti-Oskar (1:3000), mouse monoclonal anti-Orb 4HB (1:50, Developmental Studies Hybridoma Bank), mouse monoclonal anti-Orb 6H4 (1:50, Developmental Studies Hybridoma Bank), rabbit anti-Lupli (1:10000, affinity purified), rabbit anti-GFP (1:1000, Molecular Probes), mouse monoclonal anti-HA (1:1000, HA11, Berkeley Antibody Company), mouse monoclonal anti-β Galactosidase (1:2000, Promega). Ovaries were washed 2 times for 20 minutes in blocking buffer. Ovaries were then blocked in PBST with 10% normal goat serum (NGS) for 1 hour before incubation with Cy3 (1:750) or FITC (1:500) conjugated secondary antibodies and Alexa635 conjugated Phallodin (1:200, Molecular Probes) in PBST for 2 hours. Ovaries were washed repeatedly in PBST, and mounted in mounting medium (2% n-propylgallate, 80% glycerol). Analyses were performed using a Leica SP2 confocal microscope and images were edited using Adobe Photoshop CS.

2.8.2 Lupli immunostaining of egg chambers

Protocol used to stain for Lupli protein in wid type, $stau^{D3}$ and $grk^{2B6/2B12}$ mutant egg chambers. Ovaries were dissected in cold PBS, fixed in 4% paraformaldehyde in PBS for 30 minutes and washed 5 times for 5 min in PBST (PBS with 0.1% Triton-X). Ovaries were washed in 1:1 PBST/hybridization buffer (50% Formamide, 5X SSC, 0.1% Tween-20) for 5 minutes, then in hybridization buffer for 5 minutes. Ovaries were prehybridized in 1 ml hybridization buffer for at least 1.5 hours at 65°C Ovaries were hybridized 50 µl hybridization buffer at 65°C overnight. Ovaries were washed in hybridization buffer for 20 minutes at 65°C. They were then washed in 1:1 hybridization buffer/PBST 20 minutes at 65°C. Ovaries were washed for 4 times 20 minutes in PBT at 65°C, then in blocking buffer (0.3% Triton-X, 0.5% BSA in PBS) for 2 hours at room temperature. Ovaries were incubated with primary antibodies in blocking buffer at 4°C for 20 hours. Primary antibodies used: rabbit anti-Lupli

(1:10000, affinity purified), rat anti-Staufen (1:2000), mouse monoclonal anti-HA (1:1000, HA11, Berkeley Antibody Company). Ovaries were washed 2 times for 10 minutes in blocking buffer, then incubated in PBT with 10% NGS for 2 hours. Ovaries were incubated with secondary antibodies in PBT at 4°C overnight. Ovaries were then washed in PBT 3 times for 10 minutes, then mounted in mounting medium (2% n-propylgallate, 80% glycerol) and analyzed by confocal microscopy.

2.9 Software/Websites

- Jalview
- Graphpad Prism
- Ensembl http://www.ensembl.org/
- FlyBase http://flybase.bio.indiana.edu/
- BLAST http://www.ncbi.nlm.nih.gov/BLAST/
- InParanoid http://inparanoid.sbc.su.se/
- TreeFam http://www.treefam.org/
- ClustalW http://www.ebi.ac.uk/clustalw/index.htm
- DrosDel http://www.drosdel.org.uk/
- FlyAtlas http://flyatlas.org/
- ELM http://elm.eu.org/
- The Drosophila Gateway Collection http://www.ciwemb.edu/labs/murphy/Gateway%20vectors.html
- Drosophila Genomics Resource Center https://dgrc.cgb.indiana.edu/

Chapter 3

Results

3.1 GFP-based protein trap screen

Several of the factors, such as Barentsz, Staufen or Y14, involved in localization and translation of *oskar* mRNA co-localize with the transcript at the posterior pole of the oocyte. Most of the genes encoding these proteins have been identified in loss-of-function screens, which have proven to be extremely powerful. However, it is likely that other interesting factors were missed, due to problems such as redundancy. Therefore, in order to identify novel components involved in *oskar* mRNA control, we decided to search for proteins that localize to the posterior pole of the oocyte together with *oskar* mRNA.

3.1.1 Principle

We performed a protein trap screen by randomly generating GFP-fusion proteins and scoring for their localization to the posterior pole of the oocyte. To achieve this, we used a vector containing a GFP cassette flanked by splicing-acceptor and splicing-donor sites (Figure 3.1 A). This cassette was mobilized and randomly inserted into the *Drosophila* genome (see below). In the cases where the cassette was inserted into an intronic region flanked by two protein-coding exons, the artifical "GFP exon" was spliced normally. If the cassette inserted in the correct orientation, as well as

the correct reading frame of the gene, the transcript gave raise to a GFP-fusion protein. As this is only the case for one out of six insertions, production of a GFP-tagged protein was a rare event. Furthermore, detection of the fluorescent protein required stable and relatively high levels of expression to detect it. When this was the case, we analyzed its pattern of expression with the assumption that it mimiked the distribution of the mature, untagged protein.

3.1.2 Techniques

The generation of the GFP-trap lines was performed as follows. Transgenic flies were generated using a vector containing a GFP-cassette, as described in Figure 3.1 A, as well as the ends of a P transposable element [as described in Morin et al., 2001] to allow random insertion of the GFP-exon into the genome in presence of the transposase. A transgenic line that does not express any GFP was selected , and males of this line were then crossed to virgin females expressing the P transposase (P1 cross, Figure 3.1 B). Flies of the P1 progeny, so-called "jumpstarters", contained both the GFP-exon and the transposase, and therefore had the capacity to mobilize the cassette in their germline. Male jumpstarters were crossed to wild type virgins (F1 cross, Figure 3.1 B), and an automated embryo sorter was used to identify the rare GFP-expressing embyros, thus allowing selection for successful insertions in the progeny. The frequency of GFP^+embryos was about 1/5,000 ("transposition frequency"), which was presumably due to an insertion of the GFP-exon into an intron, giving rise to a GFP-fusion protein. The GFP^+ animals were then raised to adulthood and crossed individually to double-balancer fllies (F2 cross, Figure 3.1 B). The resulting GFP-trap lines were then screened for subcellular distribution of GFP in the ovary. Interesting lines were kept and stocks generated. In order to determine which gene was tagged with GFP in the individual lines, the insertion sites were mapped by inverse PCR (iPCR) and subsequent sequencing. All the resulting data, e.g. expression patterns, sequencing data, etc, were then entered into a web-based database (Figure 3.2).

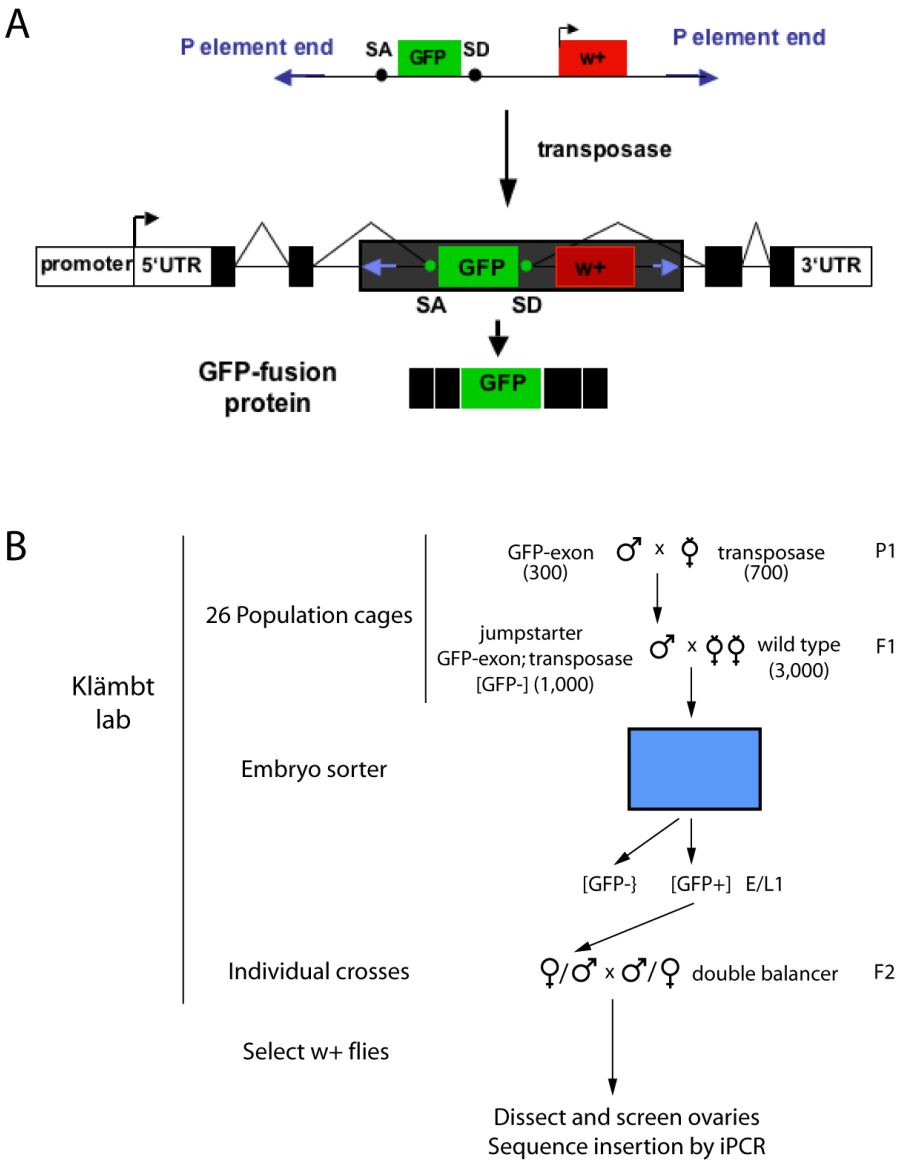

Figure 3.1: Principle of GFP-based protein trap screen
(A) The vector (top) contains a GFP-exon consisting of the GFP-coding region flanked by splice-acceptor (SA), and splice-donor (SD) sites, as well as the ends of a transposable element, the P element. The vector is mobilized within the *Drosophila* genome (middle) using the transposase. If inserted into an intron, the GFP-exon will get spliced and creates a GFP-fusion protein, if in frame and on the correct strand (bottom). (B) Generation of GFP-trap lines. In the P1 generation, transgenic lines containing the vector described in (A) were crossed against virgins containing the transposase to generate the jumpstarter males, which are GFP^-. These jumpstarter males were then crossed against wild type virgins (F1). The F1 progeny was screened for GFP using an embryo sorter. GFP^+ embryos (E) or L1 larvae (L1) were raised to adulthood and crossed to double balancer flies (F2). The w^+ flies were selected, as only these contain the vector (see above), and the ovaries were dissected and screened for GFP distribution. The F1 crosses were performed in 26 population cages. In brackets is indicated the approximate numbers of flies used per cage. No genotypes are indicated.

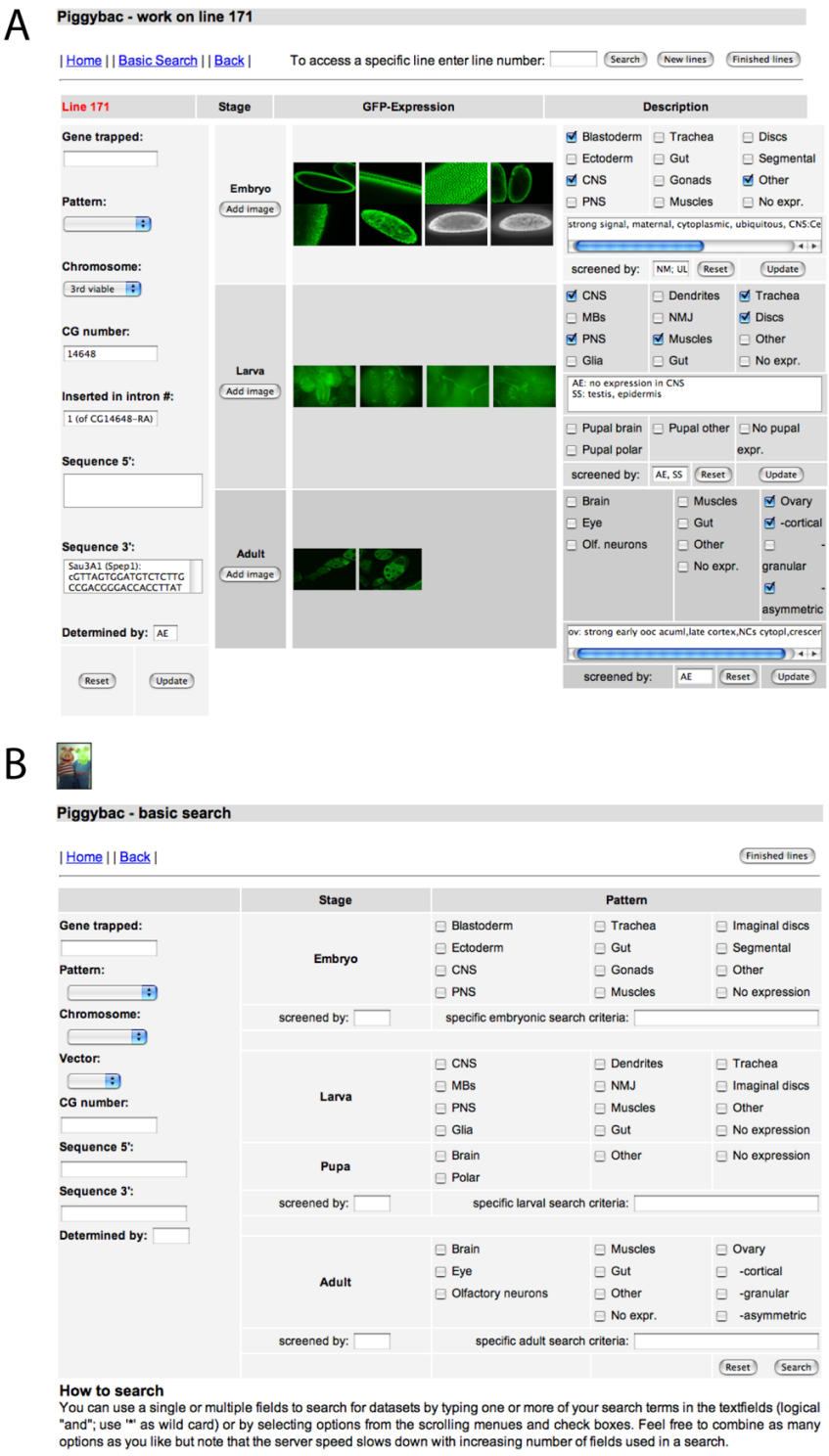

Figure 3.2: Layout of the Protein-trap database
(A) Information on one single line including genomic data (left), i.e. name of the gene, sequencing data, images (middle) and description (right) of the observed GFP expression pattern in the different tissus and developmental stages. (C) Worksheet into which all the data can be uploaded. (B) Search page that allows automatic search for specific expression profile.

3.1.3 The Protein-trap consortium

This project was performed within a consortium headed by Christian Klämbt, University of Münster, and comprised of ten labs [1]. The production of the GFP trap lines, including the generation of the original transgenic lines used to generate the jumpstarters, the crosses, the embryo sorting, and the establishment of the database, were performed in the Klämbt lab (Figure 3.1 B). The lines were then shipped to the different participating labs and screened for expression patterns in the tissue of interest, e.g. embryonic nervous system, larval wing imaginal discs, or neuromuscular junctions. The majority of the sequencing was performed in the Ephrussi lab.

The aim was to begin with a medium-scale "pilot" screen using a P element transposable element-based, to establish the screening procedure, to contribute to development and improvement of the database (Figure 3.2), and adjust the logistics necessary for such a multi-lab project.

3.1.4 Observed patterns

In collaboration with Anna Cyrklaff and Florence Besse, I screened a total of 347 lines.[2] Among these, 298 lines were GFP$^+$ in the ovary. As illustrated in Figure 3.3, we observed a variety of expression patterns. Insertion into 14-3-3ϵ in line 184, for example, showed a strong nuclear signal in the entire egg chamber, as well as a cortical signal in the oocyte (Figure 3.3 A). The signal in line 162 was exclusively extracellular (Figure 3.3 B), whereas line 90 showed a granular pattern in the follicular epithelium with GFP accumulating at the apical side of the cells (Figure 3.3 C, arrows). The GFP signal in line 324 was excluded from the nurse cells but was present in the cytoplasm of the oocyte, the follicular epithelium, and the border cells (Figure 3.3 D, arrow head). These examples illustrate how the different

[1] The participating labs were the groups of Suzanne Eaton, Dresden, Anne Ephrussi, Heidelberg, Christian Dahmann, Dresden, Marcos Gonzales-Gaitan, Dresden, Christian Klaembt, Muenster, Eli Knust, Duesseldorf, Arno Mueller, Duesseldorf, Andreas Wodarz, Duesseldorf, and Stephan Sigrist, Goettingen, Gaia Tavosanis, Munich.

[2] We have also screened for polarized GFP patterns in the Mushroom body neurons in the larval brains (not described here).

GFP-fusions can be expressed in distinct cell types and targeted to specific locations within one cell.

3.1.5 Several lines with posterior enrichment

To identify potential candidates involved in *oskar* mRNA regulation, we were specifically screening for lines that displayed a strong posterior crescent in stage 9 and stage 10 oocytes, where the *osk*-RNP normally localizes. In several lines we did observe an enriched signal at the oocyte posterior (Figure 3.3 E-I). In lines 171 and 309 the GFP fusion was strongly expressed in the cytoplasm of the nurse cells, and cortical in the oocyte, with a slight enrichment at the posterior pole (Figure 3.3 E, F). Line 185 showed a nuclear pattern with a dot at the posterior end, whereas in lines 263 and 303 a posterior crescent was observed (Figure 3.3 G-I). However, in none of the lines GFP localized exclusively to the posterior pole.

It was interesting that in two lines (line 263 and line 303), the proteins trapped have previously been shown to be localized to the posterior pole of the oocyte and to be involved in *oskar* regulation (Figure 3.3 H, I). *Ypsilon Schachtel (yps),* trapped in line 303, acts antagonistically to *orb* in *oskar* localization and translation and is part of an *osk*-Exu-Orb RNP complex [Wilhelm et al., 2000, Mansfield et al., 2002]. *rab11,* trapped in line 263, is required for *oskar* mRNA transport to the posterior pole [Dollar et al., 2002]. Furthermore, the GFP patterns in these two lines do indeed recapitulate the localization of the endogenous proteins in wild type ovaries, as revealed by immunostaining using antibodies directed against Yps and Rab11 [Dollar et al., 2002, Mansfield et al., 2002]. These results therefore validate our approach of a GFP-based protein trap screen to identify novel components involved in *oskar* mRNA regulation.

3.1.6 Refining posteriorly enriched lines

Even though that during this screen we originally identified 22 lines out of the 347 that displayed a posterior enrichment of GFP in the oocyte, several reasons led

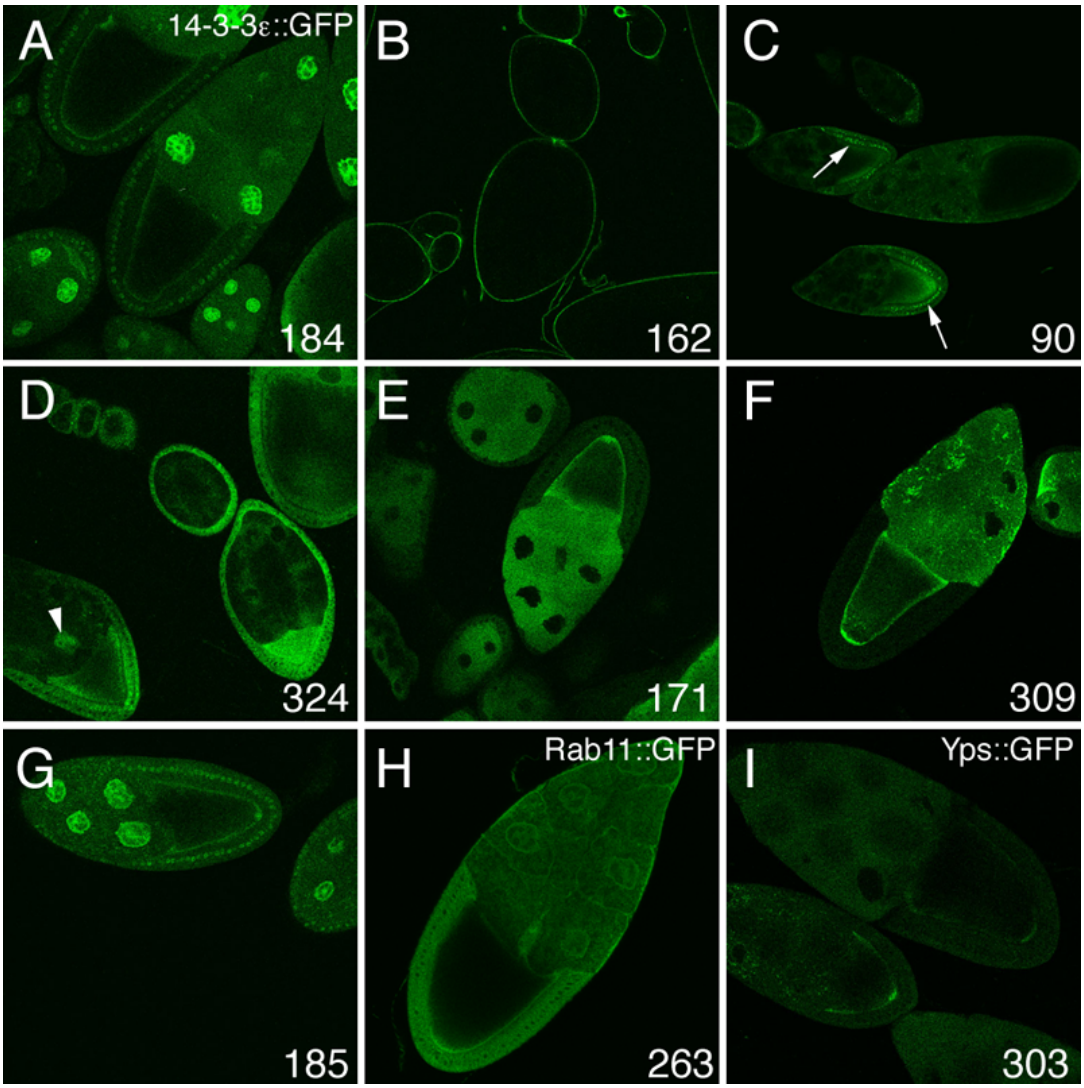

Figure 3.3: GFP trap expression patterns in the ovary
(A) GFP insertion into 14-3-3ϵ (line 184) displays a signal in all nuclei in the egg chamber and around the cortex of the oocyte and the nurse cells (low levels). (B) In line 162, GFP localizes extracellularly to the egg chambers. (C) In line 90, GFP is cytoplasmic in the oocyte, and localizes as granules to the apical side of the follicular epithelium (arrows). (D) Expression of GFP in line 324 is cytoplasmic in the oocyte, the follicular epithelium and the border cells (arrow head). (E-I) Lines with an enriched signal at the posterior of the oocyte. Line 171 (E) shows a cytoplasmic signal in the nurse cells and a cortical signal in the oocyte, similar to line 309 (F). Line 185 (G) shows a nuclear signal in all the cells, as well as a dot at the posterior. Insertion into *rab-11* (line 263, H) shows a cytoplasmic signal in the follicular cellls and border cells, and a posterior crescent in the oocyte. (I) Insertion into *yps* (line 303) shows a posterior crescent of GFP in the oocyte.

line	gene	posterior enrichment	RNA bdg/metab	chr. position
68	CG10686 (tral)	yes	yes	204861 (3L)
76	CG14648 (growl)	yes	no	229388 (3R)
77	5' of CG14709	maybe	no	7394934
112	? (outside of gene)	maybe	?	127560 (3L)
121	CG9884 (oaf)+CG31605 (bsg)	yes	no	?
171	CG14648 (growl)	yes	yes	229771 (3L)
202	? (outside of gene)	maybe	?	7575436 (X)
216	CG14648 (growl)	yes	no	229771 (3L)
217	CG14648 (growl)	yes	no	229487 (3L)
244	CG14648 (growl)	yes	no	229771 (3L)
279	?	maybe	?	?
303	CG5654 (yps)	yes	yes	12117260 (3L)
305	?	maybe	?	?
309	?	yes	?	?
413	?	yes	?	?
424	?	yes	?	?

Figure 3.4: Lines displaying a posterior enrichment of GFP
Eleven lines show a posterior GFP enrichment, whereas five of them are insertions into the same gene (*CG14648*, *growl*). Five lines do potentially show a posterior enrichment. The table also indicates for which gene an involment in RNA metabolism is predicted or has been demonstrated. Furthermore, the precise position of the insertion site is indicated (right row).

me to the conclusion not to pursue the analysis for any of them. First, thorough subsequent analysis reveiled that only 11 lines out of these 22 lines displayed a clear posterior GFP signal, whereas for five lines it was hard to dermine and eight lines had to be considered as false positives (Table 3.4). Second, sequencing analysis of the insertion site in line 112 and line 202 was not conclusive, as the insertion mapped to a region outside of any gene, therefore unlikely to be responsible for the GFP signal observed. The most likely explanation for this is that there was another GFP insertion, but which could not be mapped. In addition, five lines still need to be mapped. Fourth, the only lines which trapped proteins predicted to be involved in RNA metabolism, line 68 (*tral*), line 303 (*yps*) have already been described [see above, Mansfield et al., 2002, Wilhelm et al., 2000, 2005]. This was in contrast to an independent GFP-trap line that I already started characterizing, namely *P64C9*, and I therefore continued to work on that new line.

3.1.7 Conclusion

Taken together, the results of this screen provide a proof of principle for such an approach to identify interesting candidate genes based on their expression pattern.

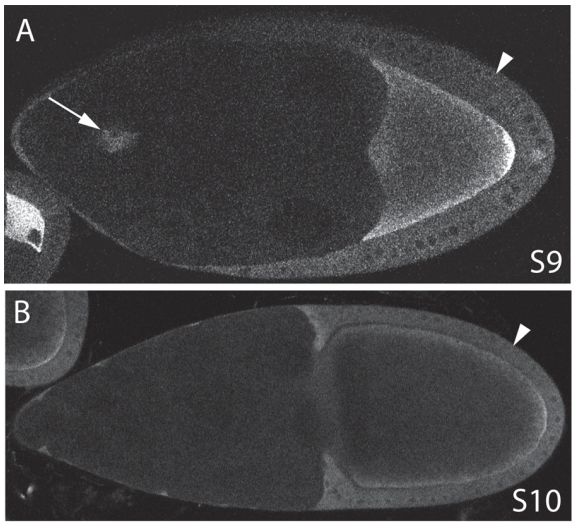

Figure 3.5: GFP expression pattern in *P64C9* egg chambers
Stage 9 (A) and stage 10 (B) *P64C9* egg chamber showing a cortical accumulation of GFP in the oocyte and a strong signal at the posterior pole, in the cytoplasm of the surrounding follicular epithelium (arrow head) and the migrating border cell (arrow).

Furthermore, they show that new genes can be discovered that have not been described previously. However, I abandoned this screen due to my stronger interest in another project, in which I tried to establish the *Drosophila* mushroom body (MB) as a model system to study neuronal RNA localization. Unfortunately, for technical restrictions and unsatisfactory results while working with the MB, I turned back to *oskar* localization in the ovary and focused the second half of my PhD time on one particularly interesting GFP-trap line found previously in the lab, line *P64C9*. This new project is described in the following chapters of this thesis.

3.2 Lupli, a novel RRM domain protein

3.2.1 GFP-trap line *P64C9* shows a posterior enrichment in the oocyte

A P element-based GFP trap screen had previously been performed in our lab to identify novel components of the *oskar* RNP complex.[3] In this screen, line 366,

[3]The lines were originally generated by Hanne Varmark (Tano Gonzalez' lab) and screened by Shoko Yoshida and Anne Cyrklaff for GFP-fusions accumulating at the posterior pole of the *Drosophila* oocyte.

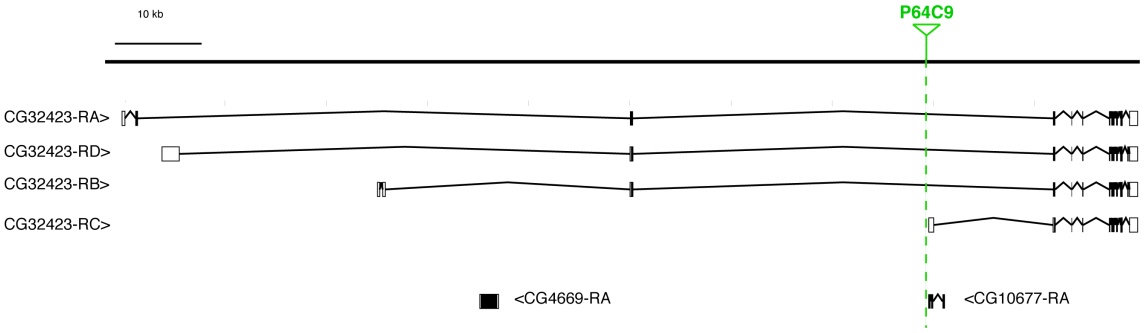

Figure 3.6: Insertion of GFP into *CG32423* in line *P64C9*
Genomic locus of *CG32423* (horizontal thick black bar) showing the location of the GFP exon in line *P64C9* (green triangle). The four predicted transcripts RA, RB, RC and RD of CG32423 are shown with the 5' on the left. The site of insertion predicts incorporation of the GFP exon into all but the shortest transcripts upon splicing. *CG4669* and *CG10677* are transcribed from the opposite strand (indicated by <). UTR sequence is denoted in white, protein-coding sequence in black. Transcripts as annotated by FlyBase Release 4.3.

which was originally identified by Shoko Yoshida and then named *P64C9*, showed a strong cytoplasmic GFP signal in the follicular epithelium, as well as in the migrating border cells. Line *P64C9* also displayed a cortical GFP signal in the oocyte, and interestingly, GFP enrichment at the posterior pole during stage 9 and stage 10 of oogenesis (Figure 3.5 on the previous page). This pattern coincides with the localization of *oskar* mRNA during these stages.

3.2.2 *P64C9* is a Lupli::GFP fusion

Mapping of the line *P64C9* by iPCR revealed an insertion of GFP into an intron of the gene *CG32423* (Figure 3.6). This gene was recently refered to as *alan shepard* in a conference abstract due to its apparent implication in gravitaxis [Bjorum, 2006]. However, the gene has so far not been described in any publication. I therefore decided to name this gene *lupli*[4].

The *lupli* locus spans approximately 120 kb on *Drosophila*. EST data and computational analysis predict four different transcripts of which two, the long (RA) and short (RC) isoforms, are present in the ovary, as shown by RT-PCR, using specific

[4]After several months of referring to it as "my gene" and "my protein", my lab mates simply called it "*Lu*kas' *p*rotein". The "-li" is the swiss-german ending for "small", which resulted in the gene name "*lupli*".

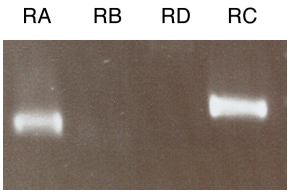

Figure 3.7: *lupli* transcripts in the ovary
RT-PCR was performed to specifically amplify the four predicted transcripts from ovarian RNA of wild type females (see 2.3.3 on page 41)

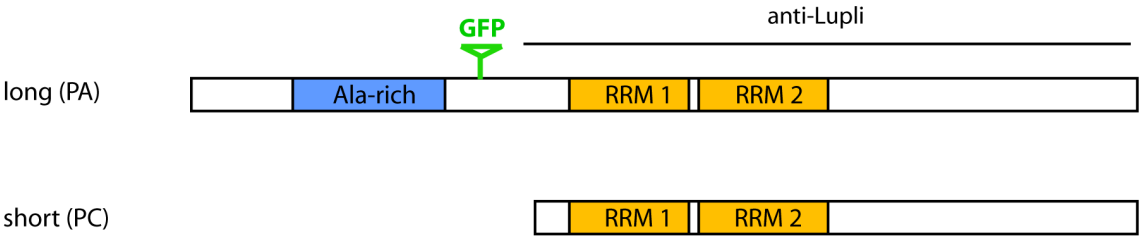

Figure 3.8: Lupli protein
Schematic representation of the two Lupli isoforms present in the ovary. The long (PA) and short (PC) isoforms, have an identical C-terminal that contains two RNA-recognition motifs (RRM 1 and RRM 2, orange boxes). The long isoform (PA) contains an alanine-rich, low complexity region in the N-terminal region (blue box). The site of GFP insertion in line *P64C9* (green triangle) is prediced to affect the long Lupli isoform only. The peptide expressed for antibody production is indicated (black bar).

primers (Figure 3.7). Proteins predicted from those transcripts contain two common RNA recognition motifs (RRM) in their common C-terminal. In addition, the N-terminal of the long isoform (PA) contains a low complexity, alanine-rich region, which is unlikely to contain any globular domains (Figure 3.8).

3.2.3 *lupli* is conserved during evolution

A search for possible *lupli* orthologs using Ensembl, FlyBase, and TreeFam, suggested that *lupli* is a conserved gene belonging to the family of RNA-binding motif, single-stranded interacting proteins (RBMS). In mammals, this family comprises three members - RBMS1, RBMS2 and RBMS3 (Figure 3.9 on the following page) - which are evolutionarily all equally distant related to *lupli*. The phylogenetic tree also indicates that there exists only a single *lupli* gene in flies, mosquitoes and worms, and that there are probably no paralogs in these organisms. The human RBMS1 and RBMS2 were first identified as *c-myc* gene single-strand binding

Figure 3.9: Lupli is the *Drosophila* ortholog of three mamalian RBMS proteins
A phylogenetic was generated to show the relationship between different Lupli orthologs across evolution. The positions, within the tree, of the human RBMS1, RBMS3 (NP_055298_HUMAN) and RBMS2 proteins are marked by blue boxes (from top to bottom, respectively). Lupli (PA, red box) is equally distantly related to the three human RBMS proteins. There are no closely related Lupli paralogs in *Drosophila*, nor in mosquito (green box) or *C. elegans* (purple box). This tree was automatically generated in TreeFam, using the long Lupli isoform (PA) as input.

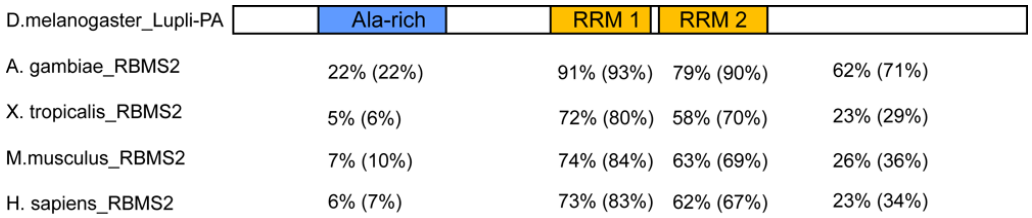

Figure 3.10: Sequence conservation of Lupli across evolution
Schematic representation of the individual parts of the long Lupli isoform (PA) and their degree of conservation compared to RBMS2 in other species. The percentages correspond to sequence identity and similarity (in brackets) compared to the long Lupli isoform (Lupli-PA).

protein (MSSP) [Negishi et al., 1994, Kanaoka and Nojima, 1994]. Both, RBMS1 and RBMS2, are single-stranded DNA-binding proteins that act in transcriptional regulation [Kanaoka and Nojima, 1994, Takai et al., 1994, Iida et al., 1997, Negishi et al., 1994]. RBMS3, in contrast, does not seem to be a transcription factor, but is thought to have a cytoplasmic role and has been demonstrated to bind A/U-rich stretches of RNA [Penkov et al., 2000].

3.2.4 RRM protein and function prediction

All the Lupli orthologs contain two RNA recognition motifs (RRM) that have been highly conserved during evolution (Figure 3.10). The C-terminus of Lupli protein is less well conserved, sharing 23% identity with the human RBMS2. The RRM domain is one of the most commonly found protein domains in eukaryotes. In the *Drosophila* genome, a search using Ensembl revealed that over 140 fly proteins contain one or several RRMs. Although the presence of an RRM is generally highly predictive of RNA binding activity, some RRM-containing proteins do not interact with RNA, but with single-stranded DNA (ssDNA), or even with other proteins. One such example is Y14, which binds via its RRMs to Mago [Maris et al., 2005, Fribourg et al., 2003].

The two RRM folds present in Lupli and its orthologs are composed of 75 and 90 amino acids, respectively (Figure 3.11). They both contain the two characteristic motifs RNP1 (consensus sequence [RK]-G-[FY]-[GA]-[FY]-[ILV]-X-[FY]) and RNP2

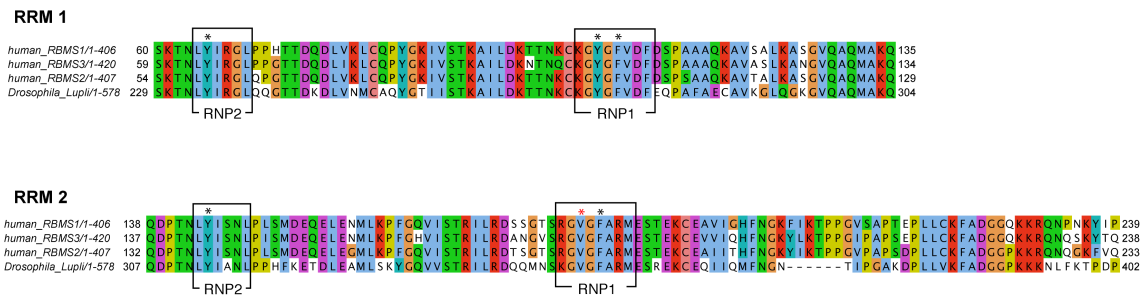

Figure 3.11: Conservation of RRM domains in Lupli and its human orthologs
Sequence alignment of the two RRM domains in human RBMS1, RBMS2, RBMS3 and *Drosophila* Lupli with the following Ensembl Peptide IDs: RBMS1 (ENSP00000294904), RBMS2 (ENSP00000262031), RBMS3 (ENSP00000373277), Lupli-PA (CG32423-PA). The conserved RNP 1 and RNP 2 are highlighted with a black frame [Maris et al., 2005, see also Material and Methods]. The aromatic residues important for primary RNA binding (black asterisk) and the conserved Valine (red asterisk), which does not fit the consensus sequence, but could still enable RNA binding, are marked. The alignment was generated with ClustalW [Thompson et al., 1994] and coloured using the ClustalX scheme in Jalview [Clamp et al., 2004]. Orange: glycine (G); gold: proline (P); blue: small and hydrophobic amino acids (A,V,L,I,M,F,W); green: hydroxyl and amine amino acids (S,T,N,Q); magenta: negatively charged amino acids (D,E); red: positively charged amino acids (R,K); dark blue: histidine (H) and tyrosine (Y).

([ILV]-[FY]-[ILV]-X-N-L) [Maris et al., 2005]. The three aromatic amino acids that contribute to primary RNA binding, namely RNP 1 positions 3 and 5 and RNP 2 position 2, are perfectly conserved between RRM domain 1 of the Lupli orthologs, as well as the RNP 2 of RRM domain 2 (Figure 3.11). The only exception is the residue at position 3 in RNP 1 of RRM domain 2, which, although conserved - is not an aromatic residue, but a valine (Figure 3.11). However, this does not exlude a possible RNA-binding activity, as has been shown for other proteins, such as Sex-lethal [Maris et al., 2005]. This strong conservation of the RRMs of Lupli and its three human orthologs points towards an importance in function (Figure 3.11).

In light of the published experimental data on RBMS proteins, this analysis emphasizes that one cannot distinguish between DNA- or RNA-binding based on the sequence of the two RNP motifs, as, in contrast to RBMS1 and RBMS2, RBMS3 is thought to mediate its function through binding to RNA [Penkov et al., 2000]. It suggests that Lupli might function in RNA regulation possibly through direct interaction with RNA. Together with the localization pattern of Lupli::GFP at the

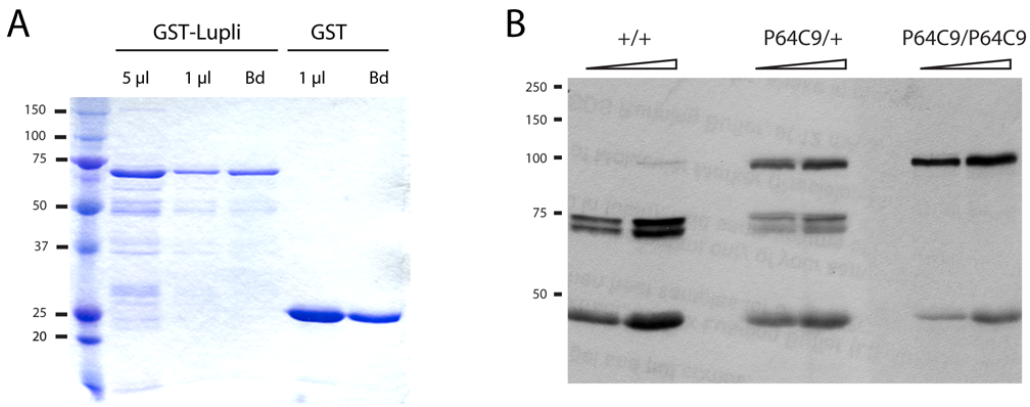

Figure 3.12: Generation and specificity of anti-Lupli antibody
(A) GST-Lupli (C-terminal region, left), predicted to be around 65 kD, was expressed, and different amounts of purified protein (5 μl and 1 μl) or sepharose beads (Bd) were loaded on a denaturing protein gel. GST alone was loaded as comparison (right) (see Materials and Methods 2.5 on page 46). Some remaining protein can be seen on the beads, indicating the elution was not complete. (B) western blot from ovarian extracts of wild type (+/+) females, or females bearing either one (*P64C9*/+), or two (*P64C9*/*P64C9*) copies of Lupli::GFP, were probed with anti-Lupli antibody.

posterior pole of the oocyte, Lupli seemed an exciting new protein to investigate for potential role in *oskar* RNA regulation.

3.3 Lupli distribution during oogenesis

3.3.1 Generation of anti-Lupli antibody

Due to the site of insertion of the GFP-cassette, the GFP pattern observed in line *P64C9* should reflect the distribution of the endogenous Lupli (see Figures 3.6 and 3.8). But as the GFP tag could affect localization of the endogenous protein, I decided to produce an antibody against the C-terminus shared by all isoforms (Figure 3.8). This region was cloned, expressed and purified as a GST-fusion (see Figure 3.8). The serum of rats and rabbits injected with this antigen was then tested for immunoreactivity against Lupli on ovarian extracts (3.12 B). The predicted size of the short Lupli isoform is 40,0 kDa and for the long isoform 60,7 kDa. On western blots of wild type ovarian extracts, one band at 45 kDa and a doublet at around 70 kDa can be observed (see 3.12). Such a difference between observed and calculated size was also seen with MSSP-1, the human RBMS1, and might be due to

the amino acid composition or postranslational modifications of the protein [Negishi et al., 1994]. When extracts form *P64C9* flies were used, the upper doublet shifted to about 100 kDa, which can be attributed to the addition of GFP with a molecular weight of 23 kDa. The mobility of the lower band remains unchanged in all three genotypes, and most likely corresponds to the short Lupli isoform (see below). These data suggest that the newly generated antibody is specific for Lupli, confirming the hypothesis that the insertion of the GFP cassette in *P64C9* tags the long isoform exclusively.

3.3.2 Long Lupli is a phosphoprotein

Western blot analysis of wild type ovarian extract showed a doublet migrating at around 70 kDa (see Figure 3.12 B), suggesting a posttranslational modification of the long Lupli isoform (Figure 3.12 B). To test whether Lupli is phosphorylated, I incubated wild type extracts with phosphatase. As shown in figure 3.13, the top band disappeared when using the phosphatase alone, whereas it reappeared when phosphatase inhibitors were added. There also seems to be a faint third band in between, which might be due to a post-translational modification distinct from phosphorylation. These results suggests that the long Lupli isoform is a phosphoprotein and that it exists in both phosphorylated and non-phosphorylated states in the wild type ovary.

3.3.3 Lupli expression pattern during oogenesis

To test whether the observed pattern of Lupli::GFP in *P64C9* corresponded to the one of endogenous Lupli I performed immunostaining using the anti-Lupli antibody. In wild type ovaries Lupli is expressed in the cytoplasm both of germline cells and of somatic cells in the germarium, and accumulates in the oocyte early oogenesis (Figure 3.14) . During mid-oogenesis Lupli localizes to the cortex of the oocyte and, at stages 9 and 10A Lupli is enriched at the posterior pole (Figure 3.15). This pattern of expression is highly reminiscent of *oskar* mRNA (see Introduction 1.4) [Ephrussi

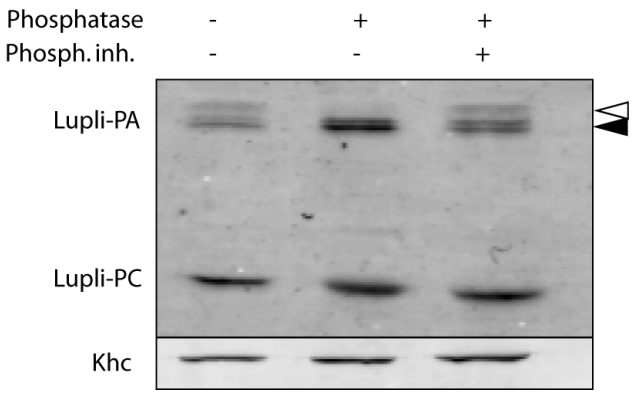

Figure 3.13: Long Lupli a phospho-protein
Western blot of wild type ovarian extract (left lane), after phosphatase treatment (middle), or after phosphatase treatment, in the presence of phosphatase inhibitors (right), probed with anti-Lupli antibody. Kinesin heavy-chain (Khc) was used as a loading control. The top band (white arrow head) of the long isoform triplet (PA) is likely to be due to phosphorylation, as it disappears upon phosphatase treatment The two lower bands (black arrow head) of the long isoform, as well as the single band of the small isoform (PC), do not change.

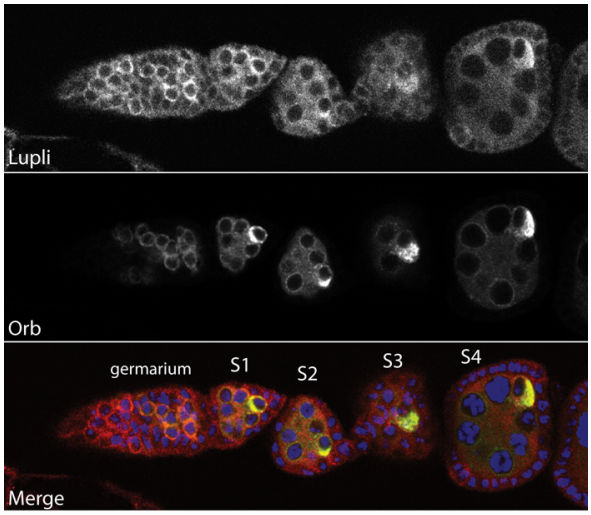

Figure 3.14: Lupli expression in the germarium and during early oogenesis
Wild type ovaries were stained for Lupli (red) and Orb (green), a germline and oocyte marker [Lantz et al., 1992, 1994]. Lupli is expressed very early in the germline and in the soma of the germarium, and accumulates in the oocyte at oogenesis progression.

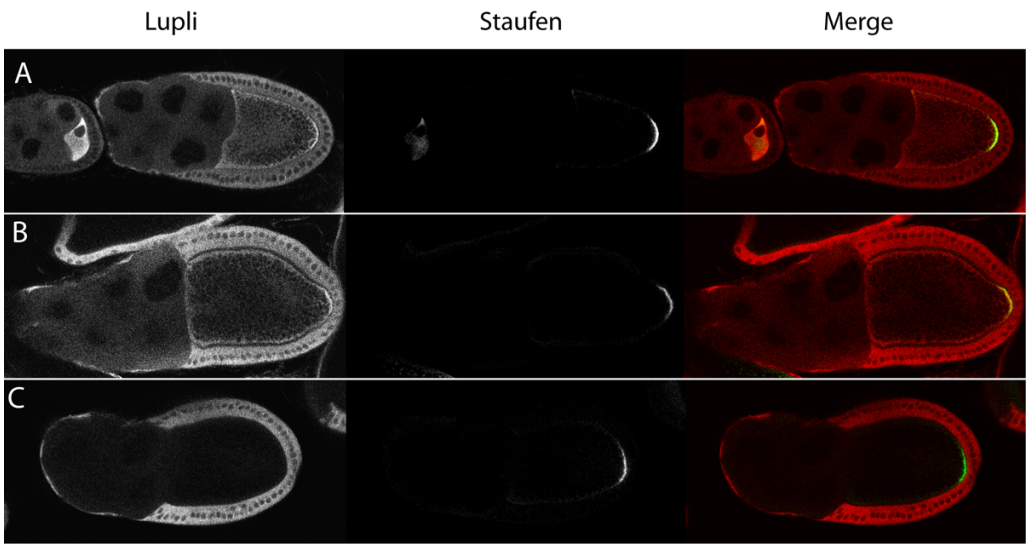

Figure 3.15: Endogenous Lupli localizes to the posterior of the oocyte together with *oskar* mRNA
Wild type (A,B) and, as a negative control, *lupli*$^{\Delta C}$ germline clone (C, see Materials and Methods 3.6.1 on page 74) ovaries were stained for Lupli (left) and Staufen (middle) proteins. (A-C) Lupli is expressed at low levels in the cytoplasm of the oocyte, the follicular epithelium, as well as of the nurse cells. Lupli is enriched and colocalizes with Staufen, a marker of the *osk*-RNP, at the posterior pole oocyte of stage 9 (A) and stage 10A (B) egg chambers. Confocal micrographs were taken with the same settings.

et al., 1991, Kim-Ha et al., 1991], and the Lupli signal indeed colocalizes with Staufen at the posterior pole of stage 9 and 10 egg chambers (Figure 3.15). During these stages, Lupli is also strongly expressed in the cytoplasm of the follicular epithelial cells, and to a weaker extent in the nurse cells (compare A and B to C in Figure 3.15). In general, the distribution of endogenous Lupli is very similar to that of Lupli::GFP in the protein trap line *P64C9* (Figure 3.5 on page 60), in which only the long Lupli isoform is tagged. The anti-Lupli antibody can not distinguish between the two isoforms, as it was raised against the common C-terminal region of the isoforms. To assess whether there is a difference in the expression pattern of the two isoforms, I expressed them individually, fused to an HA-tag. By immunostaining, I detected no difference in their expression patterns in the egg chamber, and both showed an enrichment at the posterior pole (Figure 3.16).

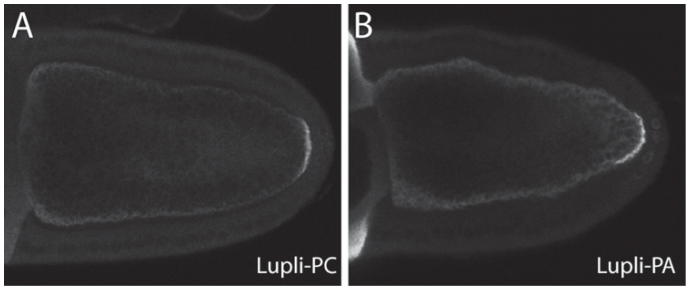

Figure 3.16: Distribution of Lupli isoforms in the oocyte
Stage 10 egg chambers, expressing either HA-tagged short (PC) or long (PA) Lupli under control of the pCog-GAL4 driver, were stained using an anti-HA antibody. Both Lupli isoforms are enriched at the posterior pole of the oocyte.

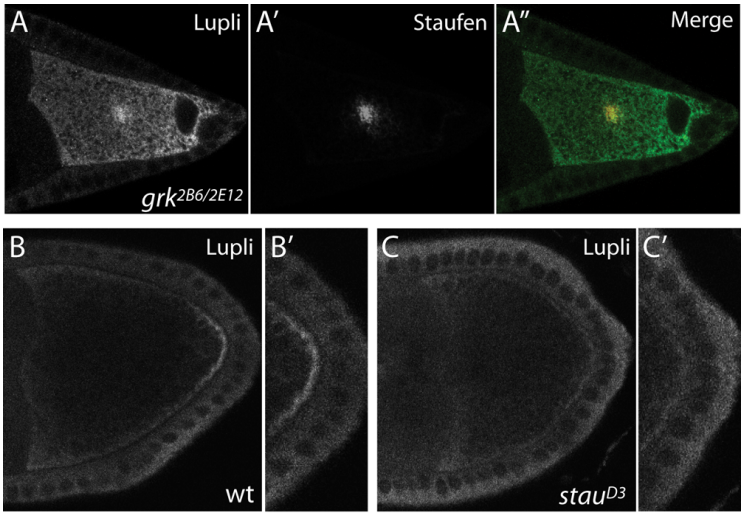

Figure 3.17: The posterior enrichment of Lupli depends on *oskar* mRNA
(A) In egg chambers of the strong *gurken* allelic combination $grk^{2B6/2E12}$, Lupli accumulates together with Staufen in the center of the oocyte. Wild type (B) and $stau^{D3}$ (C) stage 9 egg chambers were stained for Lupli. Lupli is enriched at the posterior pole of wild type oocytes (B,B'), whereas it is reduced in $stau^{D3}$ oocytes (C,C'). These are representative confocal micrographs taken with the same settings.

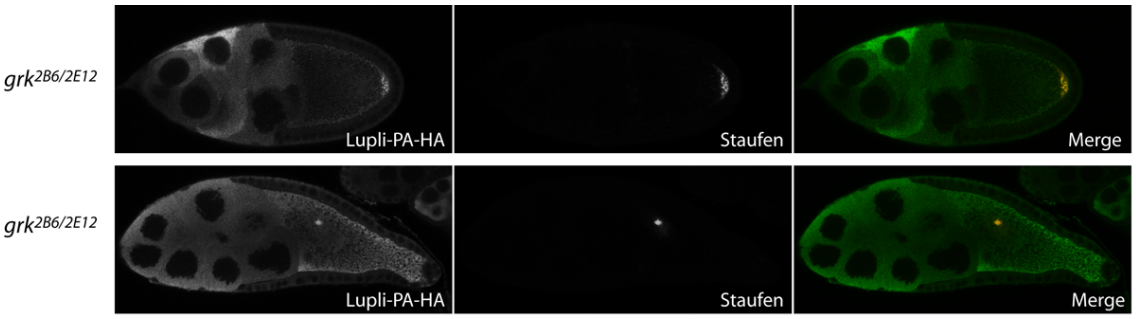

Figure 3.18: Colocalization of long Lupli-HA with Staufen in a *gurken* mutant oocytes
Long HA-tagged Lupli (PA) was overexpressed using a pCog-GAL4 driver, and stained for HA in control (top) and $grk^{2B6/2E12}$ (bottom) egg chambers. The tagged long Lupli isoform colocalizes with Staufen in the center of the oocyte in a *grk* mutant background.

3.4 Lupli is a novel component of the *oskar* RNP

Given that Lupli protein contains two RRMs and colocalizes with *oskar* mRNA at the posterior pole of the oocyte, I hypothesized that it might be part of the *oskar* RNP complex. To test if Lupli localization is dependent on *oskar* mRNA, I examined Lupli distribution in two mutant backgrounds, in which the posterior localization of *oskar* mRNA is perturbed. First, I examined Lupli distribution in a *gurken* (*grk*) mutant background, in which *oskar* mRNA, and its partner Staufen, are mislocalized to the center of the oocyte, due to mispolarization of the microtubule skeleton [Gonzalez-Reyes et al., 1995, Roth et al., 1995]. In this background, Lupli colocalizes together with Staufen in the middle of the oocyte (Figure 3.17). This is also true for the long Lupli isoform, when it is overexpressed in a *grk* mutant background (Figure 3.18). This suggests that Lupli travels with *oskar* RNP complex to the posterior. Second, in $staufen^{D3}$ mutant oocytes, in which *oskar* mRNA fails to localize to the posterior pole [Ephrussi et al., 1991, Johnston et al., 1991, Kim-Ha et al., 1991], Lupli is no longer enriched at the posterior at stage 9, (Figure 3.17 B). This suggests that Lupli distribution at the posterior pole of the oocyte might require the localization of *oskar* mRNA.

To test if Lupli localization at the posterior is indeed dependent on *oskar* mRNA, and not on Oskar protein, I examined Lupli localization in $osk^{54/84}$ mutant background. In this heteroallelic combination no Oskar protein produced. This does not

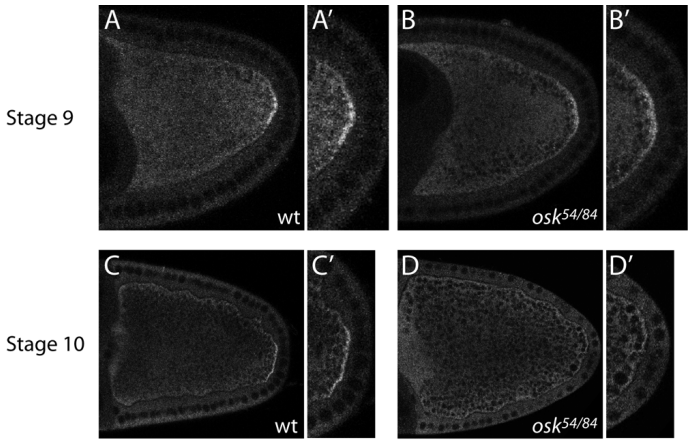

Figure 3.19: Posterior enrichment of Lupli does not depend on Oskar protein
Stage 9 wild type (A,C) and mutant (B,D) egg chambers were stained for Lupli. (A,A') Lupli is enriched at the posterior pole of wild type (A,A') and of *oskar* protein-null mutant (B,B') oocytes. (C-D) The Lupli enrichment is strongly reduced at the posterior of Stage 10 egg chambers.

affect the inital localization the *oskar* transcript, but its anchoring at the posterior pole [Lehmann and Nusslein-Volhard, 1991, 1986, Ephrussi et al., 1991, Kim-Ha et al., 1991, Rongo et al., 1995]. In $osk^{54/84}$ Lupli is enriched at the posterior pole of the oocytes at stage 9 as in wild type (Figure 3.19 A, B), but is reduced at stage 10 (Figure 3.19 C, D). Lupli colocalization with *osk* mRNA therefore does not depend on Oskar protein. Taken together, these results suggest that Lupli and *oskar* mRNA travel together to the posterior pole, strengthening the hypothesis that they might be part of the same localization complex in vivo.

3.5 Lupli associates with the *oskar* 3' UTR

The above results, as well as the prediction that Lupli might bind RNA through its RRMs, suggest an association of Lupli with *oskar* mRNA. To test if Lupli protein can bind *oskar* RNA, I performed affinity pull-down experiments. After incubation of different biotinylated fragments of *oskar* and control RNA with ovarian extracts, the RNAs were precipitated using streptavidin coated beads and the proteins associating with RNAs were examined by western blot (Figure 3.20 A). Under low salt conditions (40 mM KCl), both Lupli isoforms, as well as Bruno were copurified with the 3' UTR

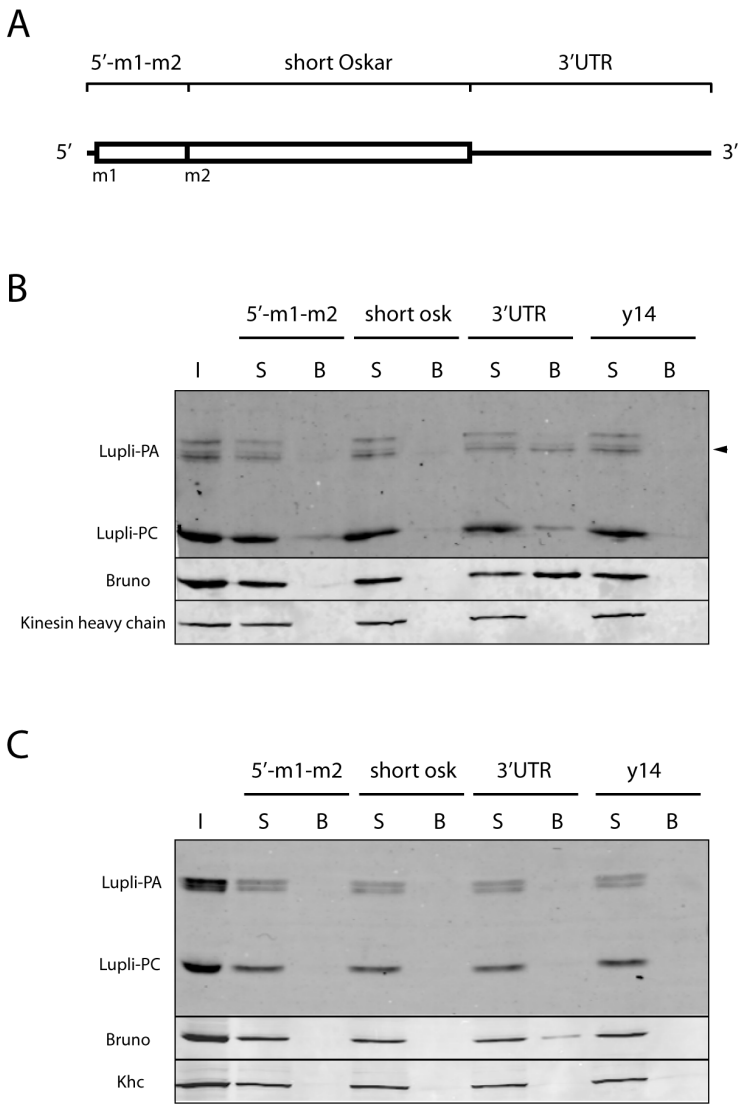

Figure 3.20: Lupli binds biotinylated *oskar* 3'UTR

(A) A diagram of the different regions of *oskar* mRNA used for the affinity RNA pull-down assay. Shown are the protein coding sequence (box), the untranslated regions (UTR, line), and the alternate start codons, m1 and m2, giving rise to Long, and Short Oskar, respectively. The region between m1 and m2 including the 5'UTR (5'-m1-m2), the coding region of Short Oskar, and the *oskar* 3'UTR were used as probes in the binding experiments shown below.

(B) Lupli copurifies with the *oskar* 3'UTR in affinity pull-down assays, when beads were washed 40 mM KCl. Biotinylated *osk* RNA probes were used to affinity-purify interacting proteins from wild type ovarian extracts, then washed, and the bound proteins were then revealed by western blot and probed for Lupli, Bruno (a protein that has been demonstrated to bind to the *oskar* 3'UTR [Kim-Ha et al., 1995]), and Kinesin heavy chain (Khc), used as loading control. The lanes show the supernatant (S) and bound fractions (B), as well as the input (left lane, I) of ovarian extract. The non-phosphorylated (arrow head) form of long (PA) and short (PC) Lupli copurify with *oskar* 3'UTR but not with other parts of the RNA, or the unrelated RNA *y14*. The faint bands of Lupli-PC and Bruno observed in the bound fraction of 5'-m1-m2 probably reflects leakage from a neighboring well, as they could not be reproduced.

(C) Lupli does not co-purify with the *oskar* 3'UTR when beads were washed when 150 mM KCl, in contrast to Bruno, which can still associate with *oskar* 3'UTR under these conditions.

of *oskar* mRNA. In constrast, they did not seem to associate with any other part of the *oskar* transcript, or to an unrelated mRNA (Figure 3.20 B). Interestingly, only the long non-phosphorylated Lupli isoform seems to associate with the 3' UTR (Figure 3.20 B). In the same assay, but under higher salt conditions (150 mM KCl), only Bruno could be detected to associate with the *oskar* 3'UTR (Figure 3.20 C), suggesting that Lupli binds to the *oskar* 3' UTR with a lower affinity than Bruno. These results indicate that Lupli associates with the *oskar* 3' UTR. Together with the previous results, which show an association of Lupli and *oskar* mRNA in vivo, it suggests that Lupli is part of the *oskar* mRNA localization complex to the posterior of the oocyte.

3.6 Lupli function in *oskar* mRNA localization

3.6.1 *lupli*$^{\Delta C}$ - an RRM-deletion mutant

To investigate whether *lupli* function is required for *oskar* localization and/or translation, I wished to perform loss-of-function experiments using a null mutant. As such a *lupli* allele was not available, I decided to create a *lupli* null allele. Several constraints had to be taken into account. First, the huge size of the *lupli* locus made it difficult to delete the entire gene by imprecise excision of a transposable element inserted in the locus (Figure 3.21 A). Second, deletion of only one transcriptional start site would affect the expression of only one isoform, and would therefore not be a strong mutant (Figure 3.21 and 3.6).Third, two additional genes, *CG10677* and *CG4669*, present in *lupli* introns must not be affected in the new mutant. I therefore decided to delete the genomic region encoding the two RRMs, as they were the only predicted domains in Lupli and were most likely to be essential for its function (Figure 3.21 A). By performing ends-out homogous recombination, I replaced this 6.7 kb genomic region with a marker cassette (see Material and Methods 2.4 on page 42) [Gong and Golic, 2003, 2004]. Of the 226 generated lines, 51 had an insertion of the cassette on the desired chromosome. For one of these lines, *lupli*$^{\Delta C}$, I could confirm,

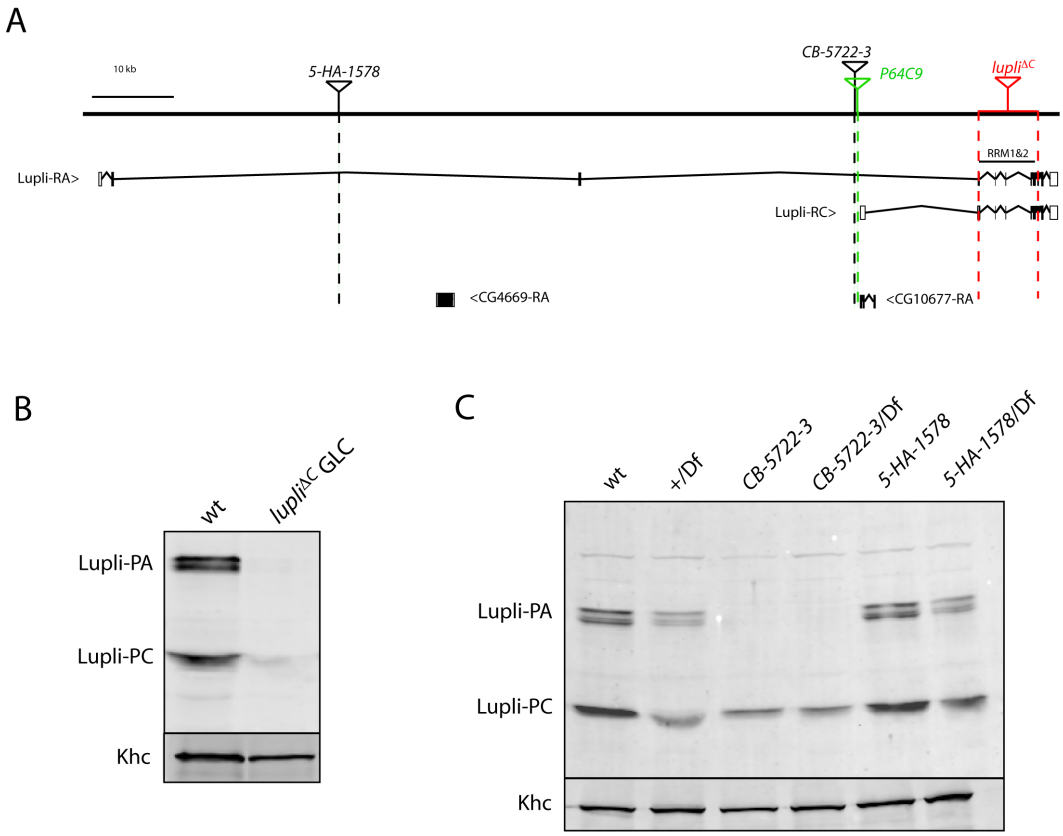

Figure 3.21: *lupli* locus and mutants

(A) Splicing pattern of the long (RA) and short (RC) *lupli* transcripts. Exons are depicted as black, UTRs as white boxes. The region encoding the two RRMs (black bar) of *lupli*, the region deleted by homologous recombination in *lupli*$^{\Delta C}$ (red trangle and lines), the insertion sites of the two P elements *5-HA-1578* and *CB-5722-3* (black triangle), as well as the insertion site of the GFP-cassette of trap line *P64C9* (green triangle), are shown. *CG4669* and *CG10677* are located on the opposite strand, and their predicted transcripts are not affected by any of the insertions (data not shown).

(B) Western blot comparing Lupli levels in wild type and *lupli*$^{\Delta C}$ GLC ovarian extracts. Kinesin heavy chain (Khc) was used as a loading control. Lupli is very strongly reduced in *lupli*$^{\Delta C}$.

(C) Western blot of wild type and mutant ovarian extracts. Blots were probed for Lupli and Kinesin heavy chain (Khc). The long Lupli isoform (Lupli-PA) is absent in *CB-5722-3/CB-5722-3* and *CB-5722-3/Df* flies, whereas the levels of the short isoform (Lupli-PC) is reduced. In *5-HA-1578* extracts, no significant difference in Lupli levels was detected.

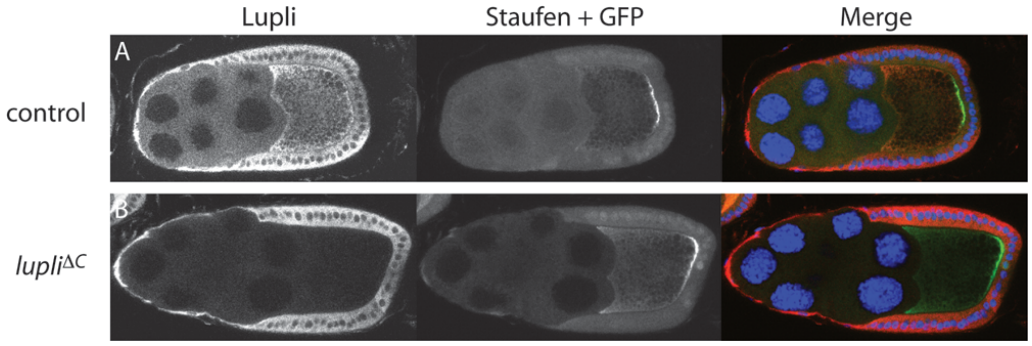

Figure 3.22: *lupli*$^{\Delta C}$ egg chambers show no defects in localization of osk-RNP *lupli*$^{\Delta C}$ germline clones (bottom) and control (top) were stained for Lupli (red, to select for germline clones) and Staufen (green).

by PCR, the absence of the targeted region, as well as the presence of the cassette (see Material and Methods 2.4 on page 42). In addition, western blot analysis using ovarian extracts from *lupli*$^{\Delta C}$ GLC ovaries further confirmed that the RRM encoding region of *Lupli* is indeed deleted, as hardly any protein was detected (Figure 3.21B). This experiment also confirmed the specificity of the Lupli antibody.

lupli$^{\Delta C}$ flies are homozygous lethal and the flies die as pharate adults, suggesting an essential role for *lupli* during late pupal development. A few adult escaper flies could be recovered at 18 °C, but they were very sick, displayed defects in pigmentation, wing eversion, locomotion and died after a few days. They also did not develop any ovaries that could be analysed. These findings indicate one or several important functions for *lupli* in *Drosophila.*

To investigate *lupli* function during oogenesis, I used the *lupli*$^{\Delta C}$ allele to create germline clones (GLC), using the FRT-FLP technique [Chou and Perrimon, 1996]. *lupli*$^{\Delta C}$ homozygous germ cells were either selected for the absence of GFP, or by the dominant female-sterile mutation *ovo*^{D} (see 2.2 on page 36). Mutant egg chambers proceeded normally through oogenesis and showed no defects in *oskar* localization or translation at any point of oogenesis (Figure 3.21). This indicates that *lupli* is either not essential for *osk* regulation or that *lupli*$^{\Delta C}$ is not a null mutant. Western blot analysis of *lupli*$^{\Delta C}$ GLC ovaries showed extremely low levels of Lupli protein, which is most likely residual protein from wild type follicle cells. But as the epitopes used for generating the anti-Lupli antibody are for the most part deleted in *lupli*$^{\Delta C}$

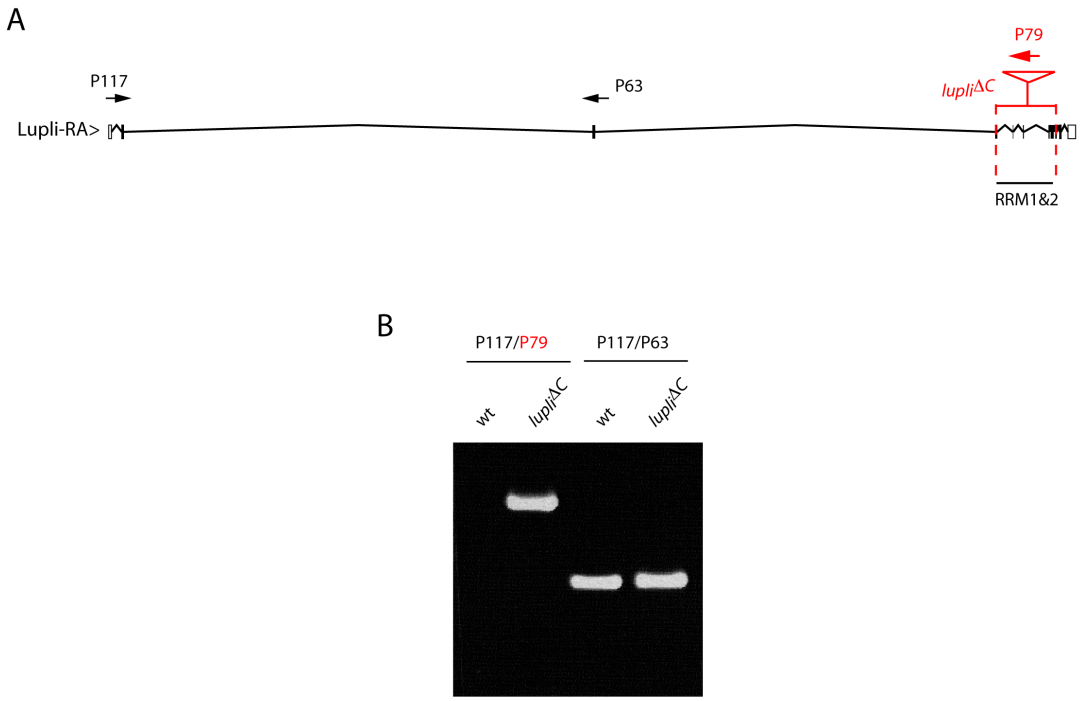

Figure 3.23: A truncated long Lupli transcript is present in *lupli*$^{\Delta C}$
(A) Diagram indicating the hypothetical mutant Lupli-RA transcript as it is presumably present in *lupli*$^{\Delta C}$. Primers (P117, P118, P76; black arrows) were chosen in the exons of the long Lupli transcript to amplify from a wild type or mutant cDNA library. A different primer (P79, red arrow) matches a region of the cassette that was introduced into the genome to replace the two RRMs of *lupli*, and will therefore only amplify mutant Lupli-RA transcripts if used in combination with the other oligos shown. (B) Ethidium-bromide gel showing the products of an RT-PCR using the primers indicated in (A). As template, two different cDNA libraries were used, generated from either wild type or *lupli*$^{\Delta C}$ homozygous pupae. The long Lupli transcript is still present in homozygous *lupli*$^{\Delta C}$ animals.

it made detection of a residual truncated long Lupli isoform impossible with this antibody. By RT-PCR, however, I could detect a transcript in homozygous *lupli*$^{\Delta C}$ pupae (Figure 3.23), indicating that this transcript is stable and might then be translated. This therefore raised the possiblity that a residual long Lupli protein lacking the C-terminal RRMs might be present in *lupli*$^{\Delta C}$ germ cells and able to perform its function in *oskar* regulation. I therefore searched for other alleles that would affect the long Lupli isoform.

3.6.2 P element alleles of *lupli*

To explore if *lupli* is required for posterior localization of *oskar* mRNA, I used two fly stocks carrying P element alleles of *lupli*. Both, *CB-5722-3* and *5-HA-*

1578, generated by DrosDel [Ryder et al., 2004], are P element insertions into the intronic regions of the long Lupli isoform (see Figure 3.21A). Crossing both stocks to a deficiency chromosome that encompasses the *lupli* locus, revealed that *CB-5722-3/Df* flies are semi-lethal, but *5-HA-1578/Df* are viable. Analysis by western blot shows that in *CB-5722-3/Df* the long Lupli isoform is absent and the short isoform is reduced. In *5-HA-1578/Df*, however, no obvious change of Lupli levels was detectable.

Both P elements, *CB-5722-3* and *5-HA-1578*, are independent insertions into the *lupli* locus (Figure 3.21 on page 75). However, two other genes, *CG4669* and *CG10677*, are predicted on the opposite strand within the *lupli* locus and their function could, in principle, be affected by the two P element alleles. Neither of the two genes have been described so far, and no antibodies were available to test for a change in protein levels in wild type versus *lupli* mutant extracts. I attempted tried to amplify the predicted transcript of *CG10677* by quantitative PCR (qPCR), using cDNA produced from wild type ovaries or adult flies but did not succeed. There are also no ESTs available for this gene, nor does it seem to be expressed in any specific tissue by microarray in the FlyAtlas database[5]. This suggests that the predicted *CG10677* is not a real gene and I therefore did not further continue the analysis.[6] For *CG4669* I could detect a transcript in the adult fly, but only at very low levels in the ovary. It was therefore hard to detect any difference in transcript levels between wild type and *lupli* mutant ovaries by qPCR. Taken together, these results suggest that *CG4669* and *CG10677* are unlikely to be affected by the two *lupli* P element alleles used.

3.6.3 *oskar* localization in *lupli* alleles

To test whether *oskar* mRNA localization was affected in the two *lupli* P element alleles, I performed immunostaining on mutant and wild type egg chambers using Staufen as a marker for the *oskar* RNP. In *5-HA-1578/Df* and *CB-5722-3/Df*

[5]FlyAtlas `http://flyatlas.org/`

[6]In the latest FlyBase release 5.2 (August 2007) the gene *CG10677* is no longer annotated.

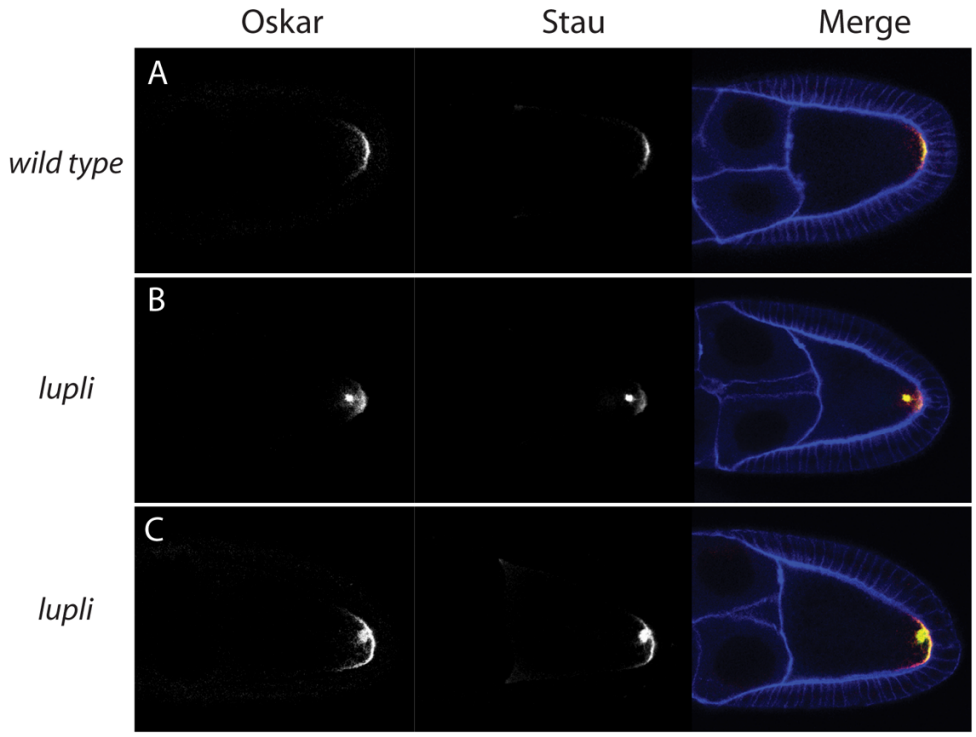

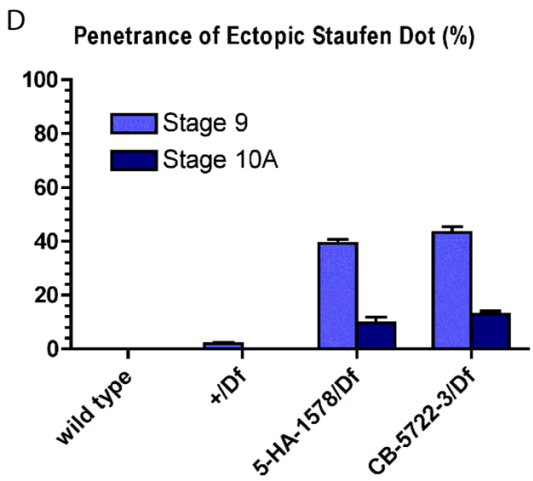

E

genotype	Stage 9			Stage 10A		
	Y	SD	N	Y	SD	N
wild type	0.0	0.0	127	0.0	0.0	63
+/Df	1.9	3.7	104	0.0	0.0	71
5-HA-1578/Df	39.1	14.5	92	9.7	17.1	72
CB-5722-3/Df	43.2	13.6	44	12.9	9.3	70

Figure 3.24: *lupli* is required for proper localization of Staufen and Oskar at the posterior pole
(A-C) Immunostaining for Staufen and Oskar protein in stage 9 egg chambers. In wild type oocytes (A) Staufen and Oskar localize tightly to the posterior cortex. In *lupli* mutants, an ectopic spot of Staufen and Oskar protein is formed, either in close proximity (B), or connected to (C) the posterior pole of the oocyte. (D) Diagram showing the percentage of egg chambers displaying an ectopic dot of Staufen and Oskar. 39.1% of *5-HA-1578/Df*, and 43.2% of *CB-5722-3/Df* of the observed stage 9 egg chambers show this ectopic dot. This penetrance decreases at stage 10A where 9.7% of *5-HA-1578/Df* , 12.9% of *CB-5722-3/Df* oocytes show the phenotype. (E) Table showing the values corresponding to the diagram shown in (D), displaying the percentage of ectopic dot phenotype (Y), the standard deviation (SD), and the total number (N) of egg chambers observed.

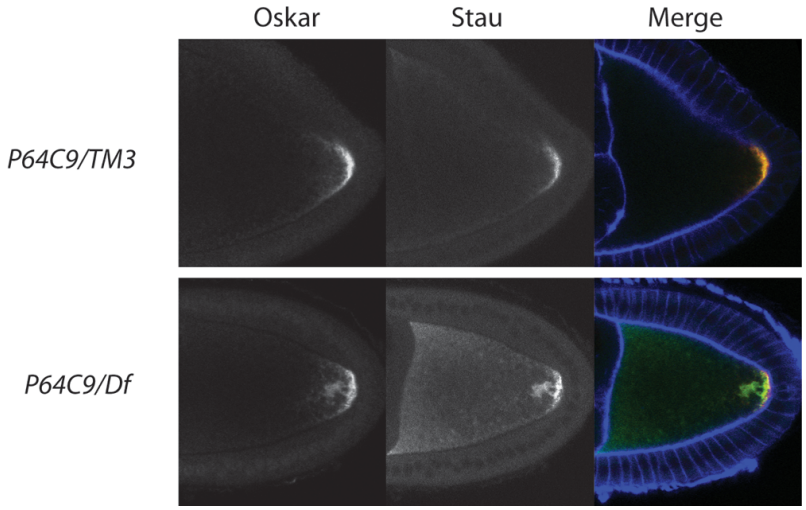

Figure 3.25: *P64C9* is a *lupli* allele and displays the same phenotype as other *lupli* alleles
In 38% (n=42) of stage 9 *P64C9/Df* oocytes Staufen, a marker for *oskar* mRNA, and Oskar protein are detectable as an ectopic aggregate next to the crescent at the posterior pole.

oocytes, Staufen is normally distributed until stage 8 of oogenesis. At stage 9, however, Staufen is found in an ectopic dot that is in immediate proximity of, or connected to the crescent at the posterior pole in 39.1% of *5-HA-1578/Df* (n=92), and 43.2% of *CB-5722-3/Df* (n=44) egg chambers (Figure 3.24). Furthermore, Oskar protein always colocalizes with Staufen in this ectopic dot, indicating either that Oskar protein is ectopically expressed, or that is expressed at the posterior, but is not anchored properly at the posterior pole. Furthermore, the trap line *P64C9* displays an identical phenotype, indicating that it is a new *lupli* allele (Figure 3.25). At stage 10A, the penetrance of this phenotype in mutant egg chambers decreases to 9.7% for *5-HA-1578/Df* (n=72), and 12.9% for *CB-5722-3/Df* (n=70) egg chambers. At later stages, *lupli* mutant egg chambers appear completely wild type. These results suggest that *lupli* has role in localization of *oskar* mRNA to the posterior pole of the oocyte. As three independent and different alleles display the same phenotype in the oocyte, the mutations in the *lupli* gene are quite likely the cause of the phenotype observed.

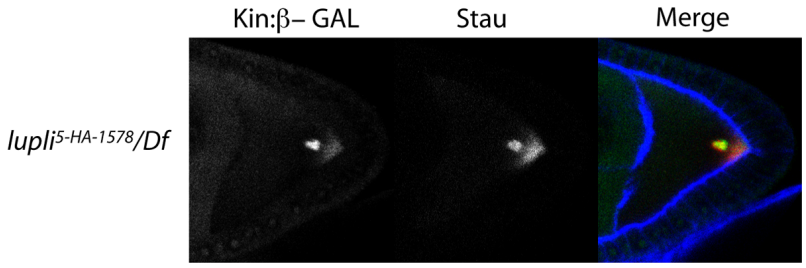

Figure 3.26: lupli is required for oocyte polarity
Kin::β-GAL forms an ectopic dot in *5-HA-1578/Df* stage 9 egg chambers that colocalizes with Staufen.

3.6.4 Microtubule polarity is affected *lupli* mutants

To assess whether defects in *oskar* mRNA/Staufen localization in *lupli* mutant oocytes might be caused by an improperly polarized microtubule (MT) cytoskeleton, I examined the overall polarity of the oocyte MTs. I made use of the Kinesin-β-galactosidase (Kin::β-GAL) fusion protein, which marks MT plus ends and is localized to the posterior pole of the oocyte at stage 9, therefore serving as an oocyte polarity marker (see Section 1.4.2) [Clark et al., 1994]. Unlike wild type oocytes, in which the MTs colocalize together with Kin::β-GAL at the posterior pole, in *5-HA-1578/Df* oocytes Kin::β-GAL forms an ectopic dot in close proximity to the posterior pole, always colocalizing with Staufen, thus revealing an aberrant organization of the oocyte MT cytoskeleton (Figure 3.26). Similar results were also obtained with *CB-5722-3/Df*. This indicates that *lupli* is required for establishment or maintenance of proper oocyte MT polarity. Furthermore, these results suggest that the observed mislocalization of the *oskar* RNP complex observed in *lupli* mutant oocytes is a consequence of MT polarity defects.

3.6.5 *lupli* affects Oskar protein levels

The above results indicate that *lupli* affects localization of Oskar protein at the posterior cortex in stage 9 egg chambers. I wished to assess if not only localization, but also levels of Oskar protein were affected. Indeed, by western blot, I could observe an approximately two-fold reduction of Oskar protein in *lupli* mutant ovarian extracts (Figure 3.27).

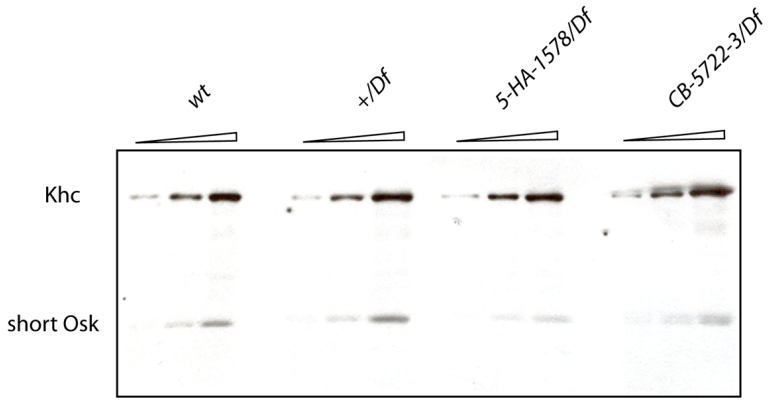

Figure 3.27: Oskar protein levels are reduced in *lupli* mutant ovaries
Different amounts of wild type and mutant ovarian extracts were probed with anti-Oskar antibody. anti-Khc antibody was used as a loading control. The levels of long Osk were too low to detect any difference in levels, therefore only short Osk is indicated.

There is a direct relationship between the amount of Oskar protein and the concentration of pole plasm components that are required for abdomen and germline formation at the posterior pole of the embryo (see Section 1.3.4 on page 22) [Ephrussi et al., 1991, Ephrussi and Lehmann, 1992, Kim-Ha et al., 1991]. In particular, a reduction in Oskar protein levels leads to patterning defects in embryos coming from *oskar* mutant mothers, which then usually results in lethality. To test if the observed reduction in Oskar protein in *lupli* mutant ovaries has any effect on the further development of the embryo, I scored the lethality of embryos derived from *5-HA-1578/Df* and *CB-5722-3/Df* females. I could not observe any difference in the hatching rates of embryos produced by *lupli* and wild type females (Figure 3.28). I therefore excluded the possibility of patterning defects in embryos coming from *lupli* mutant mothers. This is maybe not surprising, as a rather normal posterior crescent of Oskar protein is observed from stage 10 onwards. Furthermore, a two-fold reduction in Oskar protein levels might not be enough to cause defects in patterning of the embyro.

Germline development is more sensitive to Oskar levels than embryonic patterning. I therefore assessed if the reduction in Oskar protein level might affect the germline development in *lupli* mutant progeny ("grandchild-less phenotype", see Section 1.3.4 on page 22). To this end, I counted the number of ovaries of females

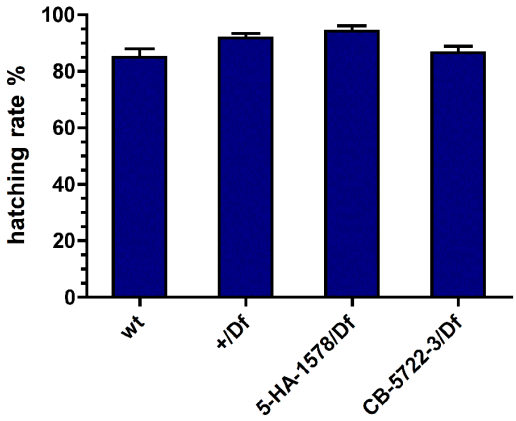

Figure 3.28: Hatching rates of eggs laid by *lupli* mutant mothers are not affected
The hatching rates of eggs produced by wild type or *lupli* mutant mothers were 85.07% (n=355) for wild type, 91.86% (n=492) for +/Df, 93.70% (n=372) for *5-HA-1578/Df*, 86.59% (n=507) for *CB-5722-3/Df*.

genotype of mothers	2 ovaries	1 ovary	0 ovary
wild type	61	0	0
+/Df	75	0	0
5-HA-1578/Df	59	0	0
CB-5722-3/Df	68	0	0

Table 3.1: Germline functions normally in *lupli* progeny
This table indicates the numbers of females coming form progeny of *wild type*, *+/Df*, *5-HA-1578/Df* and *CB-5722-3/Df* females crossed against wild type males. They were dissected and their number of ovaries was counted.

derived from *5-HA-1578/Df* and *CB-5722-3/Df* mothers (Table 3.1). I observed no reduction in the number ovaries developed by any of the different daughters analyzed. These results suggest that *lupli* modulates Oskar protein levels, but that these levels are still above the threshold required for the development of the egg into fertile adults.

Chapter 4

Discussion

4.1 Limits of the protein trap approach

In a medium scale GFP-based protein trap screen carried out in the context of a consortium of laboratories, I screened 347 lines, of which 298 showed expression of GFP in the ovary. A wide variety of expression patterns was observed, validating the use of such an approach to identify novel proteins by their expression pattern.

We mapped by iPCR the P element insertion sites in the lines displaying the most interesting expression patterns for the consortium (Figure 4.1). 40 out of the 56 lines sequenced had insertions in introns, presumably giving rise to the GFP-fusion proteins. For the remaining lines, the mapping data indicated that the insertion did not lie in an intron. In fact, 12 of these "non-intronic lines" have an insert in the 5' region of a gene, which might indicate the existence of new splicing isoforms. 4 insertions did not correspond to any annotated gene, which might reflect an insertion into a new, un-annotated gene [Morin et al., 2001]. However, the observed GFP pattern might also be due to a second insertion, which we were not able to map properly.

Interestingly, there was a strong bias towards insertions into certain genes (Figure 4.1). This was surprising, considering the huge number of possible insertions in the entire genome. Although several of the lines in which the proteins 14-3-3ϵ, Rab11

line	gene	insert position (scaffold)2	intron size (bp)
68	trailer hitch	204861 (AE03541)	987
72	calreticulin	167936 (AE003683)	269
76	CG14648	134706 (AE003606)	1189
101,171,216,244	"	135089 (AE003606)	1189
217	"	134805 (AE003606)	1189
80	CG3036	289739 (AE003757)	7407
84	"	283753 (AE003757)	7407
106	shaggy	31526 (AE003425)	27820
118	"	12808 (AE003425)	27820
232	"	8767 (AE003425)	27820
234,249	"	24909 (AE003425)	27820
456	"	8831 (AE003425)	27820
94	basigin	283430 (AE003619)	15955
108	"	282991 (AE003619)	15955
121	"	269937 (AE003619)	15955
132	"	283210 (AE003619)	15955
252	"	283677 (AE003619)	15955
121	out at first	263143 (AE003583)	2078
141	CG31305	43301 (AE003692)	2207
145, 147,164,	14-3-3ε	83722 (AE003721)	
209,242,243	"	83722 (AE003721)	4524
280	"	83759 (AE003721)	
151	Thioredoxin reductase-1	127301 (AE003443)	3363
156,190,191,	rab11	134236 (AE003733)	2091
263	"	134236 (AE003733)	
173	nervana 2	148841 (AE003495)	4496
193	vimar	314158 (AE003790)	6815
199	simjang	71722 (AE003547)	19640
227	nucleoplasmin	115237 (AE003772)	233
303	ypsilon schachtel	116043 (AE003542)	1137
354,356	Rtnl1	115206 (AE003535)	11387
397	nuclear fallout	115206 (AE003535)	11386

Figure 4.1: Mapping details of genes trapped by GFP
Most of the *shaggy* and *basigin* lines differ in their insertion site. Other genes were trapped several times independently by identical insertion sites.

and Growl were tagged, contained an insertions at the exact same position and might result from the same clonal event, independent insertions into the same intron were also recovered (Figure 4.1). This may partly be due to the huge size of introns in some of these genes (about 28 kb and 16 kb in the cases of *shaggy* and *basigin,* respectively). However, stochastic reasons can only partially explain this bias. First, other genes with equally large introns were not hit. Second, some genes that were repetitively hit have introns of average size (e.g. 1.2 kb for *CG14648*). This indicates that there are hotspots for integration of the transposable element in the genome.

The P element, which was used in our vector, is known to insert into hotspots, primarily within the regulatory regions of genes [Spradling et al., 1999]. As our aim

was to create intronic insertions, such a bias of the P element is not useful for our purposes [Morin et al., 2001, Spradling et al., 1999]. To overcome this problem, we used constructs based on a different transposable element, piggyBac, which was reported to have more random integration [Hacker et al., 2003, Thibault et al., 2004]. However, the frequency at which GFP^+ embryos were recovered when mobilizing the piggyBac constructs proved to be much lower (approximately 1/100000), than for the P element based vector (frequency approximately 1/5000, Christian Klämbt, personal communication). Furthermore, very similar results were described in a recently published protein trap screen by Buszczak and co-workers [Buszczak et al., 2007], who identified a large number of lines using P element-based constructs, but obtained a low frequency of GFP^+ flies with the piggyBac construct. It is therefore questionable if piggyBac is indeed a more suitable transposable element for this type of screen. However, the decrease in transposition frequency might simply depend on the construct itself, rather than the fact that it is piggyBac-based, as variations between different vectors could be observed (Christian Klämbt, personal communication). Thus, before performing a piggyBac-based screen, it would be important to optimize the jumping capability of the vector in order to perform a large scale GFP-trap screen.

Another alternative to at least partially overcome the problems of hotspots, is simply to generate more lines. Our pilot screen was a medium-scale screen, far from saturation. Approaching saturation by the generation of more lines should therefore increase the total number of different genes hit.

4.2 Lupli - a component of the *oskar* RNP

Lupli protein was discovered due to its posterior enrichment in GFP-trap line *P64C9*. I could confirm this expression pattern by immunostaining, using an antibody against the bacterially-expressed protein. The colocalization of Lupli with Staufen in wild type, *staufen* and *gurken* mutant background indicates that at least a fraction of

the Lupli protein pool expressed in the oocyte travels with *oskar* mRNA to the posterior pole. This suggests that Lupli is a novel component of the *oskar* RNP complex in vivo. Therefore, our visual GFP-trap screen may provide an alternative method to the classical biochemical and genetic approaches used in the past for the identification of new *oskar* RNP components.

The result of the affinity pull-down assay suggests an association of both Lupli isoforms with the *oskar* 3' UTR in ovarian extracts, further strengthening the hypothesis that Lupli is in a complex with *oskar* mRNA. UV cross-linking experiments using radiolabeled *oskar* mRNA and purified Lupli protein could reveal whether such an interaction is direct. An interesting recent study of the human Lupli ortholog RBMS3 showed by gel mobility-shift experiments that this protein binds directly to a specific 60 nucleotide-long A/U-rich region within the 3' UTR of Prx1 mRNA, a transcript encoding a transcription factor involved in hepatic collagen synthesis [Fritz and Stefanovic, 2007]. Several A/U-rich elements have been characterized in the *oskar* 3' UTR, such as the binding sites for Hrp48 [Gunkel et al., 1998, Werner, 2005, Yano et al., 2004], and IMP, the *Drosophila* ortholog of zip code-binding protein 1 (ZBP-1) [Munro et al., 2006]. The IMP-binding elements (IBEs) in the *oskar* 3' UTR are required for *oskar* translational activation at the posterior pole of the oocyte. However, *imp* mutant flies do not show any defect in *oskar* regulation, and the authors have hypothesized the existence of an unknown factor X that can also bind to IBEs and acts redundantly with IMP. It would therefore be interesting to examine whether this factor might be Lupli, by testing if Lupli localizes to the posterior pole of the oocyte in transgenic flies in which the only *oskar* mRNA expressed contains mutated IBEs to which IMP can not bind.

My results also indicate that only the non-phosphorylated long isoform associates with *oskar* 3' UTR (Figure 3.20 on page 73). This suggests a mechanism whereby binding of Lupli to *oskar* mRNA might be regulated by phosphorylation. A bioinformatic search using the ELM database[1] reveals many phosphorylation sites

[1]ELM database `http://elm.eu.org/`

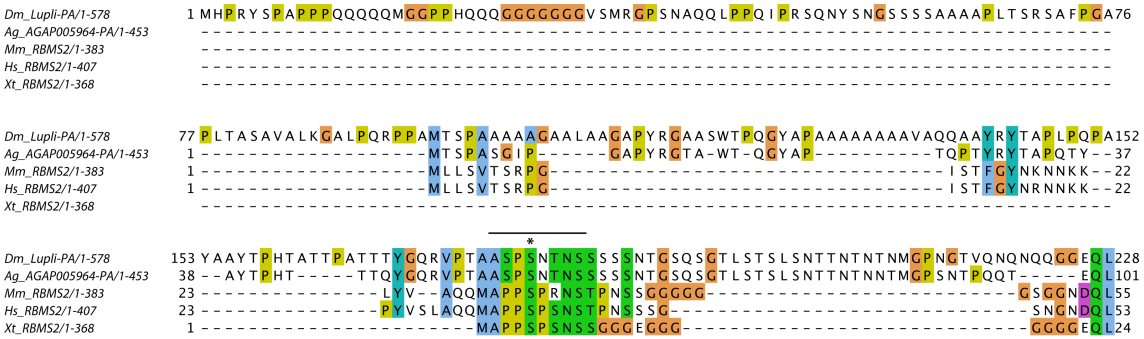

Figure 4.2: A Potential GKS-3 phosphorylation site in the N-terminal of long Lupli is conserved
Multiple alignment of *Drosophila* Lupli-PA and RBMS2 orthologs with the following Ensembl Peptide IDs: *A. gambiae* (AGAP005964-PA), *M. musculus* (ENSMUSP00000089664), *H. sapiens* (ENSP0000026203). The black line depicts the conserved GSK-3 recognition site (consensus [X]-[X]-[X]-[ST]-[X]-[X]-[X]-[ST]), a star indicates the predicted phosphorylation site. The method for generating the alignment and coloring was as in Figure 3.11 on page 65).

in long Lupli. However, most of these are not conserved. Interestingly, a consensus recognition site for glycogen-synthase kinase (GSK-3) is present in the N-terminal region of Lupli and its orthologs (Figure 4.2). Furthermore, *shaggy*, the *Drosophila* GSK-3β ortholog, is expressed during oogenesis, as revealed by the pattern of several of our GFP-trap lines, and as previously described [Jordan et al., 2006]. It would therefore be interesting to generate mutations in the predicted GSK-3 phosphorylation sites of Lupli to test the in vivo relevance of such a predicted phosphorylation site in *oskar* binding and regulation.

4.3 Phenotype

4.3.1 Absence of phenotype in *lupli*$^{\Delta C}$

To analyse the function of *lupli* in *oskar* regulation, I created a mutant by homologous recombination. The allele produced, *lupli*$^{\Delta C}$, seems to be closer to a loss-of-function mutation than other P element alleles used (*5-HA-1578* and *CB-57722-3*), as homozygous *lupli*$^{\Delta C}$ flies are lethal, and no protein was detected using the an-

tibody I generated. However, no aberrant phenotype was observed in homozygous mutant germline clone ovaries. This could be for several reasons. First, it is in principle possible that the insertion in *lupli* is not the cause of the *oskar* phenotype in *5-HA-1578* and *CB-57722-3* mutants. This can only be resolved by rescueing the phenotype with a wild type *lupli* transgene. I have attempted to rescue these mutants using the cDNAs of either the long or the short *lupli* isoform, tagged with HA. Unfortunately, I have not been successful so far, which might be due to sub-optimal expression levels, timing, the HA-tag, the driver, or the need for simultaneous expression of the long and the short Lupli isoform. I am currently in the process of optimizing the rescue experiment. Nevertheless, several facts argue in favor of *lupli* being the cause of the observed phenotype. Three P element insertions in the *lupli* locus, *5-HA-1578*, *CB-57722-3*, and *P64C9*, which were generated independently using different vectors, display the same phenotype concerning *oskar* localization to the posterior pole. Also, it is unlikely that *CG4669*, the only other gene in the *lupli* locus, is affected by the mutant alleles used. Indeed, it is only expressed at very low levels during oogenesis, and I could not detect any changes in levels in wild type versus mutant egg chambers. It therefore seems unlikely that a gene other than *lupli* is responsible for the ectopic dot of *oskar* mRNA in stage 9 *lupli* mutant egg chambers.

Second, *lupli* may not be required exclusively in the germline. The homozygous *lupli*$^{\Delta C}$ oocytes were mainly surrounded by a wild type follicular epithelium, expressing Lupli at normal levels. Lupli could have a non cell-autonomous effect from the follicular epithelium on *oskar* mRNA in the oocyte. Therefore, Lupli protein in the follicular epithelial cells would be sufficient to rescue an *oskar* localization phenotype in a *lupli* mutant oocyte. It is hard to address if this is indeed the case, as one would have to generate *lupli*$^{\Delta C}$ clones simultaneously in the germline and the follicular cells, which is difficult. Increasing the frequency of recombination and analyzing more samples should help resolve this issue.

Third, a residual peptide sufficient to perform the function of Lupli, might still be

present in *lupli*$^{\Delta C}$ clones, This seems unlikely, as one would expect the two deleted RRMs in the Lupli C-terminus to be essential for its function. Furthermore, the N-terminus of Lupli only contains an alanine-rich region and is not predicted to encode any folded domains. Unfortunately, I have not been able to detect such a truncated peptide, as the anti-Lupli antibody was raised against the C-terminus common to all isoforms. However, in homozygous *lupli*$^{\Delta C}$ pupae, a transcript encoding such a peptide could be detected by RT-PCR (Figure 3.23 on page 77). It therefore can not be excluded that such a residual peptide is expressed and that it may be able to perform some of the function of full-length Lupli protein in *oskar* regulation.

4.3.2 Ectopic dot phenotype and MT polarity

In my experiments I could observe an ectopic dot of Staufen and Oskar proteins close to the posterior of *lupli* mutant oocytes, mainly at stage 9, with a recovery at later stages (Figure 3.24 on page 79). This phenotype differs from that of other *oskar* localization mutants, such as *staufen*, *barentsz*, or *y14*. In these mutants, *oskar* mRNA is not concentrated in a dot, but dispersed or at the anterior of the oocyte, and no Oskar protein is detected [van Eeden et al., 2001, Ephrussi et al., 1991, Hachet and Ephrussi, 2001, Kim-Ha et al., 1991]. This suggests that Lupli might be required at a late and specific stage of *oskar* regulation, as in *lupli* mutants the *oskar* RNP seems to be transported to the posterior of the oocyte, but does not form a tight crescent at the cortex. This could be explained in two ways. First, the *oskar* RNP complex does manage to reach the cortex, but fails to anchor there, as observed in the absence of Moesin, Homer/Bifocal, or Long Osk [Babu et al., 2004, Jankovics et al., 2002, Polesello et al., 2002, Rongo et al., 1995]. In these mutants, however, an abnormal distribution of Oskar is observed only in late stage 10 oocytes. The second and much more likely explanation is that the *oskar* RNP does never efficiently reach the posterior cortex in *lupli* mutants and accumulates ectopically as a dot, as observed. Novel techniques of live-cell imaging might give more insight into the kinetics of *oskar* mRNA in *lupli* oocytes in the future.

The ectopic Staufen/Oskar dot is always associated with ectopic Kin::β-GAL (Figure 3.26 on page 81), indicating that MT polarity is affected in *lupli*. There are at least three possible ways to explain this phenotype. First, the ectopic dot in *lupli* mutants could simply be a consequence of the polarity defects in *lupli* oocytes. Second, Lupli might have pleiotropic functions, one in MT regulation and the other in *oskar* mRNA transport. Hrp48, for example, has different functions, which can be distinguished using different *hrp48* alleles [Huynh et al., 2004, Yano et al., 2004]. A similar scenario could therefore be the case for Lupli. But as no *lupli* alleles that allows one to distinguish between the two effects have been recovered so far, it has not been possible to address if this scenario is taking place. Third, Lupli might directly affect *oskar* mRNA localization, which then would cause a defect in MT polarity. Support for such a hypothesis comes from a recent study that suggests a role of Oskar protein in the maintenance of oocyte polarity [Zimyanin et al., 2007]. The authors observe that Oskar protein is required for efficient recruitement of MT plus ends to the posterior pole. Furthermore, ectopic Oskar protein can recruit the MT plus-ends through PAR-1, which leads the authors to suggest that Oskar protein acts in a positive feedback loop that regulates MT polarity. This therefore raises the possibility that the observed polarity defects in *lupli* mutants are a consequence, rather than a cause, of the observed ectopic Staufen dots. In this scenario, Lupli would directly be involved in short-range transport of the *oskar* RNP complex from the posterior region to the cortex. In *lupli* mutants, short-range transport would therefore be affected, leading to ectopic Oskar expression close to the posterior pole, as it is observed. This ectopic accumulation, in turn, would then recruit the MT plus ends away from the cortex to the ectopic Staufen/Oskar dot. To test this model, it would therefore be interesting to look at *lupli* mutants in an Oskar protein-null background.

4.3.3 *lupli* and Oskar levels

My results indicate that Oskar levels are approximately two-fold lower in *lupli* mutant ovarian extracts, compared with wild type. This could be for several reasons. Lupli might directly affect the stability of Oskar protein. But, as my experiments indicate an association of Lupli with the *oskar* 3' UTR, it seems therefore more probable that Lupli acts on the level of the transcript. Interestingly, in the study by Fritz and Branco, it was observed that overexpression of RBMS3 caused an increase of *Prx1* transcript levels [Fritz and Stefanovic, 2007]. They showed that the stability of a reporter transcript was increased if it contained the wild type, but not a mutant RBMS3-binding region. This suggested that RBMS3 binding to and stabilization of the *Prx1* transcript might cause the increased level of Prx1 protein in cells overexpressing RBMS3. By analogy, the observed decrease in Oskar protein levels in *lupli* mutants might therefore be due to reduced *oskar* mRNA stability. This could be tested by evaluating the relative stability of *oskar* transcripts in wild type and *lupli* mutant ovaries.

Oskar protein levels might also be regulated at the translational level. As shown by Munro *et al.*, the IBEs in the *oskar* 3' UTR are required for translational activation of *oskar* mRNA [Munro et al., 2006]. If the hypothesis that Lupli binds to the IBEs were correct (see Section 4.2), one could therefore speculate that Lupli is in fact the cause of reduced Oskar protein levels in IBE mutant ovaries.

4.4 Conclusion

In a protein-trap screen, I identified several lines displaying an enrichment of GFP-fusion proteins at the posterior pole of the *Drosophila* oocyte. I characterized an independently generated line, in which the gene identified encodes a novel RRM-containing protein that I named Lupli. By immunostaining, I showed that endogenous Lupli protein displays the same distribution pattern in the oocyte as GFP::Lupli. Lupli associates with the 3' UTR of *oskar* mRNA and is a component

of the *oskar* RNP complex in vivo. I showed that the late short-range transport of *oskar* mRNA to the cortex is defective in *lupli* mutant oocytes at stage 9, and that the microtubule cytoskeleton is not properly polarized. Furthermore, Oskar protein levels are reduced in *lupli* mutant ovaries. My work thus led to the identification of Lupli as a new component of the *oskar* RNP complex, and suggests that its function is required for proper localization and expression of *oskar* in *Drosophila* oocytes.

Acknowledgments

I am deeply grateful to Anne Ephrussi for giving me the chance to carry out my PhD project in her lab. Her continuous support, passion for science and the opportunity to function independtly were invaluable for me.

I would like to thank the members of my EMBL thesis advisory committee, Darren Gilmour, G. Elisabeth Pollerberg and Pernille Rørth, for their scientific and important strategic advise during my PhD. Many thanks also to the additional members of my university defense committee, Eileen Furlong and Jochen Wittbrodt, for investing the time in reading and evaluating my thesis.

I am indebted and immensly thankful to Florence Besse, from whom I received the majority of my training, covering the entire range from basic fly genetics over experimental design to scientific writing. Merci Flo for all your patience with me! I also learned a tremendous amount about scientific thinking in general, and RNA localization in specific, as well as many essential techniques from Sonia Lopez de Quinto, whom I want to thank for the time and energy she invested into my project. I also would like to express my appreciation to all the other members of the Ephrussi lab, past and present, for their continuous help, exciting discussions, as well as friendship, Jean-Baptiste Coutelis, Anna Cyrklaff, Shih-Jung Fan, Sanjay Ghosh, Helena Jambor, Virginie Marchand, Sandra Müller, Yelena Riordan, Alvar Trucco, Shoko Yoshida, and "the new one", Ronny Gstir. I especially want to thank Piyi Papadaki, who has become a great friend over these years, and with whom I share fantastic culinary and subaquatic experiences I will never forget.

I also would like to express my gratitude to the following people for their scientific advice, reagents, or just general help on various aspects of my PhD: Peter Bieling, Aidan Budd, Natascha Bushati, Julie Cahu, Eoghan Harrington, Christian Klämbt and the Protein-trap consortium, Cleo Kozlowski, Kasia Oktaba, Hsin-Ho Sung, Hanne Varmark, Ann-Mari Voie.

Close to my heart are these people I met during my time at EMBL, whom I want to thank for their great, and hopefully still long-lasting friendship: Gros

bisous pour “mon liebling” Mirana Ramialison, Matthieu Pichaud, Julie Cahue, filakia poli! to Valia Stamataki and Alexandra Boutla, thanks to Eoghan Harrington, Meikel Diepholz and Natascha Bushati, merci vilmal to Annette Schmidt, my “very professional friends” Kasia “Palerita” Oktaba and Konrad Förstner, as well as the loveliest Taiwanese couple ever, Hsin-Ho Sung and Yawen Chen.

A big hug goes to Joni Winkler, “my rockstar friend”, for his life-long friendship, and because he helps me, together with Susanne Gnekow, to keep my feet down on the ground.

This work is dedicated to my family as without them nothing would have been possible: Eva-Maria, mum and dad for their love, their confidence and their 30-year long support in anything I do, especially of course, in getting closer to my goal of becoming a “Tierforscher”.

I was supported by an E-STAR fellowship funded by the FP6 Marie Curie Host fellowship for Early Stage Research Training under contract number MEST-CT-2004-504640.

Bibliography

Kavita Babu, Yu Cai, Sami Bahri, Xiaohang Yang, and William Chia. Roles of bifocal, homer, and f-actin in anchoring oskar to the posterior cortex of drosophila oocytes. *Genes Dev*, 18(2): 138–143, Jan 2004. doi: 10.1101/gad.282604. URL `http://dx.doi.org/10.1101/gad.282604`.

S.M. Bjorum. Two genes affecting drosophila gravitaxis. In *A. Dros. Res. Conf. 47 : 615B.*, 2006.

N. Bobola, R. P. Jansen, T. H. Shin, and K. Nasmyth. Asymmetric accumulation of ash1p in postanaphase nuclei depends on a myosin and restricts yeast mating-type switching to mother cells. *Cell*, 84(5):699–709, Mar 1996.

F. Bohl, C. Kruse, A. Frank, D. Ferring, and R. P. Jansen. She2p, a novel rna-binding protein tethers ash1 mrna to the myo4p myosin motor via she3p. *EMBO J*, 19(20):5514–5524, Oct 2000. doi: 10.1093/emboj/19.20.5514. URL `http://dx.doi.org/10.1093/emboj/19.20.5514`.

A. H. Brand and N. Perrimon. Targeted gene expression as a means of altering cell fates and generating dominant phenotypes. *Development*, 118(2):401–415, Jun 1993.

R. P. Brendza, L. R. Serbus, J. B. Duffy, and W. M. Saxton. A function for kinesin i in the posterior transport of oskar mrna and staufen protein. *Science*, 289(5487):2120–2122, Sep 2000.

Michael Buszczak, Shelley Paterno, Daniel Lighthouse, Julia Bachman, Jamie Planck, Stephenie Owen, Andrew D Skora, Todd G Nystul, Benjamin Ohlstein, Anna Allen, James E Wilhelm, Terence D Murphy, Robert W Levis, Erika Matunis, Nahathai Srivali, Roger A Hoskins, and Allan C Spradling. The carnegie protein trap library: a versatile tool for drosophila developmental studies. *Genetics*, 175(3):1505–1531, Mar 2007. doi: 10.1534/genetics.106.065961. URL `http://dx.doi.org/10.1534/genetics.106.065961`.

Byeong-Jik Cha, Laura R Serbus, Birgit S Koppetsch, and William E Theurkauf. Kinesin i-dependent cortical exclusion restricts pole plasm to the oocyte posterior. *Nat Cell Biol*, 4(8): 592–598, Aug 2002. doi: 10.1038/ncb832. URL `http://dx.doi.org/10.1038/ncb832`.

T. B. Chou and N. Perrimon. The autosomal flp-dfs technique for generating germline mosaics in drosophila melanogaster. *Genetics*, 144(4):1673–1679, Dec 1996.

T. B. Chou, E. Noll, and N. Perrimon. Autosomal p[ovod1] dominant female-sterile insertions in drosophila and their use in generating germ-line chimeras. *Development*, 119(4):1359–1369, Dec 1993.

Michele Clamp, James Cuff, Stephen M Searle, and Geoffrey J Barton. The jalview java alignment editor. *Bioinformatics*, 20(3):426–427, Feb 2004. doi: 10.1093/bioinformatics/btg430. URL `http://dx.doi.org/10.1093/bioinformatics/btg430`.

I. Clark, E. Giniger, H. Ruohola-Baker, L. Y. Jan, and Y. N. Jan. Transient posterior localization of a kinesin fusion protein reflects anteroposterior polarity of the drosophila oocyte. *Curr Biol*, 4(4):289–300, Apr 1994.

G. Dalgleish, J. L. Veyrune, J. M. Blanchard, and J. Hesketh. mrna localization by a 145-nucleotide region of the c-fos 3'–untranslated region. links to translation but not stability. *J Biol Chem*, 276(17):13593–13599, Apr 2001. doi: 10.1074/jbc.M001141200. URL `http://dx.doi.org/10.1074/jbc.M001141200`.

D. Ding, S. M. Parkhurst, S. R. Halsell, and H. D. Lipshitz. Dynamic hsp83 rna localization during drosophila oogenesis and embryogenesis. *Mol Cell Biol*, 13(6):3773–3781, Jun 1993.

Gretchen Dollar, Eric Struckhoff, Jason Michaud, and Robert S Cohen. Rab11 polarization of the drosophila oocyte: a novel link between membrane trafficking, microtubule organization, and oskar mrna localization and translation. *Development*, 129(2):517–526, Jan 2002.

G. Drewes, A. Ebneth, U. Preuss, E. M. Mandelkow, and E. Mandelkow. Mark, a novel family of protein kinases that phosphorylate microtubule-associated proteins and trigger microtubule disruption. *Cell*, 89(2):297–308, Apr 1997.

W. Driever and C. Nusslein-Volhard. The bicoid protein determines position in the drosophila embryo in a concentration-dependent manner. *Cell*, 54(1):95–104, Jul 1988a.

W. Driever and C. Nusslein-Volhard. A gradient of bicoid protein in drosophila embryos. *Cell*, 54 (1):83–93, Jul 1988b.

Jason E Duncan and Rahul Warrior. The cytoplasmic dynein and kinesin motors have interdependent roles in patterning the drosophila oocyte. *Curr Biol*, 12(23):1982–1991, Dec 2002.

A. Ephrussi and R. Lehmann. Induction of germ cell formation by oskar. *Nature*, 358(6385): 387–392, Jul 1992. doi: 10.1038/358387a0. URL `http://dx.doi.org/10.1038/358387a0`.

A. Ephrussi, L. K. Dickinson, and R. Lehmann. Oskar organizes the germ plasm and directs localization of the posterior determinant nanos. *Cell*, 66(1):37–50, Jul 1991.

M. Erdelyi, A. M. Michon, A. Guichet, J. B. Glotzer, and A. Ephrussi. Requirement for drosophila cytoplasmic tropomyosin in oskar mrna localization. *Nature*, 377(6549):524–527, Oct 1995. doi: 10.1038/377524a0. URL `http://dx.doi.org/10.1038/377524a0`.

D. Ferrandon, L. Elphick, C. NÃŒsslein-Volhard, and D. St Johnston. Staufen protein associates with the 3'utr of bicoid mrna to form particles that move in a microtubule-dependent manner. *Cell*, 79(7):1221–1232, Dec 1994.

Kevin M Forrest and Elizabeth R Gavis. Live imaging of endogenous rna reveals a diffusion and entrapment mechanism for nanos mrna localization in drosophila. *Curr Biol*, 13(14):1159–1168, Jul 2003.

Sebastien Fribourg, David Gatfield, Elisa Izaurralde, and Elena Conti. A novel mode of rbd-protein recognition in the y14-mago complex. *Nat Struct Biol*, 10(6):433–439, Jun 2003. doi: 10.1038/nsb926. URL `http://dx.doi.org/10.1038/nsb926`.

Dillon Fritz and Branko Stefanovic. Rna-binding protein rbms3 is expressed in activated hepatic stellate cells and liver fibrosis and increases expression of transcription factor prx1. *J Mol Biol*, 371(3):585–595, Aug 2007. doi: 10.1016/j.jmb.2007.06.006. URL `http://dx.doi.org/10.1016/j.jmb.2007.06.006`.

Hans Georg Frohnhofer and Christiane Nusslein-Volhard. Organization of anterior pattern in the drosophila embryo by the maternal gene bicoid. *Nature*, 324:120–125, 1986.

J. B. Glotzer, R. Saffrich, M. Glotzer, and A. Ephrussi. Cytoplasmic flows localize injected oskar rna in drosophila oocytes. *Curr Biol*, 7(5):326–337, May 1997.

K. G. Golic. Site-specific recombination between homologous chromosomes in drosophila. *Science*, 252(5008):958–961, May 1991.

Wei J Gong and Kent G Golic. Ends-out, or replacement, gene targeting in drosophila. *Proc Natl Acad Sci U S A*, 100(5):2556–2561, Mar 2003. doi: 10.1073/pnas.0535280100. URL `http://dx.doi.org/10.1073/pnas.0535280100`.

Wei J Gong and Kent G Golic. Genomic deletions of the drosophila melanogaster hsp70 genes. *Genetics*, 168(3):1467–1476, Nov 2004. doi: 10.1534/genetics.104.030874. URL `http://dx.doi.org/10.1534/genetics.104.030874`.

Graydon B Gonsalvez, Carl R Urbinati, and Roy M Long. Rna localization in yeast: moving towards a mechanism. *Biol Cell*, 97(1):75–86, Jan 2005. doi: 10.1042/BC20040066. URL `http://dx.doi.org/10.1042/BC20040066`.

A. Gonzalez-Reyes, H. Elliott, and D. St Johnston. Polarization of both major body axes in drosophila by gurken-torpedo signalling. *Nature*, 375(6533):654–658, Jun 1995. doi: 10.1038/375654a0. URL `http://dx.doi.org/10.1038/375654a0`.

N. C. Grieder, M. de Cuevas, and A. C. Spradling. The fusome organizes the microtubule network during oocyte differentiation in drosophila. *Development*, 127(19):4253–4264, Oct 2000.

I. Groisman, Y. S. Huang, R. Mendez, Q. Cao, W. Theurkauf, and J. D. Richter. Cpeb, maskin, and cyclin b1 mrna at the mitotic apparatus: implications for local translational control of cell division. *Cell*, 103(3):435–447, Oct 2000.

N. Gunkel, T. Yano, F. H. Markussen, L. C. Olsen, and A. Ephrussi. Localization-dependent translation requires a functional interaction between the 5' and 3' ends of oskar mrna. *Genes Dev*, 12(11):1652–1664, Jun 1998.

O. Hachet and A. Ephrussi. Drosophila y14 shuttles to the posterior of the oocyte and is required for oskar mrna transport. *Curr Biol*, 11(21):1666–1674, Oct 2001.

Olivier Hachet and Anne Ephrussi. Splicing of oskar rna in the nucleus is coupled to its cytoplasmic localization. *Nature*, 428(6986):959–963, Apr 2004. doi: 10.1038/nature02521. URL `http://dx.doi.org/10.1038/nature02521`.

Udo Hacker, Sverker Nystedt, Mojgan Padash Barmchi, Carsten Horn, and Ernst A Wimmer. piggybac-based insertional mutagenesis in the presence of stably integrated p elements in drosophila. *Proc Natl Acad Sci U S A*, 100(13):7720–7725, Jun 2003. doi: 10.1073/pnas.1230526100. URL `http://dx.doi.org/10.1073/pnas.1230526100`.

K. S. Hoek, G. J. Kidd, J. H. Carson, and R. Smith. hnrnp a2 selectively binds the cytoplasmic transport sequence of myelin basic protein mrna. *Biochemistry*, 37(19):7021–7029, May 1998. doi: 10.1021/bi9800247. URL `http://dx.doi.org/10.1021/bi9800247`.

Jean-Rene Huynh, Trent P Munro, Katia Smith-Litiere, Jean-Antoine Lepesant, and Daniel St Johnston. The drosophila hnrnpa/b homolog, hrp48, is specifically required for a distinct step in osk mrna localization. *Dev Cell*, 6(5):625–635, May 2004.

M. Iida, T. Taira, H. Ariga, and S. M. Iguchi-Ariga. Induction of apoptosis in hela cells by mssp, c-myc binding proteins. *Biol Pharm Bull*, 20(1):10–14, Jan 1997.

Ferenc Jankovics, Rita Sinka, Tamas Lukacsovich, and Miklos Erdelyi. Moesin crosslinks actin and cell membrane in drosophila oocytes and is required for oskar anchoring. *Curr Biol*, 12(23): 2060–2065, Dec 2002.

R. P. Jansen. mrna localization: message on the move. *Nat Rev Mol Cell Biol*, 2(4):247–256, Apr 2001. doi: 10.1038/35067016. URL `http://dx.doi.org/10.1038/35067016`.

Jens Januschke, Louis Gervais, Sajith Dass, Julia A Kaltschmidt, Hernan Lopez-Schier, Daniel St Johnston, Andrea H Brand, Siegfried Roth, and Antoine Guichet. Polar transport in the drosophila oocyte requires dynein and kinesin i cooperation. *Curr Biol*, 12(23):1971–1981, Dec 2002.

Jens Januschke, Louis Gervais, Laurent Gillet, Guy Keryer, Michel Bornens, and Antoine Guichet. The centrosome-nucleus complex and microtubule organization in the drosophila oocyte. *Development*, 133(1):129–139, Jan 2006. doi: 10.1242/dev.02179. URL `http://dx.doi.org/10.1242/dev.02179`.

D. St Johnston, W. Driever, T. Berleth, S. Richstein, and C. Nusslein-Volhard. Multiple steps in the localization of bicoid rna to the anterior pole of the drosophila oocyte. *Development*, 107 Suppl:13–19, 1989.

D. St Johnston, D. Beuchle, and C. Nusslein-Volhard. Staufen, a gene required to localize maternal rnas in the drosophila egg. *Cell*, 66(1):51–63, Jul 1991.

Daniel St Johnston. Moving messages: the intracellular localization of mrnas. *Nat Rev Mol Cell Biol*, 6(5):363–375, May 2005. doi: 10.1038/nrm1643. URL `http://dx.doi.org/10.1038/nrm1643`.

O. Johnstone and P. Lasko. Translational regulation and rna localization in drosophila oocytes and embryos. *Annu Rev Genet*, 35:365–406, 2001. doi: 10.1146/annurev.genet.35.102401.090756. URL `http://dx.doi.org/10.1146/annurev.genet.35.102401.090756`.

Katherine C Jordan, Valerie Schaeffer, Karin A Fischer, Elizabeth E Gray, and Hannele Ruohola-Baker. Notch signaling through tramtrack bypasses the mitosis promoting activity of the jnk

pathway in the mitotic-to-endocycle transition of drosophila follicle cells. *BMC Dev Biol*, 6:16, 2006. doi: 10.1186/1471-213X-6-16. URL `http://dx.doi.org/10.1186/1471-213X-6-16`.

Yoshimitsu Kanai, Naoshi Dohmae, and Nobutaka Hirokawa. Kinesin transports rna: isolation and characterization of an rna-transporting granule. *Neuron*, 43(4):513–525, Aug 2004. doi: 10.1016/j.neuron.2004.07.022. URL `http://dx.doi.org/10.1016/j.neuron.2004.07.022`.

Y. Kanaoka and H. Nojima. Scr: novel human suppressors of cdc2/cdc13 mutants of schizosaccharomyces pombe harbour motifs for rna binding proteins. *Nucleic Acids Res*, 22(13):2687–2693, Jul 1994.

R. L. Kelley. Initial organization of the drosophila dorsoventral axis depends on an rna-binding protein encoded by the squid gene. *Genes Dev*, 7(6):948–960, Jun 1993.

J. Kim-Ha, J. L. Smith, and P. M. Macdonald. oskar mrna is localized to the posterior pole of the drosophila oocyte. *Cell*, 66(1):23–35, Jul 1991.

J. Kim-Ha, P. J. Webster, J. L. Smith, and P. M. Macdonald. Multiple rna regulatory elements mediate distinct steps in localization of oskar mrna. *Development*, 119(1):169–178, Sep 1993.

J. Kim-Ha, K. Kerr, and P. M. Macdonald. Translational regulation of oskar mrna by bruno, an ovarian rna-binding protein, is essential. *Cell*, 81(3):403–412, May 1995.

R. C. King. The meiotic behavior of the drosophila oocyte. *Int Rev Cytol*, 28:125–168, 1970.

E. H. Kislauskis, Z. Li, R. H. Singer, and K. L. Taneja. Isoform-specific 3'-untranslated sequences sort alpha-cardiac and beta-cytoplasmic actin messenger rnas to different cytoplasmic compartments. *J Cell Biol*, 123(1):165–172, Oct 1993.

E. H. Kislauskis, X. Zhu, and R. H. Singer. beta-actin messenger rna localization and protein synthesis augment cell motility. *J Cell Biol*, 136(6):1263–1270, Mar 1997.

Malgorzata Kloc, N. Ruth Zearfoss, and Laurence D Etkin. Mechanisms of subcellular mrna localization. *Cell*, 108(4):533–544, Feb 2002.

M. E. Lane and D. Kalderon. Rna localization along the anteroposterior axis of the drosophila oocyte requires pka-mediated signal transduction to direct normal microtubule organization. *Genes Dev*, 8(24):2986–2995, Dec 1994.

V. Lantz, L. Ambrosio, and P. Schedl. The drosophila orb gene is predicted to encode sex-specific germline rna-binding proteins and has localized transcripts in ovaries and early embryos. *Development*, 115(1):75–88, May 1992.

V. Lantz, J. S. Chang, J. I. Horabin, D. Bopp, and P. Schedl. The drosophila orb rna-binding protein is required for the formation of the egg chamber and establishment of polarity. *Genes Dev*, 8(5):598–613, Mar 1994.

R. Lehmann and C. Nusslein-Volhard. Abdominal segmentation, pole cell formation, and embryonic polarity require the localized activity of oskar, a maternal gene in drosophila. *Cell*, 47(1):141–152, Oct 1986.

R. Lehmann and C. Nusslein-Volhard. The maternal gene nanos has a central role in posterior pattern formation of the drosophila embryo. *Development*, 112(3):679–691, Jul 1991.

Kin-Mei Leung, Francisca P G van Horck, Andrew C Lin, Rachel Allison, Nancy Standart, and Christine E Holt. Asymmetrical beta-actin mrna translation in growth cones mediates attractive turning to netrin-1. *Nat Neurosci*, 9(10):1247–1256, Oct 2006. doi: 10.1038/nn1775. URL `http://dx.doi.org/10.1038/nn1775`.

M. Levadoux-Martin, J. E. Hesketh, J. H. Beattie, and H. M. Wallace. Influence of metallothionein-1 localization on its function. *Biochem J*, 355(Pt 2):473–479, Apr 2001.

P. Li, X. Yang, M. Wasser, Y. Cai, and W. Chia. Inscuteable and staufen mediate asymmetric localization and segregation of prospero rna during drosophila neuroblast cell divisions. *Cell*, 90 (3):437–447, Aug 1997.

R. M. Long, R. H. Singer, X. Meng, I. Gonzalez, K. Nasmyth, and R. P. Jansen. Mating type switching in yeast controlled by asymmetric localization of ash1 mrna. *Science*, 277(5324): 383–387, Jul 1997.

R. M. Long, W. Gu, E. Lorimer, R. H. Singer, and P. Chartrand. She2p is a novel rna-binding protein that recruits the myo4p-she3p complex to ash1 mrna. *EMBO J*, 19(23):6592–6601, Dec 2000. doi: 10.1093/emboj/19.23.6592. URL `http://dx.doi.org/10.1093/emboj/19.23.6592`.

Nina MacDougall, Alejandra Clark, Eilidh MacDougall, and Ilan Davis. Drosophila gurken (tgfalpha) mrna localizes as particles that move within the oocyte in two dynein-dependent steps. *Dev Cell*, 4(3):307–319, Mar 2003.

P. Mahon, K. Partridge, J. H. Beattie, L. A. Glover, and J. E. Hesketh. The 3' untranslated region plays a role in the targeting of metallothionein-i mrna to the perinuclear cytoplasm and cytoskeletal-bound polysomes. *Biochim Biophys Acta*, 1358(2):153–162, Sep 1997.

Massimo Mallardo, Anke Deitinghoff, Juliane Muller, Bernhard Goetze, Paolo Macchi, Christopher Peters, and Michael A Kiebler. Isolation and characterization of staufen-containing ribonucleoprotein particles from rat brain. *Proc Natl Acad Sci U S A*, 100(4):2100–2105, Feb 2003. doi: 10.1073/pnas.0334355100. URL `http://dx.doi.org/10.1073/pnas.0334355100`.

Jennifer H Mansfield, James E Wilhelm, and Tulle Hazelrigg. Ypsilon schachtel, a drosophila y-box protein, acts antagonistically to orb in the oskar mrna localization and translation pathway. *Development*, 129(1):197–209, Jan 2002.

Christophe Maris, Cyril Dominguez, and Frederic H-T Allain. The rna recognition motif, a plastic rna-binding platform to regulate post-transcriptional gene expression. *FEBS J*, 272(9):2118–2131, May 2005. doi: 10.1111/j.1742-4658.2005.04653.x. URL `http://dx.doi.org/10.1111/j.1742-4658.2005.04653.x`.

F. H. Markussen, A. M. Michon, W. Breitwieser, and A. Ephrussi. Translational control of oskar generates short osk, the isoform that induces pole plasma assembly. *Development*, 121(11): 3723–3732, Nov 1995.

Kelsey C Martin. Local protein synthesis during axon guidance and synaptic plasticity. *Curr Opin Neurobiol*, 14(3):305–310, Jun 2004. doi: 10.1016/j.conb.2004.05.009. URL `http://dx.doi.org/10.1016/j.conb.2004.05.009`.

D. R. Micklem, R. Dasgupta, H. Elliott, F. Gergely, C. Davidson, A. Brand, A. GonzÃ¡lez-Reyes, and D. St Johnston. The mago nashi gene is required for the polarisation of the oocyte and the formation of perpendicular axes in drosophila. *Curr Biol*, 7(7):468–478, Jul 1997.

D. R. Micklem, J. Adams, S. Grunert, and D. St Johnston. Distinct roles of two conserved staufen domains in oskar mrna localization and translation. *EMBO J*, 19(6):1366–1377, Mar 2000. doi: 10.1093/emboj/19.6.1366. URL `http://dx.doi.org/10.1093/emboj/19.6.1366`.

Stephan Miller, Masahiro Yasuda, Jennifer K Coats, Ying Jones, Maryann E Martone, and Mark Mayford. Disruption of dendritic translation of camkiialpha impairs stabilization of synaptic plasticity and memory consolidation. *Neuron*, 36(3):507–519, Oct 2002.

S. E. Mohr, S. T. Dillon, and R. E. Boswell. The rna-binding protein tsunagi interacts with mago nashi to establish polarity and localize oskar mrna during drosophila oogenesis. *Genes Dev*, 15 (21):2886–2899, Nov 2001. doi: 10.1101/gad.927001. URL `http://dx.doi.org/10.1101/gad.927001`.

X. Morin, R. Daneman, M. Zavortink, and W. Chia. A protein trap strategy to detect gfp-tagged proteins expressed from their endogenous loci in drosophila. *Proc Natl Acad Sci U S A*, 98(26): 15050–15055, Dec 2001. doi: 10.1073/pnas.261408198. URL `http://dx.doi.org/10.1073/pnas.261408198`.

Trent P Munro, Sunjong Kwon, Bruce J Schnapp, and Daniel St Johnston. A repeated imp-binding motif controls oskar mrna translation and anchoring independently of drosophila melanogaster imp. *J Cell Biol*, 172(4):577–588, Feb 2006. doi: 10.1083/jcb.200510044. URL `http://dx.doi.org/10.1083/jcb.200510044`.

Y. Negishi, Y. Nishita, Y. Saegusa, I. Kakizaki, I. Galli, F. Kihara, K. Tamai, N. Miyajima, S. M. Iguchi-Ariga, and H. Ariga. Identification and cdna cloning of single-stranded dna binding proteins that interact with the region upstream of the human c-myc gene. *Oncogene*, 9(4): 1133–1143, Apr 1994.

F. S. Neuman-Silberberg and T. Schupbach. The drosophila dorsoventral patterning gene gurken produces a dorsally localized rna and encodes a tgf alpha-like protein. *Cell*, 75(1):165–174, Oct 1993.

F. S. Neuman-Silberberg and T. Schupbach. The drosophila tgf-alpha-like protein gurken: expression and cellular localization during drosophila oogenesis. *Mech Dev*, 59(2):105–113, Oct 1996.

P. A. Newmark and R. E. Boswell. The mago nashi locus encodes an essential product required for germ plasm assembly in drosophila. *Development*, 120(5):1303–1313, May 1994.

P. A. Newmark, S. E. Mohr, L. Gong, and R. E. Boswell. mago nashi mediates the posterior follicle cell-to-oocyte signal to organize axis formation in drosophila. *Development*, 124(16):3197–3207, Aug 1997.

A. Norvell, R. L. Kelley, K. Wehr, and T. Schupbach. Specific isoforms of squid, a drosophila hnrnp, perform distinct roles in gurken localization during oogenesis. *Genes Dev*, 13(7):864–876, Apr 1999.

Amanda Norvell, Alain Debec, Daniel Finch, Lisa Gibson, and Brandi Thoma. Squid is required for efficient posterior localization of oskar mrna during drosophila oogenesis. *Dev Genes Evol*, 215 (7):340–349, Jul 2005. doi: 10.1007/s00427-005-0480-2. URL `http://dx.doi.org/10.1007/s00427-005-0480-2`.

Christiane N Nusslein-Volhard. The bicoid morphogen papers (i): account from cnv. *Cell*, 116(2 Suppl):S1–5, 2 p following S9, Jan 2004.

H. Ochman, A. S. Gerber, and D. L. Hartl. Genetic applications of an inverse polymerase chain reaction. *Genetics*, 120(3):621–623, Nov 1988.

Isabel M Palacios. How does an mrna find its way? intracellular localisation of transcripts. *Semin Cell Dev Biol*, 18(2):163–170, Apr 2007. doi: 10.1016/j.semcdb.2007.01.008. URL `http://dx.doi.org/10.1016/j.semcdb.2007.01.008`.

Isabel M Palacios and Daniel St Johnston. Kinesin light chain-independent function of the kinesin heavy chain in cytoplasmic streaming and posterior localisation in the drosophila oocyte. *Development*, 129(23):5473–5485, Dec 2002.

Isabel M Palacios, David Gatfield, Daniel St Johnston, and Elisa Izaurralde. An eif4aiii-containing complex required for mrna localization and nonsense-mediated mrna decay. *Nature*, 427 (6976):753–757, Feb 2004. doi: 10.1038/nature02351. URL `http://dx.doi.org/10.1038/nature02351`.

D. Penkov, R. Ni, C. Else, S. Pinol-Roma, F. Ramirez, and S. Tanaka. Cloning of a human gene closely related to the genes coding for the c-myc single-strand binding proteins. *Gene*, 243(1-2): 27–36, Feb 2000.

Cedric Polesello, Isabelle Delon, Philippe Valenti, Pierre Ferrer, and FranÃ§ois Payre. Dmoesin controls actin-based cell shape and polarity during drosophila melanogaster oogenesis. *Nat Cell Biol*, 4(10):782–789, Oct 2002. doi: 10.1038/ncb856. URL `http://dx.doi.org/10.1038/ncb856`.

V. Riechmann and A. Ephrussi. Axis formation during drosophila oogenesis. *Curr Opin Genet Dev*, 11(4):374–383, Aug 2001.

C. Rongo, E. R. Gavis, and R. Lehmann. Localization of oskar rna regulates oskar translation and requires oskar protein. *Development*, 121(9):2737–2746, Sep 1995.

P. Rorth. Gal4 in the drosophila female germline. *Mech Dev*, 78(1-2):113–118, Nov 1998.

S. Roth, F. S. Neuman-Silberberg, G. Barcelo, and T. Schupbach. cornichon and the egf receptor signaling process are necessary for both anterior-posterior and dorsal-ventral pattern formation in drosophila. *Cell*, 81(6):967–978, Jun 1995.

Edward Ryder, Fiona Blows, Michael Ashburner, Rosa Bautista-Llacer, Darin Coulson, Jenny Drummond, Jane Webster, David Gubb, Nicola Gunton, Glynnis Johnson, Cahir J O'Kane, David Huen, Punita Sharma, Zoltan Asztalos, Heiko Baisch, Janet Schulze, Maria Kube, Kathrin Kittlaus, Gunter Reuter, Peter Maroy, Janos Szidonya, Asa Rasmuson-Lestander, Karin Ekstrom, Barry Dickson, Christoph Hugentobler, Hugo Stocker, Ernst Hafen, Jean Antoine Lepesant, Gert Pflugfelder, Martin Heisenberg, Bernard Mechler, Florenci Serras, Montserrat Corominas, Stephan Schneuwly, Thomas Preat, John Roote, and Steven Russell. The drosdel collection: a set of p-element insertions for generating custom chromosomal aberrations in drosophila melanogaster. *Genetics*, 167(2):797–813, Jun 2004. doi: 10.1534/genetics.104.026658. URL `http://dx.doi.org/10.1534/genetics.104.026658`.

C. Saunders and R. S. Cohen. The role of oocyte transcription, the 5'utr, and translation repression and derepression in drosophila gurken mrna and protein localization. *Mol Cell*, 3(1):43–54, Jan 1999.

T. Schupbach. Germ line and soma cooperate during oogenesis to establish the dorsoventral pattern of egg shell and embryo in drosophila melanogaster. *Cell*, 49(5):699–707, Jun 1987.

Laura R Serbus, Byeong-Jik Cha, William E Theurkauf, and William M Saxton. Dynein and the actin cytoskeleton control kinesin-driven cytoplasmic streaming in drosophila oocytes. *Development*, 132(16):3743–3752, Aug 2005. doi: 10.1242/dev.01956. URL `http://dx.doi.org/10.1242/dev.01956`.

J. M. Shulman, R. Benton, and D. St Johnston. The drosophila homolog of c. elegans par-1 organizes the oocyte cytoskeleton and directs oskar mrna localization to the posterior pole. *Cell*, 101(4):377–388, May 2000.

A. C. Spradling, D. Stern, A. Beaton, E. J. Rhem, T. Laverty, N. Mozden, S. Misra, and G. M. Rubin. The berkeley drosophila genome project gene disruption project: Single p-element insertions mutating 25 *Genetics*, 153(1):135–177, Sep 1999.

Josefa Steinhauer and Daniel Kalderon. The rna-binding protein squid is required for the establishment of anteroposterior polarity in the drosophila oocyte. *Development*, 132(24):5515–5525, Dec 2005. doi: 10.1242/dev.02159. URL `http://dx.doi.org/10.1242/dev.02159`.

Josefa Steinhauer and Daniel Kalderon. Microtubule polarity and axis formation in the drosophila oocyte. *Dev Dyn*, 235(6):1455–1468, Jun 2006. doi: 10.1002/dvdy.20770. URL `http://dx.doi.org/10.1002/dvdy.20770`.

O. Steward and E. M. Schuman. Protein synthesis at synaptic sites on dendrites. *Annu Rev Neurosci*, 24:299–325, 2001. doi: 10.1146/annurev.neuro.24.1.299. URL `http://dx.doi.org/10.1146/annurev.neuro.24.1.299`.

T. Takai, Y. Nishita, S. M. Iguchi-Ariga, and H. Ariga. Molecular cloning of mssp-2, a c-myc gene single-strand binding protein: characterization of binding specificity and dna replication activity. *Nucleic Acids Res*, 22(25):5576–5581, Dec 1994.

P. A. Takizawa and R. D. Vale. The myosin motor, myo4p, binds ash1 mrna via the adapter protein, she3p. *Proc Natl Acad Sci U S A*, 97(10):5273–5278, May 2000. doi: 10.1073/pnas.080585897. URL `http://dx.doi.org/10.1073/pnas.080585897`.

P. A. Takizawa, A. Sil, J. R. Swedlow, I. Herskowitz, and R. D. Vale. Actin-dependent localization of an rna encoding a cell-fate determinant in yeast. *Nature*, 389(6646):90–93, Sep 1997. doi: 10.1038/38015. URL `http://dx.doi.org/10.1038/38015`.

W. E. Theurkauf, S. Smiley, M. L. Wong, and B. M. Alberts. Reorganization of the cytoskeleton during drosophila oogenesis: implications for axis specification and intercellular transport. *Development*, 115(4):923–936, Aug 1992.

Stephen T Thibault, Matthew A Singer, Wesley Y Miyazaki, Brett Milash, Nicholas A Dompe, Carol M Singh, Ross Buchholz, Madelyn Demsky, Robert Fawcett, Helen L Francis-Lang, Lisa Ryner, Lai Man Cheung, Angela Chong, Cathy Erickson, William W Fisher, Kimberly Greer, Stephanie R Hartouni, Elizabeth Howie, Lakshmi Jakkula, Daniel Joo, Keith Killpack, Alex Laufer, Julie Mazzotta, Ronald D Smith, Lynn M Stevens, Christiana Stuber, Lory R Tan, Richard Ventura, Alesa Woo, Irena Zakrajsek, Lora Zhao, Feng Chen, Candace Swimmer, Casey Kopczynski, Geoffrey Duyk, Margaret L Winberg, and Jonathan Margolis. A complementary transposon tool kit for drosophila melanogaster using p and piggybac. *Nat Genet*, 36(3):283–287, Mar 2004. doi: 10.1038/ng1314. URL `http://dx.doi.org/10.1038/ng1314`.

J. D. Thompson, D. G. Higgins, and T. J. Gibson. Clustal w: improving the sensitivity of progressive multiple sequence alignment through sequence weighting, position-specific gap penalties and weight matrix choice. *Nucleic Acids Res*, 22(22):4673–4680, Nov 1994.

G. H. Thomsen and D. A. Melton. Processed vg1 protein is an axial mesoderm inducer in xenopus. *Cell*, 74(3):433–441, Aug 1993.

P. Tomancak, F. Piano, V. Riechmann, K. C. Gunsalus, K. J. Kemphues, and A. Ephrussi. A drosophila melanogaster homologue of caenorhabditis elegans par-1 acts at an early step in

embryonic-axis formation. *Nat Cell Biol*, 2(7):458–460, Jul 2000. doi: 10.1038/35017101. URL `http://dx.doi.org/10.1038/35017101`.

F. J. van Eeden, I. M. Palacios, M. Petronczki, M. J. Weston, and D. St Johnston. Barentsz is essential for the posterior localization of oskar mrna and colocalizes with it to the posterior pole. *J Cell Biol*, 154(3):511–523, Aug 2001. doi: 10.1083/jcb.200105056. URL `http://dx.doi.org/10.1083/jcb.200105056`.

Nathalie F Vanzo and Anne Ephrussi. Oskar anchoring restricts pole plasm formation to the posterior of the drosophila oocyte. *Development*, 129(15):3705–3714, Aug 2002.

J. L. Veyrune, G. P. Campbell, J. Wiseman, J. M. Blanchard, and J. E. Hesketh. A localisation signal in the 3' untranslated region of c-myc mrna targets c-myc mrna and beta-globin reporter sequences to the perinuclear cytoplasm and cytoskeletal-bound polysomes. *J Cell Sci*, 109 (Pt 6):1185–1194, Jun 1996.

C. Wang and R. Lehmann. Nanos is the localized posterior determinant in drosophila. *Cell*, 66(4): 637–647, Aug 1991.

Schallum Werner. Characterizing the binding-attributes of hrp48 and mapping the binding sites in oskar mrna. Master's thesis, Faculty of Biology Technische Unversitaet Darmstadt and EMBL Developmental Biology Programme Heidelberg, 2005.

J. E. Wilhelm, J. Mansfield, N. Hom-Booher, S. Wang, C. W. Turck, T. Hazelrigg, and R. D. Vale. Isolation of a ribonucleoprotein complex involved in mrna localization in drosophila oocytes. *J Cell Biol*, 148(3):427–440, Feb 2000.

James E Wilhelm, Michael Buszczak, and Suzanne Sayles. Efficient protein trafficking requires trailer hitch, a component of a ribonucleoprotein complex localized to the er in drosophila. *Dev Cell*, 9(5):675–685, Nov 2005. doi: 10.1016/j.devcel.2005.09.015. URL `http://dx.doi.org/10.1016/j.devcel.2005.09.015`.

T. Xu and G. M. Rubin. Analysis of genetic mosaics in developing and adult drosophila tissues. *Development*, 117(4):1223–1237, Apr 1993.

Tamaki Yano, Sonia Lopez de Quinto, Yasuhisa Matsui, Anna Shevchenko, Andrej Shevchenko, and Anne Ephrussi. Hrp48, a drosophila hnrnpa/b homolog, binds and regulates translation of oskar mrna. *Dev Cell*, 6(5):637–648, May 2004.

Young J Yoon and Kimberly L Mowry. Xenopus staufen is a component of a ribonucleoprotein complex containing vg1 rna and kinesin. *Development*, 131(13):3035–3045, Jul 2004. doi: 10.1242/dev.01170. URL `http://dx.doi.org/10.1242/dev.01170`.

H. L. Zhang, T. Eom, Y. Oleynikov, S. M. Shenoy, D. A. Liebelt, J. B. Dictenberg, R. H. Singer, and G. J. Bassell. Neurotrophin-induced transport of a beta-actin mrnp complex increases beta-actin levels and stimulates growth cone motility. *Neuron*, 31(2):261–275, Aug 2001.

Vitaly Zimyanin, Nick Lowe, and Daniel St Johnston. An oskar-dependent positive feedback loop maintains the polarity of the drosophila oocyte. *Curr Biol*, 17(4):353–359, Feb 2007. doi: 10.1016/j.cub.2006.12.044. URL `http://dx.doi.org/10.1016/j.cub.2006.12.044`.